INVESTIGATION INTO A PROMINENT 38KHZ SCATTERING LAYER IN THE NORTH SEA

Angus Mair

A Thesis Submitted for the Degree of PhD
at the
University of St. Andrews

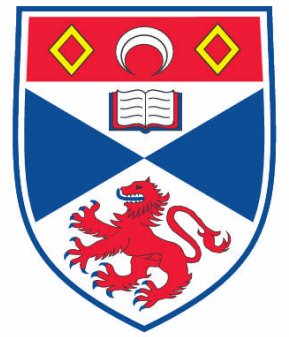

2008

Investigation into a prominent 38 kHz scattering layer in the North Sea

Angus MacDonald Mair

PhD thesis

Date of submission: 28 February 2008

I, Angus MacDonald Mair, hereby certify that this thesis, which is approximately 25000 words in length, has been written by me, that it is the record of work carried out by me and that it has not been submitted in any previous application for a higher degree.

Date: **Signature of candidate:**

I was admitted as a research student on 1 October 2002 and as a candidate for the degree of PhD on 1 October 2002; the higher study for which this is a record was carried out in the University of St Andrews between 2002 and 2006.

Date: **Signature of candidate:**

I hereby certify that the candidate has fulfilled the conditions of the Resolution and Regulations appropriate for the degree of PhD in the University of St Andrews and that the candidate is qualified to submit this thesis in application for that degree.

Date: **Signature of supervisor:**

In submitting this thesis to the University of St Andrews I understand that I am giving permission for it to be made available for use in accordance with the regulations of the University Library for the time being in force, subject to any copyright vested in the work not being affected thereby. I also understand that the title and abstract will be published, and that a copy of the work may be made and supplied to any bona fide library or research worker, that my thesis will be electronically accessible for personal or research use, and that the library has the right to migrate my thesis into new electronic forms as required to ensure continued access to the thesis. I have obtained any third-party copyright permissions that may be required in order to allow such access and migration.

Date: **Signature of candidate:**

Acknowledgements

I would like to extend thanks to my supervisors, Dr **Andrew Brierley** of the University of St Andrews Gatty Marine Laboratory and Dr **Paul Fernandes** of FRS Marine Laboratory, Aberdeen, for their continued help and advice in allowing me to complete this thesis.

As senior scientist on the survey cruises when my data were collected, **John Simmonds** is deserving of thanks and appreciation.

Members of staff at FRS who were a great help include **Phil Copland**, **Eric Armstrong**, **Mike Stewart** and **Stuart Halewood** (since moved to Bermuda). Their cheerful disposition and expertise are a continuing source of inspiration. Without their help in coaxing life out of certain pieces of ageing equipment, this study would not have been possible. **Steve Hay**, **Jens Rasmussen** and **John Fraser** also helped on many occasions with the identification of small animals and fish larvae.

Much help in sourcing, maintaining, preparing and using plankton sampling mechanisms was offered by **John Dunn**. For this I am truly grateful. John's positive outlook on life and his work is second to none - a man of many and varied interests, he continues to be a great ambassador for FRS.

Anne LeBourges-Dhaussy and her colleagues at IRD, Brest, France were of great help in explaining inverse methods and their applications—*merci beaucoup*!

I fully appreciate the efforts of **Jon Watkins** (British Antarctic Survey) and **Anne Magurran** of the University of St Andrews in finally whipping this thesis into shape.

The **Master and crew of FRV Scotia** also deserve thanks for their assistance and willingness in deploying and recovering various plankton samplers at all hours of the day and night, often immediately following a fish haul when they really deserved a break. Thanks to certain members of the crew are also due for pointing out favoured places of refreshment in the port of Lerwick! My colleagues at the **SFPA** have provided me with far more information regarding the mechanisms driving the commercial fishery than I would otherwise have found.

Overdue thanks to my secondary school biology teacher, Dr **Bruce Simms** (retired), of Robert Gordon's College, Aberdeen, for sparking my interest.

Finally, and most importantly, those who have had to put up with me over the last few years of study and head-scratching. For their ongoing support and encouragement, my parents Captain **Robert and Mrs. Carol Mair** - without whom I would not have been possible - my sons **Robbie and Thomas**, and my partner **Ildikó (Indy)** whose love, support and belief has been invaluable.

Abstract

The aim of this study was to investigate the composition of an acoustic scattering layer in the North Sea that is particularly strong at 38 kHz. A full definition of the biological composition of the layer, along with its acoustic properties, would allow for it to be confidently removed from data collected during acoustic fish surveys, where it presents a potential source of bias. The layer, traditionally and informally referred to as consisting of zooplankton, appears similar to others observed internationally. The methodology utilised in this study consisted of biological and acoustic sampling, followed by application of forward and inverse acoustic modelling techniques. Acoustic data was collected at 38, 120 and 200 kHz in July 2003, with the addition of 18 kHz in July 2004. Net samples were collected in layers of relatively strong 38 kHz acoustic scattering using a U-tow vehicle (2003) and a MIKT net (2004). Acoustic data were scrutinised to determine actual backscattering, expressed as mean volume backscattering strength (MVBS) (dB). This observed MVBS ($MVBS_{obs}$) was compared with backscattering predicted by applying the forward problem solution ($MVBS_{pred}$) to sampled animal densities in order to determine whether those animals were responsible for the enhanced 38 kHz scattering. In most instances, $MVBS_{obs} > MVBS_{pred}$, more pronounced at 38 kHz. It was found that $MVBS_{pred}$ approached $MVBS_{obs}$ more closely with MIKT than with U-tow samples, but that the 38 kHz mismatch was present in both. Inversion of candidate acoustic models predicted gas-bearing scatterers, which are strong at 38 kHz, as most likely to be responsible for this. Potential sources of inconsistencies between $MVBS_{pred}$ and $MVBS_{obs}$ were identified. The presented forward and inverse solutions infer that although the layer often contains large numbers of common zooplankton types, such as copepods and euphausiids, these are not the dominant acoustic scatterer at 38 kHz. Rather, there remains an unidentified, probably gas-bearing scatterer that contributes significantly to observed scattering levels at this frequency. This study identifies and considerably narrows the list of candidates that are most likely to be responsible for enhanced 38 kHz scattering in the North Sea layer, and recommendations are made for potential future studies.

Contents

Chapter 1 - Introduction

Chapter 2 - General methods

Chapter 3 - The contribution made by mesozooplankton to the scattering layer

Chapter 1

Introduction

General Introduction

The use of multifrequency acoustic technology in studies of zooplankton ecology is now commonplace. Acoustic sampling is essentially non-invasive and is operationally fast enough to distinguish patches of pelagic species of a range of sizes at a number of scales both spatially and temporally (Holliday and Pieper, 1995). In most instances, however, it is still necessary to obtain physical samples to confirm the types of organism detected acoustically (Fielding *et al*., 2004*;* MacLennan and Simmonds, 1992). Acoustic data can be used to direct nets to a patch of interest, improving the chances of directly sampling the acoustically-detected targets (Greenlaw, 1979). Progressing from this, combined acoustic and net data can be used to generate acoustic-only species identification (Madureira *et al.*, 1993a). Objective identification of certain animals via differences in Mean Volume Backscattering Strength (MVBS) at different frequencies, without the need for biological sampling, has been postulated (Kang *et al*., 2002; Korneliussen and Ona, 2002; Madureira *et al*., 1993a; Watkins and Brierley, 2002). Such procedures are based on the fact that different types of plankton (e.g. copepods, euphausiids, siphonophores) have diagnostic frequency responses (Holliday, 1977).

During annual summer acoustic surveys of herring in the North Sea (ICES Area IVa) aboard the Fisheries Research Vessel (FRV) Scotia (Fig. 1.1) (e.g. Simmonds, 2003), a strong 38 kHz scattering layer is present at a depth varying between approximately 10 and 75 m. This layer is less intense at 120 and 200 kHz (Fig. 1.2). This layer is often present for extended periods over the course of the survey, and has been generally but informally believed to consist of zooplankton. However, the layer composition has not been identified because it has not been sampled with plankton nets in the course of normal fish surveys. The aim of this present study was to identify the characteristics of acoustic scatterers contained in this layer using biological sampling and acoustic data recorded at combinations of 18, 38, 120 and 200 kHz. Both forward (McNaught, 1968; Greenlaw, 1979) and inverse (Holliday, 1977; Greenlaw, 1979) methods were considered. A good overview of both has previously been published (Greenlaw and Johnson, 1983) but, in brief, the forward problem involves the sorting and identification of animals in the biological samples to determine their size and the basic shape by which they can be acoustically described (e.g. sphere). Acoustic scattering models specific to those shapes (and other characteristics, such as size) are then applied to predict backscattering at each frequency. These predictions are then compared to

simultaneously-recorded acoustic data (Pieper and Holliday, 1984). The inverse method approaches the problem from the opposite direction, where the shape and size of the dominant scatterers are predicted from multifrequency backscattering. Originally (Holliday *et al*., 1989; Pieper *et al*., 1990), observed data were used to determine the most probable abundance for a given size of plankton of a single type. In this thesis, however, a range of scattering models were inverted. This allows the type and size of the most likely scattering candidates among the expected types to be identified (Lebourges-Dhaussy and Ballé-Béganton, 2004).

Aside from the inherent scientific interest in the biological composition of a community of scatterers, proper identification of the targets causing the strong 38 kHz North Sea scattering layer will aid in the further development of software-based procedures - such as those suggested by Korneliussen and Ona (2002) - that remove such targets from echograms. The ability to do this would have a beneficial effect on acoustic surveys of fish, where 38 kHz is the most commonly used sampling frequency (MacLennan and Simmonds, 1992). This would allow greater confidence when simplifying echograms by removal of the layer in question, and may also aid in stock assessment where errors may be introduced at the data analysis stage either by mistakenly evaluating plankton as fish or discarding fish echoes informally in the belief that they are caused by zooplankton.

Fig 1.1: FRV Scotia leaving Aberdeen harbour accompanied by the harbour pilot boat, July 2003.

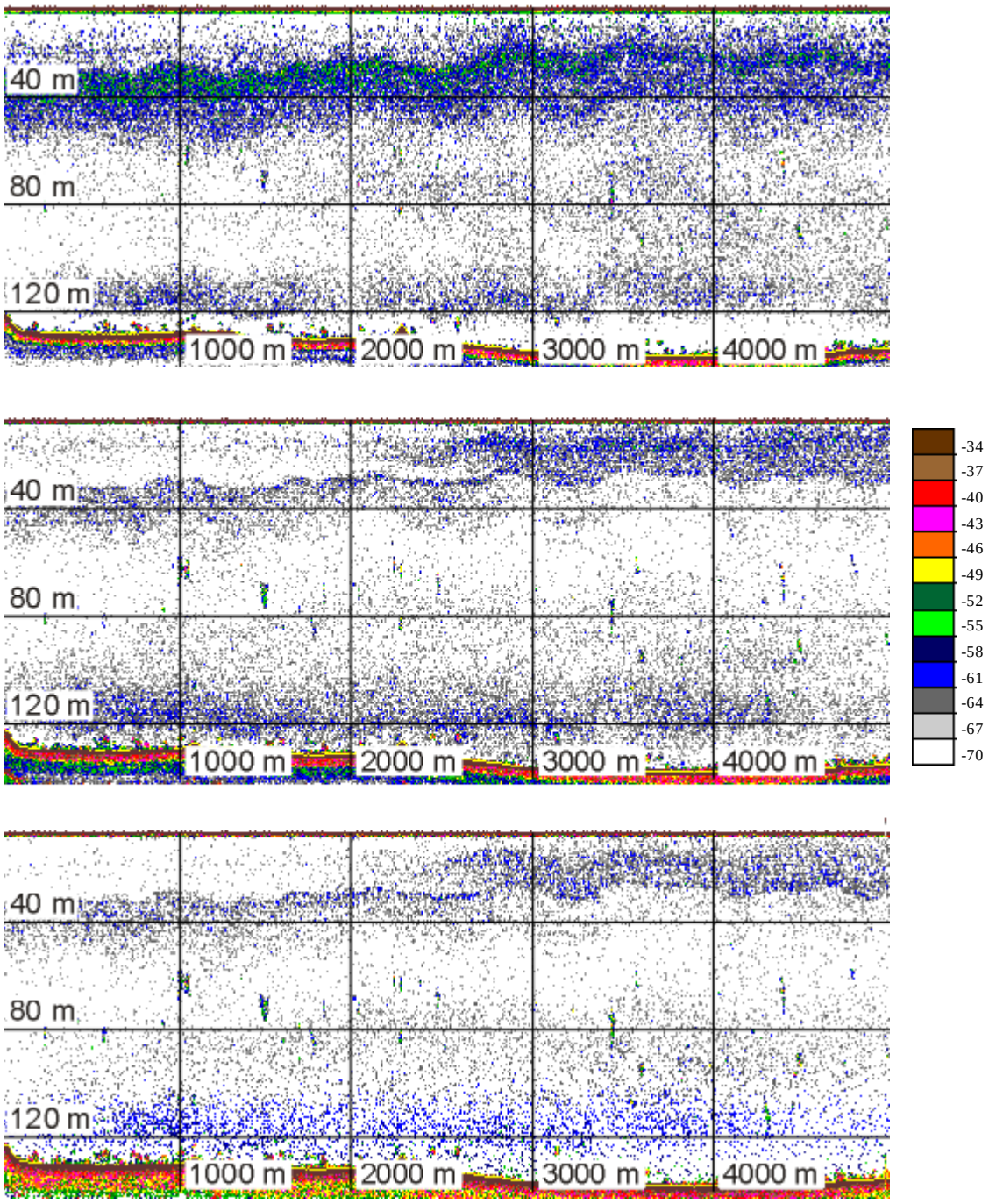

Fig. 1.2: Example echograms recorded at sound frequencies of a) 38, b) 120 and c) 200 kHz on 1st July 2003 at 59º33N 0º50W. Water depth is displayed on the left of each echogram and horizontal distance at the foot. Mean volume backscattering strength (MVBS) is shown by use of colour, with the legend showing decibel (dB) values (in 3 dB steps) for each colour used in the display. These echograms were recorded at a ship speed of approximately 10 knots. The scattering layer that is the subject of this thesis can be seen between the surface and approximately 60 m in this case.

Historical background

Investigation of the abundance and ecology of living marine resources is an important research topic because of its direct relation to the world economy. As sound propagates much more readily through water than does light, techniques based on the principles of sound propagation provide an effective means of exploring the ocean. The quantitative use of underwater sound by biological scientists is, however, a relatively new field. Although Da Vinci discovered as long ago as 1490 that listening at one end of a tube placed in the sea allowed detection of distant ships, the speed of sound in water was not initially quantified until 1827 (Colladon and Sturm, decribed in MacLennan and Simmonds, 1992). By simultaneously flashing a light and ringing an underwater bell in Lake Geneva, and calculating the difference in time to receipt, Colladon and Sturm estimated underwater sound to travel at 1450 m/s. This is remarkably close to the currently accepted value of 1500 m/s.

As is often the case, war was the catalyst which provided significant advances in the use of underwater sound. In 1918, it was noticed that submarines could be detected by listening for echoes of electrically generated sound transmissions. Although the possibility had been mentioned in the earlier years of the decade, the first successful acoustic fish detection was not reported until 1929 (Kimura, 1929). Kimura noted that reception of sound transmitted across an aquaculture pool was disturbed when fish passed through the beam. This experiment, however, utilised disruption of a forward-moving sound transmission rather than the reception of echoes (MacLennan and Simmonds, 1992). Sund (1935) was responsible for a pioneering survey which detected a layer of cod *Gadus morhua* 10 m beneath the sea surface using an echosounder operating at 16 kHz.

Further rapid development occurred between World War I and World War II, and natant commercial applications were soon realised. ASDIC (Anti Submarine Division Investigation Committee) came to be known as SONAR (Sound Navigation and Ranging) and was first used to locate fish successfully in 1946 (Renou and Tchernia, 1947). By the end of the decade, echosounders were being used widely in various commercial and scientific applications. Good summaries of historical developments to the modern day are presented by MacLennan and Holliday (1996) and Fernandes *et al.* (2002), with the general principles of fisheries acoustics well covered by MacLennan and Forbes (1984).

Aside from investigations of fish stocks, acoustics has been used extensively in zooplankton surveys and has been applied to analysis of other groups such as squid (Goss *et al.*, 2001) and jellyfish (Brierley *et al.*, 2001). Recently, the most substantial advances have been made in software-based acoustic data analysis techniques (Higginbottom *et al.*, 2000).

Due to the increased use of acoustics in biomass estimation, allied to the disparity of terminology, MacLennan and Fernandes (2000) proposed a consistent approach to acoustic scattering definitions and symbols for fisheries applications, the scope of which has been broadened to include sound source and propagation (MacLennan *et al.*, 2002). Adoption of the suggested terminology would encourage consistency in the literature, and I have endeavoured to apply it throughout this thesis.

Underwater sound propagation

An understanding of the properties of sound in an aquatic environment, particularly the manner in which it is scattered and reflected, is necessary for the scientist intending to use acoustics for the acquisition of data.

A constant waveform, such as sound, can be described either by its "frequency" or its "wavelength". Frequency refers to the number of wave cycles per second, and is measured in Hertz (Hz). One Hertz is equal to one wave cycle per second. Similarly, one kiloHertz (kHz) is equal to one thousand wave cycles per second. Wavelength is the distance measured between identical points on adjacent cycles of the waveform. Frequency is inversely related to wavelength, such that for a given velocity a higher frequency sound will have a correspondingly shorter wavelength.

The level of underwater sound is generally measured on the decibel scale. The decibel (dB) is a commonly used unit of acoustic measurement. It is a logarithmic expression of the ratio of two sound pressures, one of which is a reference point (commonly 1 µPa) and the other the measured value. Logarithmic values are used due to the wide range of sound pressures encountered (MacLennan and Simmonds, 1992).

The sound pressure level of an acoustic wave emanating from a source underwater diminishes exponentially with range, due mainly to absorption and spreading. The loss due to spreading has an inverse square relationship with distance.

Advection is the process by which water currents can refract and otherwise modify acoustic signals, and may be detected in a horizontal change of echo arrival angle (Farmer, 1996). Absorption is defined as an exponential loss of acoustic energy with reference to distance (MacLennan and Simmonds, 1992). The acoustic absorption coefficient (α), expressed in dB m^{-1} can be calculated using the equation $\alpha = 8.69\beta$, where β is the acoustic coefficient of the medium. The value α is frequency dependent - higher frequency sound will be absorbed more quickly (MacLennan and Simmonds, 1992).

The primary factor influencing absorption is friction due to water viscosity. This occurs in both salt and fresh water, but the effect is enhanced in the sea by the presence of compounds such as magnesium sulphate. Friction is caused by acoustic pressure inducing “relaxation” of these compounds into ions, particularly at frequencies between 2 and 500 kHz. Boric acid exhibits similar behaviour in the lower frequency range (MacLennan and Simmonds, 1992). Sound frequencies above this range do not cause such relaxation, due to a higher pressure oscillation rate caused by the acoustic waves. It is evident that a higher concentration of compounds in the water will result in a higher attenuation of sound.

Other factors influencing absorption which must be considered include - as well as salinity - temperature, depth and pH (MacLennan, 1990). Several attempts have been made to define the effects of such factors, with work by Shulkin and Marsh (1963) and Fisher and Simmons (1977) being refined by Francois and Garrison (1982) resulting in an absorption coefficient equation which covers temperatures from 1.8 - 30 ºC, salinities from 30 - 35 ‰ and acoustic frequencies from 400 Hz - 1 MHz, as well as considering depth and pH. This equation contains components relating to boric acid, magnesium sulphate and water viscosity. Although seawater pH can vary between 7.8 and 8.2, Maclennan and Simmonds (1992) argue that a value of 8.0 can be reasonably assumed in the absence of data.

The speed of sound in water varies around 1500ms^{-1} according to salinity, temperature and depth. Again, equations used to calculate this velocity have been refined over time with Wilson (1960), for example, providing a detailed procedure. Del Grosso and Mader (1972) and Urick (1975) published useful work on the subject, and MacKenzie (1981) furthered this to provide the currently preferred equation shown here:

Eqn. 1:

$$c = 1448.96 + 4.591T - 0.05304T^2 + 2.734 \times 10^{-4}T^3 + (1.34 - 0.01025T)(S-35) + 0.0163D + 1.675 \times 10^{-7}D^2$$

where c is the sound velocity, T is temperature (°C), S is salinity (‰) and D is depth (m).

MacLennan and Simmonds (1992) review the basic properties of underwater sound velocity, stating that it is faster in warmer, shallower water. With decreasing temperature and increasing depth, sound travels more slowly until below 500m, where water can be considered isothermic, sound speed increases.

Underwater sound scattering

The intensity of a received echo, referred to as its "amplitude", is affected primarily by the sound scattering process. On encountering an obstacle (or "target") part of the incident sound is reflected back (backscattered), generating a secondary wave. The remainder passes through the target and continues in the incident direction. The amount of sound reflected depends on the difference in acoustic impedance of the obstacle as compared to the original medium. A greater difference will result in a stronger reflection. The major component of acoustic backscatter from some fish is caused by the gas-filled swimbladder which is responsible for 90-95% of reflected energy (Foote, 1980). However, stomach content, gonadal development, fat content and depth are also influencing factors (Ona, 1990). For the same reason, air bubbles and suspended particles such as zooplankton may cause scattering which can mask echoes from targets such as fish (Foote and Stanton, 2000). Scattering from undesirable targets is termed "reverberation". Unwanted background signals originating from other sources and which are present in the absence of active sound transmission are termed "noise". Sources of background noise include oceanic turbulence and shipboard machinery (MacLennan and Simmonds, 1992, Watkins and Brierley, 1996).

For the purposes of this thesis, "Rayleigh" and "geometric" scattering are considered. The distinction arises according to the size of the target in relation to the wavelength of incident sound. Rayleigh (1945) described the complete insonification of a target which was small compared to wavelength. The target oscillates sympathetically and scatters spherically-spreading sound waves. Geometric scattering, on the other hand, describes the properties of sound reflected from a target which is large compared to the wavelength. In this case, the general law of "angle of incidence = angle of reflection" applies, although the surface

geometry and orientation of the target (the latter particularly applying to targets showing asymmetrical morphology) will have an effect (Horne, 2000). This can be summarised by stating that Rayleigh scattering involves the volume of a small target, whilst geometric scattering involves the surface of a large target. Further, scattering by a small target increases rapidly with frequency whilst frequency has little effect for large targets (MacLennan and Simmonds, 1992).

Target strength

The backscattering cross-section (s_{bs}) of a target, expressed in m^2, is a measurement of the intensity of sound of a given frequency scattered back from a target. It is given by the following equation:

Eqn. 2: $$s_{bs} = r^2(I_{scat}/I_{inc})$$

where r (m) is the distance of the measurement position from the target, I_{scat} (dB) is the intensity of the scattered wave at the measurement position and I_{inc} (dB) is the intensity of the incident wave at the target (MacLennan and Simmonds, 1992).

However, on account of the great variation in sizes of possible targets in the sea and the consequent variation in backscattering cross-section values, a logarithmic representation termed the "target strength" (TS) is usually used:

Eqn. 4: $$TS = 10log_{10}(s_{bs})$$

This gives a measure, in decibels (dB), of the acoustic reflectivity of the target (MacLennan and Simmonds, 1992). Most fish show a target strength of between –60 dB and –20 dB, although a particular target may be characterised by a range of TS values according to several factors including animal size, shape, orientation and material properties as well as acoustic frequency (Stanton and Chu, 2000). Because of this, target strength must be considered stochastic (MacLennan, 1990).

The scientific echosounder

Scientific echosounders are devices which produce a burst of sound and allow reception of

reflected, or backscattered, echoes. Many texts describe the principles by which they operate (e.g. MacLennan and Simmonds, 1992; Fernandes *et al.*, 2002). An electrical transmitter output is converted by a transducer to acoustic energy of a given frequency, and this energy is projected in a directional beam through the water. Differing sizes of transducer are required for similar beam dimensions to be produced at different frequencies. Typically, the beam width in fisheries applications is between five and fifteen degrees (MacLennan and Simmonds, 1992).

As the transmitted sound travels through the water, it may encounter obstacles such as fish or the seabed. Some of the acoustic energy will be reflected back towards the transducer, which detects the echo and converts it to electrical energy. The intensity of the received sound is referred to as the echo amplitude, and will depend on features of the obstacle encountered. For example, the strength of sound backscattered from a population of zooplankton will depend on the concentration of zooplankters, distribution of sizes and the echosounder frequency (Greenlaw, 1979). The received signal is amplified via the application of a time-varied gain (TVG) function which compensates for simple range-dependant effects. In this way, targets which are further from the receiver are amplified to a greater degree (Foote and Stanton, 2000; MacLennan and Simmonds, 1992), correcting for loss of signal over the greater range due to absorption, spreading and reflection. The depth of the target is calculated from the time difference between pulse generation and echo reception. The process is repeated with a typical interval of one second, allowing graphical output of a time-series of echoes received. VDU displays are commonly used to display this output as an "echogram" (Fig. 1.3). An echogram plots echo returns on an *x,y* axis of depth against time/distance, and can show echo amplitude by the use of colour. Similar discrete marks on the echogram can be counted to give an estimate of target abundance in a sparsely dispersed population.

Echo integration

Counting echogram marks produced by individuals may prove impossible when animals become aggregated. Echo returns from individuals will overlap and become indistinct. In order to overcome this, the technique of echo integration is used. First proposed by Dragesund and Olsen (1965), the echo integrator system sums and averages received signal intensity over a given depth range following TVG application (Foote and Stanton, 2000).

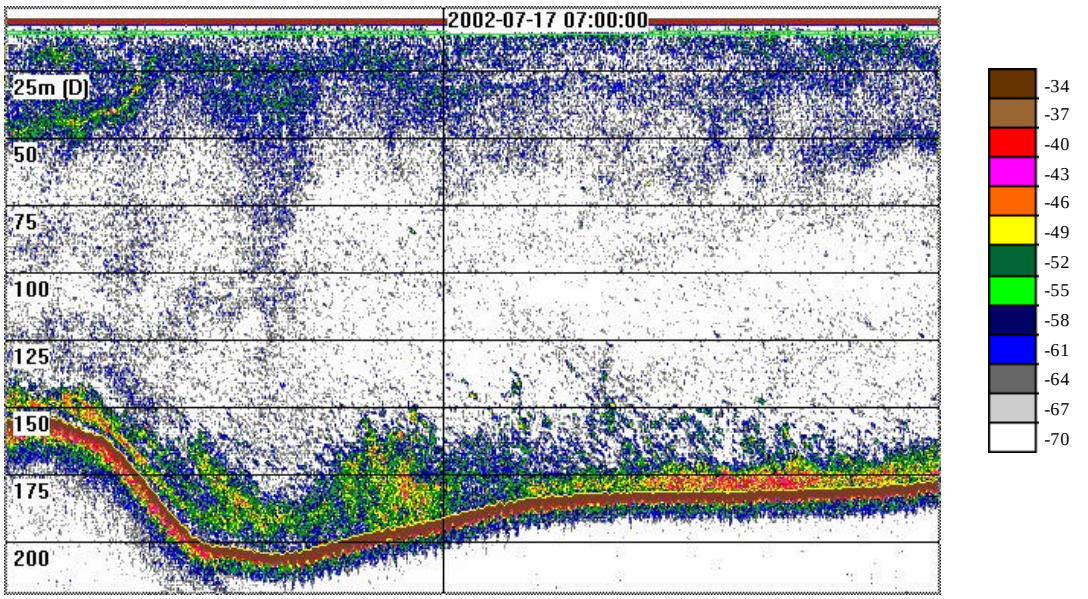

Fig. 1.3: A typical echogram as viewed on a VDU. Depth is displayed on the left, and date/time at the top of the screen. The dark red area running from 150m at left to 175m at right represents the sea bed. Increasing echo intensity is represented by colour, with the legend showing decibel (dB) levels (in 3dB steps) for each colour used. The blue area between 0 and 50m is traditionally seen as representing plankton of indeterminate population composition, whilst the stronger scatterers near the sea bed are more likely to be shoals of fish.

This gives a volume backscattering (S_v) value for a single transmission.

Averaging S_v data from a set of successive transmissions gathered along a distance travelled by the ship provides a Mean Volume Backscatter Strength (MVBS) value for the given depth range and distance. This facilitates abundance estimation of an identified target, with the primary assumption that targets are randomly distributed across the beam cross-section, such that the received integrated signal will be proportional to target density (MacLennan and Simmonds, 1992).

Background noise can be removed during the integration process by setting an integration threshold, the value of which must be carefully chosen in order not to exclude biological data. This is especially true when the desired targets are relatively weak scatterers such as zooplankton. One method of setting a threshold at depth is to use the highest MVBS value from an echogram integration interval which contains no target (Madureira *et al.*, 1993b).

Watkins and Brierley (1996) discuss a method of removing background noise by applying a post-processing TVG algorithm to unthresholded data, with the benefit that collected data remains more intact.

Calibration

In order for the interpretation of echosounder output to be consistent, the system must be calibrated prior to or during a survey. That is, the value of the given output must be compared with a standard whose acoustic properties are known, in order that density calculations made from the output will be correct (MacLennan and Simmonds, 1992). The standard procedure, approved by the International Council for the Exploration of the Sea (ICES), is described in detail in Foote *et al.* (1987). In summary, a sphere (typically tungsten carbide or copper) of known acoustic properties is wetted with a solution of fresh water and household detergent to minimise acoustic contamination by gas bubble adhesion, then suspended beneath the transducer (outside the "near field", that is, the region near the transducer where sound radiation is complex due to interference of sound radiating from different regions of the transducer) on the axis of the acoustic beam where echo energy will be at a maximum. The sphere echo is integrated for a period of time, and actual and theoretical results compared. This gives a constant of proportionality, which can be applied to other targets encountered during the survey to give accurate backscattering values (Foote and Stanton, 2000).

Backscatter from zooplankton

Zooplankton distribution is influenced by many biological and environmental factors (Haury *et al.*, 1978). The latter include large-scale physical factors from ocean gyres and currents to fronts, tides and river plumes (Herman *et al.*, 1981) which influence local factors such as microcurrents and thus the spatial variability of individuals (Holliday *et al.*, 1990). Biological factors include species as well as feeding, social and reproductive behaviour which are related to mobility capabilities (Haury and Wiebe, 1982).

Distribution may be considered either horizontally or vertically in the water column, with the latter possibly contributing towards changes in the former (Kullenberg, 1978). It may also be considered temporally. Many zooplankton species undergo diel or nocturnal vertical migration. Using acoustics in the Clyde Sea, Tarling *et al.* (2002) found that the copepod

Calanus finmarchicus ascended in the water column in late afternoon but descended again when predatory krill ascended later in the evening. Thus, time of day must be taken into account during zooplankton abundance surveys. Demer and Hewitt (1995) report that biomass estimates from an Antarctic krill survey were 49.5% higher following application of a temporal compensation function (TCF) to data that had previously disregarded such biases. Certain species of calanoid copepod exhibit seasonal vertical migration to depths of 1000 m (Lenz, 2000).

Estimation of zooplankton abundance has until recently been associated with pump and net-caught samples (Sameoto *et al.*, 2000). The use of acoustics may be an ideal alternative method, although it is currently still necessary to obtain biological samples for confirmation of the type of organism detected by acoustic methods (MacLennan and Simmonds, 1992). The initial advantage of applying acoustics to the problem is that nets can be directed to a patch of interest with the knowledge that the desired population will be sampled directly (Greenlaw, 1979). Further, objective identification of animals via differences in MVBS at different frequencies has been shown to be possible without the need for sampling (Korneliussen and Ona, 2002; Madureira *et al.*, 1993a; Watkins and Brierley, 2002).

A relatively low acoustic frequency, typically with a long wavelength relative to the expected fish size, is usually sufficient for assessment of nekton such as fish (MacLennan and Simmonds, 1992) - this is due to the presence of gas-filled swimbladders, which reflect sound well (Horne and Clay, 1998). For example, at 38 kHz, underwater sound has a wavelength of approximately 4 cm, whilst an adult fish may have a swimbladder of several cubic centimetres in volume. Thus, strong geometric backscattering would be expected at this frequency. Zooplankton acoustics, however, generally require higher frequencies with wavelengths of the order of the animal size - as wavelength increases above the size of the animal, echo amplitude decreases rapidly (McNaught, 1968; Greenlaw, 1979; Horne and Clay, 1998). Higher frequencies allow for maximisation of reflection from small zooplankton (Holliday and Pieper, 1995). For example, underwater sound at 120 kHz and 200 kHz will have approximate wavelengths of 1.2 cm and 0.7 cm respectively. Holliday *et al.* (1998) studied the structure of zooplankton assemblages using 265, 420, 1100 and 3000 kHz transducers which were selected to be particularly sensitive to the presence of small zooplankton. The primary disadvantage of using such high frequencies is that they are

quickly attenuated in water and therefore have a limited useful range.

Backscattering models

The physical properties of an acoustic target can be analysed and its backscattering characteristics modelled mathematically. With the application of such backscattering models, acoustic data can yield inherent biological information and the abundance of a particular target type can be estimated (Stanton and Chu, 2000). This requires knowledge of the biological composition of the acoustic target – knowledge that is often attained by sampling the insonified population (Sameoto *et al.*, 2000). With this knowledge, backscattering models of the animals present can be applied to the acoustic data in order to estimate relative abundance. It should be noted that any errors contained within the models will be transferred to the final result as they will become an integral part of any calculation (Greenlaw and Johnson, 1983).

There are two types of model: the empirical type involves averaging many measurements expressed as functions of frequency, organism size and orientation, whilst conceptual models assume a similarity between organisms and geometric shapes (Greenlaw and Johnson, 1983). Conceptual models are now in widespread use, and undergoing constant refinement.

The development of conceptual backscattering models can be described as improvements in resolution, with earlier approximations leading to more complex descriptions taking into account body features and appendages. Further to this, the material properties of different animal groups - such as normal orientation, density and sound speed ratios in contrast with seawater (*g* and *h* respectively) provide an area for extensive study. Using calculations of standard backscattering characteristics, the abundance of animals of a given type can be inferred from the measured backscattering strength. Holliday (1977) presented a mathematical method of size-abundance distribution estimation for marine organisms using acoustical measurements at several frequencies. Greenlaw (1977) used a range of frequencies to measure scattering strength of individual zooplankters, and Johnson (1977) modified an earlier model created by Anderson (1950) which he used to describe scattering by euphausiids and shrimp. This model treated the animals as homogenous spheres, and is known as the fluid sphere model.

Success with the fluid sphere model has been reported by authors such as Holliday *et al.* (1989) and Coyle (1998) where small animals (<1mm) such as copepods are concerned. Unfortunately, animals are generally not spherical. Acoustic scattering is a complex function of the size, shape, orientation and material properties of the target animal, as well as acoustic frequency (e.g. Stanton and Chu, 2000). Larger animals, such as some euphausiids, have a morphology which cannot be shown to conform to a spherical model (Chu *et al.*, 1992). Target strength will depend on the angle of acoustic incidence in relation to presented body area, that is, orientation of the animal (McGehee *et al.*, 1998).

Assuming morphological similarity, orientation of the live animal is an important factor which influences backscattering and the model must include assumptions about the orientation most likely to be encountered. Copepods, for example, are known to position themselves vertically in the water with the head up (Coyle, 1998; Benfield *et al.*, 2000), so that a model which assumes broadside incidence of sound will give false results. Captive krill have been shown to have a mean orientation of around 20º (Chu *et al.*, 1993), although other studies have suggested that this figure may be closer to 45º (Kils, 1981; Endo, 1993). More recently, Demer and Conti (2005) suggest 15º as a more accurate orientation for rapidly swimming antarctic krill. Such elongated organisms as euphausiids are better described by a "deformed cylinder" model, as proposed by Stanton (1989). This model assumes a circular cross-section, but allows for the general form including bend, taper and roughness of the body (Stanton and Chu, 2000) and is therefore a more accurate descriptor in this case. Watkins and Brierley (2002) report that this model performed better than the fluid sphere in predicting length of Antarctic krill when using dB difference between 120 and 38 kHz to predict krill length.

Based on the assumption that zooplankton have bodies similar in composition to surrounding water and are thus weak scatterers, Stanton *et al.* (1998) presented the Distorted Wave Born Approximation (DWBA) deformed cylinder model. This is a valid model for most angles of incidence, although Demer and Conti (2005) found it unreliable for animals at extreme orientations, and is limited with regard to material properties – the opposite of the model-series-based deformed cylinder approach. The DWBA-based model would appear to apply well to a wide range of animals with material properties similar to seawater (Stanton and Chu, 2000). One of the most recent developments is the Stochastic DWBA (or SDWBA)

model that aims to account for the stochastic nature of sound scattering, noise, and flexure in the animal's body as it swims (Demer and Conti, 2003a; 2003b). Research is ongoing in the modelling of various species of zooplankton such as *Calanus finmarchicus, Euchaeta spp.* and *Oithona spp.* (McGehee *et al.*, 2002).

Stanton *et al.* (1996) grouped animals into one of three classes according to gross anatomical class; fluid-like (e.g. small planktonic crustaceans and salps), elastic-shelled (e.g. gastropods), and gas-bearing (e.g. siphonophores). It was found that sound was scattered with different degrees of efficiency from each group. Similar echo levels (-70 dB at 200 kHz) were detected from densities of 14 m^{-3} planktonic gastropods and 190 m^{-3} salps. Thus, the elastic-shelled gastropods were shown to be much more efficient scatterers than the fluid-like salps. At 38 kHz, however, gastropods entered the Rayleigh scattering region and modelling showed that a density of 6250 m^{-3} individuals was required to produce a similar echo level. The conclusion was that the differences in morphology between zooplankton groups lead to differences in their scattering properties, with acoustic frequency being an important factor.

The most accurate technique of defining morphology for modelling purposes is digitisation. In short, a fine resolution representation of the animal's outer body is graphically produced. Stanton and Chu (2000) recommend that digitisation resolution should be around one twentieth of the acoustic wavelength, and note that approximation is still necessary in smaller animals due to the small size of appendages and other body features. McGehee *et al.* (2002) provide a thorough explanation of the procedure.

It would be expected that higher resolution models are more robust under different circumstances, but the simpler models are still applicable due to their ease of use under limited conditions (Stanton and Chu, 2000). It is envisaged that work will continue in the field of backscatter modelling, with the need to strike a balance between increased resolution and ease of use an important component. There is also a need to characterise more species at different frequencies. In any case, once a model for the backscattering properties of an animal at a given frequency is conceived, this must be allied to acoustic survey data in order to calculate the number of animals observed. The accuracy of this depends on the principle of linearity and may take the following form (e.g. Foote, 1983, McGehee *et al.*, 2002):

Eqn. 6: $S_v = N \times E[\sigma_{bs}]$

where S_v is the volume backscattering measurement made, $E[\sigma_{bs}]$ is the expected value of the backscattering coefficient from the animal in question and N is the number of such animals per unit volume. In order to calculate N, the equation is simply inverted (e.g. Horne and Jech, 1999).

It is unlikely that a single species and size/age class of zooplankton will be found in the sample area - rather several species, possibly including various life stages, will coincide (Greenlaw, 1979). This means that the equation given above (Eqn. 6) becomes too simplistic, and must be modified to include more than one possible target, as follows (Greenlaw and Johnson, 1983):

Eqn. 7: $S_v = N_1 \times E[\sigma_{bs1}] + N_2 \times E[\sigma_{bs2}] + \ldots + Nx \times E[\sigma_{bsx}]$

where x is the possible number of different species and life stages present per unit volume. Without 100% sampling of the insonified targets this equation cannot be accurately solved, and some theoretical species composition must be considered.

Multifrequency acoustics

As has already been mentioned, animals scatter sound differently according to morphology, material properties and sound frequency. Thus, an animal is likely to have two different backscattering coefficients at two different frequencies. It follows that different classes of animals may be distinguishable if insonified at multiple frequencies by their differing target strengths. This applies equally well to fish and zooplankton. Early work was done by McNaught (1968), who showed that different frequencies were more sensitive to scattering by different sizes of zooplankton. This suggested that the difference in echo levels could be utilised in calculating biomass in a size range determined by the frequencies used. The theory was ultimately tested by Pieper *et al.* (1990), whose Multifrequency Acoustic Profiling System (MAPS) used 21 frequencies spaced logarithmically from 0.1 to 10 MHz to continually measure zooplankton abundance over size classes spanning five orders of magnitude, from microns to centimetres (Pieper *et al.*, 1990).

Due mainly to industry standards, some combination of 18, 38, 120 and 200 kHz are used more commonly in multifrequency surveys (e.g. Brierley *et al.*, 2001; Kloser *et al.*, 2002; Korneliusen and Ona, 2002; Madureira *et al.*, 1993a; Watkins and Brierley, 2002), as well as 420kHz (e.g Coyle, 1998; Kirsch *et al.*, 2000). Data collected from these frequencies can be analysed for differences in MVBS (ΔMVBS) to identify different sizes of organism, with choice of frequencies closely allied to the desired target sizes (Horne and Clay, 1998). Swartzman *et al.* (1999), for example, showed an association between pollock shoals and zooplankton patches by using 38 kHz to detect the fish, and 120/200 kHz to detect plankton.

Sampling and ground truthing

The fundamental drawback of a purely acoustic survey at the present time is that no actual specimens of animals are gained and thus any biological conclusions must be considered speculative. Verification and accurate interpretation of acoustic backscattering measurements can only be achieved if the biological parameters of the area producing backscatter (often referred to as a 'patch') are known. Acoustic scatterers need to be reliably identified via ground truthing (McClatchie *et al.*, 2000). In this way, the output of the echogram can be related as directly as possible to samples of the scatterers. This is usually done by directed biological sampling or some form of photography (Foote and Stanton, 2000). Ideally, multiple sampling regimes should be used (Sameoto and Lewis, 1990). Paradoxically, it is the deficiencies in sampling procedures which have provided the incentive for acoustic surveying, which currently requires them for ground truthing (Holliday and Pieper, 1995; McClatchie *et al.*, 2000). Recent advances in the use of acoustic information for identification purposes are, however, such that ground truthing is often no longer necessary for every patch encountered once a positive identification of a similar patch has been made (Brierley *et al.*, 1998; Watkins and Brierley, 2002), and progress towards the ultimate goal of remote species identification is being made. The work described in this thesis aims to contribute to this field.

Many approaches can be used to obtain ground truth data. The information required includes species identification, size distribution and orientation distribution, but there is no current system which can provide all three (McClatchie *et al.*, 2000). Further required information, such as g and h values for the animal types sampled, cannot be gleaned simply by biological sampling. In a broader sense, sampling should be non-selective and the gear used should not

induce avoidance reactions or behavioural changes in orientation. It is necessary to have the ability to direct the sampler to the position of an echogram mark, and it must have the capacity to capture samples at discrete intervals without cross-contamination (McClatchie *et al.*, 2000).

A variety of appropriate pumps and net systems are available, a good review of which appears in Foote and Stanton (2000). Pumps offer an advantage over nets in areas of high animal density in that the volume of water filtered can be reliably measured, clogging of meshes can be monitored and contamination from surrounding layers is eliminated. However, sample scale is small compared to nets (Foote and Stanton, 2000).

Net sampling falls into several categories, including ring nets and multiple net samplers. The simple ring net (such as the WP-2) can be used easily and at low cost, but is indiscriminate (Sameoto *et al.*, 2000).

There are two main types of multiple sampling devices. The first type collects organisms on a long, continuous piece of mesh (Sameoto *et al.*, 2000). Examples include the Hardy Continuous Plankton Recorder (CPR) (Hardy, 1926), Longhurst Hardy Plankton Recorder (LHPR) (Longhurst *et al.*, 1966), Autosampling and Recording Instrumented Environmental Sampling System (ARIES) (Dunn *et al.*, 1993) and Gulf III (Gehringer, 1952). The second type of sampler utilises the method of opening and closing individual sample nets in succession. Williamson (1962, 1963) described an automatic plankton sampler using multiple nets opened and closed by a mechanical cam system. MOCNESS (Wiebe *et al.*, 1985) and BIONESS (Sameoto *et al.*, 1980) are examples of multiple net systems which can be remotely controlled from the surface. The advantage of such systems is that they can collect discrete samples which are more intact than those collected using continuous mesh. Kirsch *et al.* (2000) used a MOCNESS sampler during a 420 kHz zooplankton survey in Alaska and reported that catch resolution was insufficient to assess patches of scales less than 10m. The BIONESS has a higher towing speed, which may contribute to its greater efficiency in capturing larger zooplankton which are less able to escape a high-speed device (Sameoto *et al.*, 2000).

Greenlaw (1979) mentions problems associated with the method of counting subsamples of

net-caught plankton specimens, such as the time-lag between collection and results due to intensive analysis requirements and the need to train personnel in the required techniques, as well as errors contained within the samples, such as post-collection predation. Net clogging and avoidance contribute to errors, as does contamination from imprecise depth of net opening/closing and sample integration over the length of the tow (Holliday *et al.*, 1990). Much work has been done to improve plankton samplers (reviewed in Holliday *et al.*, 1990 and Sameoto *et al.*, 2000), with the result that data collected from today's electronic opening-closing multisamplers are far more reliable (Sameoto *et al.*, 2000).

Electronic plankton counters are now commonly used. The first such was reported by Mackas and Boyd (1979), and improved upon by Dessureault (1976), Herman and Denman (1977) and Herman and Dauphinee (1980) in the creation of a vehicle called "Batfish" which provided a continuous particle profile, utilised initially to profile chlorophyll and then zooplankton in the latter study. First described by Herman (1988), the Optical Particle Counter (OPC) provides non-video zooplankton distribution and abundance information. Particles passing through a calibrated beam of light in a sampling tunnel are counted and sized. The OPC can be towed horizontally at high speed, or used for vertical profiling (Sameoto *et al.*, 2000) but provides no information on the actual species encountered, or indeed whether particles counted are even living organisms. The Ichthyoplankton Recorder (IPR) is a modified Gulf III sampler with a sensitive video system incorporated into the codend (Lenz *et al.*, 1995). This system concentrates organisms in the net before they are measured. The Video Plankton Recorder (VPR) is a towed underwater microscope that can be used to record images of *in situ* plankton via high and low resolution video cameras (Davis *et al.*, 1996). Using this system in conjunction with an automatic identification program, Davis and Gallager (2000) were able to automatically classify video images of 11 taxa with an accuracy of 87%. Daly *et al.* (2001) describe the use of a high speed digital line scan camera in their SIPPER (Shadowed Image Particle Profiling and Evaluation Recorder) system, with the claimed advantages of imaging a large size range of organisms as well as their *in situ* spatial distribution. Underwater holography, reviewed by Foster and Watson (1997), offers the opportunity to create optical replicas of zooplankton *in situ.* The resulting holographic recording can then be analysed in the laboratory.

Recent developments

One of the problems associated with acoustic studies is the difficulty of obtaining reliable signals from the few metres of water near the surface due to background noise. For this reason, echosounders may be deployed on an instrument keel which can be dropped to a distance below the underside of the vessel to avoid surface noise - consequently, however, it becomes impossible to collect data from the surface layers above the position of the echosounder. A possible solution would be to deploy a vehicle containing either upward-looking or sideways-looking echosounders operated from the ship, for example the upward looking towfish described by Everson and Bone (1986). As an alternative, Szczucka *et al.* (2002) describe an Autonomous Hydroacoustic System (AHS) consisting of a vehicle containing a 130 kHz echosounder which sinks to the seabed and insonifies the water column in an upward direction as it rises. An autonomous underwater vehicle (AUV), Autosub-1, was used by Fernandes *et al.* (2000) during an acoustic herring survey in the North Sea. It was found that the vehicle, which collected acoustic data at 38 and 120 kHz, produced fish abundance data comparable to that of the survey vessel, which followed at 200-800 m distance. This showed that AUVs may be suitable for effective monitoring of fish stocks as well as providing evidence that fish do not avoid survey vessels. Fernandes *et al.* (2002) proposed that this vehicle may prove useful in higher frequency zooplankton studies, and this has proved to be the case. In 2001, an Autosub-2 vehicle, also collecting acoustic data at 38 and 120 kHz, was used to survey under-ice Antarctic krill populations to a distance of 27 km beyond the ice edge (Brierley *et al.*, 2002).

The ICES Working Group on Fisheries Acoustics Science and Technology (WGFAST) are currently examining the possibility of using commercial fishing vessels for acoustic data collection. This would offer the advantage of improved spatial-temporal coverage, but possible problems include lack of survey design, fish avoidance and the large amount of data requiring analysis (ICES, 2002).

The use of commercially available software such as SonarData Echoview to interpret echosounder data is now widespread, particularly in the creation of virtual echograms (Higginbottom *et al.*, 2000; Higginbottom, 2001). These consist of an on-screen combination of multifrequency data, with the resulting display highlighting targets of a desired strength. This method allows the visual separation of organisms with different scattering properties at

the frequencies concerned, such as zooplankton and fish. Korneliussen and Ona (2002) report on a real-time virtual echogram system, describing two methods of combining multifrequency data. The first, “division”, enhances the backscattering difference of a target at two frequencies by comparing the two MVBS values, whilst the second, “categorisation”, allows scatterers to be grouped together according to an expert system with several stages. The former is faster and can be used directly during survey work, whilst the latter gives a more accurate overall visualisation and may be more useful in analysing collected data. Both methods are prone to errors introduced by current hardware configurations, in particular due to poor spatial overlap of acoustic beams produced by separate transducers. Improvements whereby transducers are positioned closer together are suggested by Korneliussen and Ona (2002) and are implemented on the new Norwegian research vessel “G.O. Sars”.

Acoustic surveying techniques have shown constant progress over the last century. From an initial realisation that the presence of fish could be detected by insonifying the water column, species identification and abundance estimation have become possible. The application of multifrequency acoustics has allowed for discrimination of animal types in a volume of water, and procedures for the modelling of backscattering characteristics continue to be refined. Advances in sampling methods are ongoing, but may be eclipsed in certain circumstances by purely acoustical methodology.

The North Sea layer in an international context

Strong 38 kHz scattering layers are not found exclusively in the North Sea. In 1979, the authors of an acoustic fish survey in Burma suggested that a strong 38 kHz scattering layer was capable of masking weak fish echoes. Despite this feature being regularly observed during the survey the layer was not sampled and its constituents not identified - rather an assumption was made that “plankton” were responsible (Nakken and Aung, 1980).

Over the last decade similar layers occurring over continental shelf areas internationally have been reported, to the extent that the U.S. Office of Naval Research (ONR) has funded an ongoing study program named LOCO (“Layered Organisation in the Coastal Ocean”) (ONR, 2005). As part of this program, thin layers which appear to have similar characteristics to those in the present study have been observed, for example, in Monterey Bay, California in 2005 where they were found to consist primarily of zooplankton. These

layers are reported as rare during daylight hours, but frequently observed in the upper 10-12 m of the water column at night (Benoit-Bird K.J., College of Oceanic and Atmospheric Sciences, Oregon State University, pers. comm., 2007). The phytoplankton content of these Monterey Bay layers was also considered (Rines *et al.*, 2006).

As part of a multi-disciplinary field project in December 1996, a layer of zooplankton was acoustically observed and found to be coincident with a layer of phytoplankton which is drawn to depth by a subduction effect at the Almeria-Oran front, where the waters of the Atlantic and Mediterranean meet at the eastern end of the Alboran Sea. It was found, by analysis of high-resolution OPC data, that a further layer of smaller zooplankters did not undertake diel vertical migration, but remained concentrated near the surface (Fielding *et al.*, 2001). Acoustic detection of diel vertical migration has been clearly shown in the waters of the high Arctic, with a strong and substantial 38 kHz layer rising from a depth of 250-300 m during the day to around 150 m at night. Evidence of a much thinner, but still strong 38 kHz layer which is consistent at approximately 50 m depth can also be seen, but is not commented on by the study's authors (Keskinen *et al*, 2004).

In studies at the Mid-Atlantic Ridge area and the Gulf of Alaska, layers with similar characteristics to that found in the North Sea are apparent (Anderson *et al., 2007)*. Echograms at the Mid-Atlantic Ridge are dominated by amorphous horizontal layers which, according to the classification proposed, most likely consisted of both fish and zooplankton. A similar result was obtained in the Gulf of Alaska as part of the same study. In the Pacific, acoustic data collected around Hawaii reveals a layer comparable to that in the North Sea. This layer shows a strong component of diel vertical migration, with samples indicating that it is composed of euphausiids, small decapods and myctophid fish (Brodeur *et al.*, 2005). In 2003, Large-scale 38 kHz layers observed at around 30 m depth over the Argentinian continental shelf were sampled and found to contain dense aggregations of large gelatinous zooplankters with only traces of other animal types. It was reported that such aggregations were responsible for masking the acoustic presence of anchovy shoals (Colombo *et al.*, 2003). Gelatinous animals were also found to strongly influence the strength of similar layers observed off British Columbia, although in this instance physonect siphonophores were identified as making the major contribution to scattering (Trevorrow *et al.*, 2005).

The variety of acoustic targets held primarily responsible for enhanced scattering layers in these studies from widely dispersed areas suggests that the composition of such layers may be highly variable, and dependent on the types of organisms found locally.

The North Sea layer - an overview

Insonification of the layer under consideration in the present study at 38 kHz produces echograms similar to many of those published in the work mentioned above and hence may be of interest in an international context. The North Sea layer appears to vary between 10 and 75 m depth, and also varies in both vertical extent and acoustic density. In order to quickly visualise any major geographical variations in acoustic density and provide an impression of the extent and variability of the layer, 38 kHz acoustic data gathered over the course of two research cruises in 2003 and 2004 were manipulated in the following manner.

For each day of the research cruises during which data for the present study were collected, an echogram showing 38 kHz scattering was created using SonarData Echoview (SonarData Pty Ltd, GPO Box 1387, Hobart, Tasmania, Australia) software. The area of the water column containing the strong scattering layer was isolated across the whole of each of these echograms by defining a bounded "region" around it for each 24 hour period. This process was performed manually rather than using an algorithm in order that undulations of the layer and unusual spikes could be included.

Following this region definition, areas of high scattering characteristic of fish schools were removed from echograms using a previously-created algorithm supplied by Dr Paul Fernandes of FRS Marine Laboratory, Aberdeen. The variable computation method available in SonarData EchoView was utilised in this procedure, which was based on observations that fish schools appeared consistently on 38, 120 and 200 kHz echograms while other features were strong on some frequencies and weak on others. It was necessary to manipulate the algorithm, as it had been designed to leave fish schools on the virtual echogram whilst removing everything else. The objective of the present analysis was the opposite - to remove areas exhibiting scattering characteristic of fish. The resulting defined echogram region showed only the heavy scattering under consideration, with fish removed.

The defined region was then exported in the form of nautical area scattering coefficient

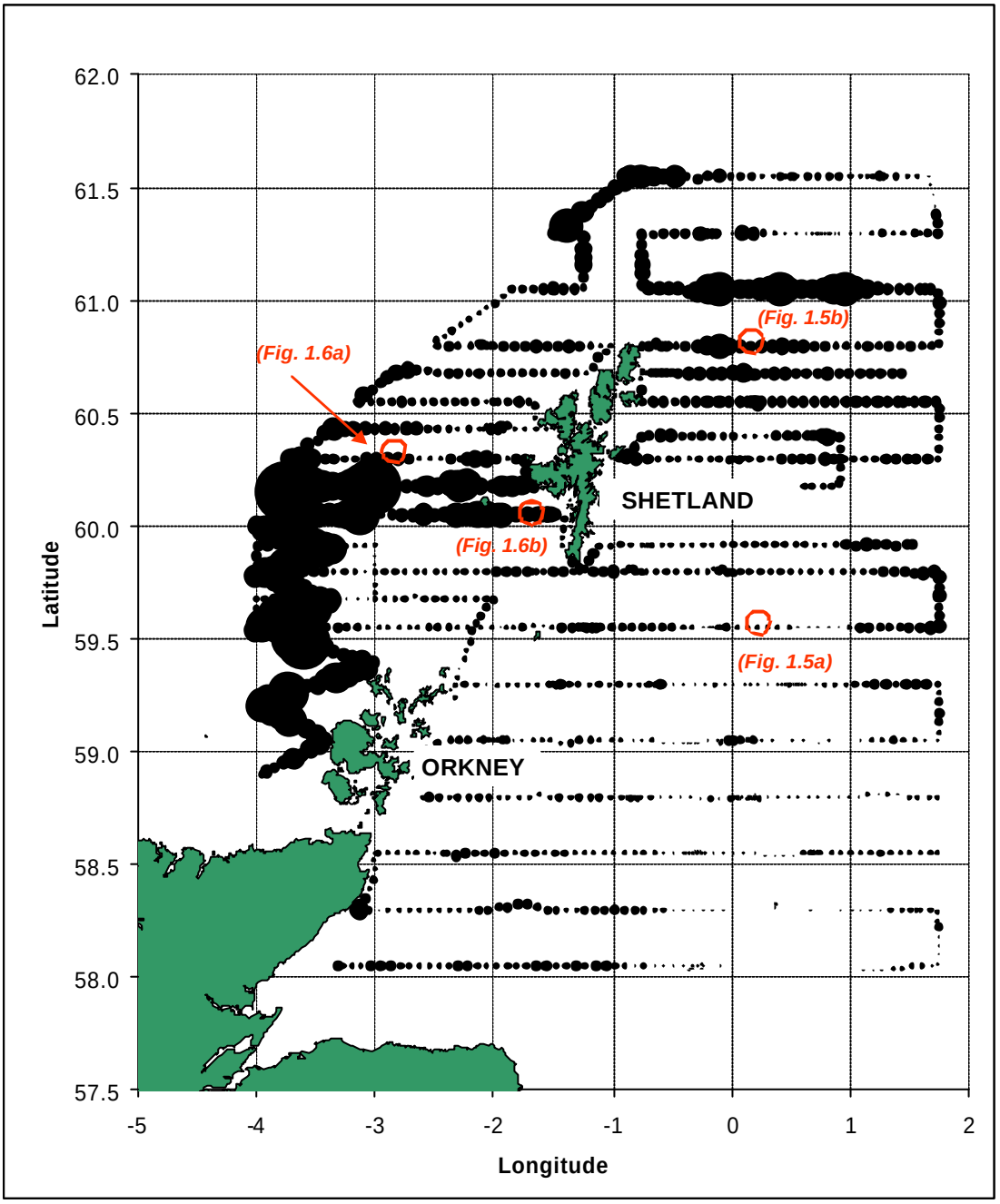

Fig 1.4: Relative acoustic density of the strong 38 kHz scattering layer in July 2003, indicated by black circles of varying sizes along the cruise track. Areas where stronger scattering was recorded are indicated by larger circles. Data were recorded during the North Sea Herring Survey, cruise 1003s. Red outline circles indicate approximate positions of the four sample echograms shown in Fig. 1.5 and Fig. 1.6, with a legend at each showing to which it refers..

a.

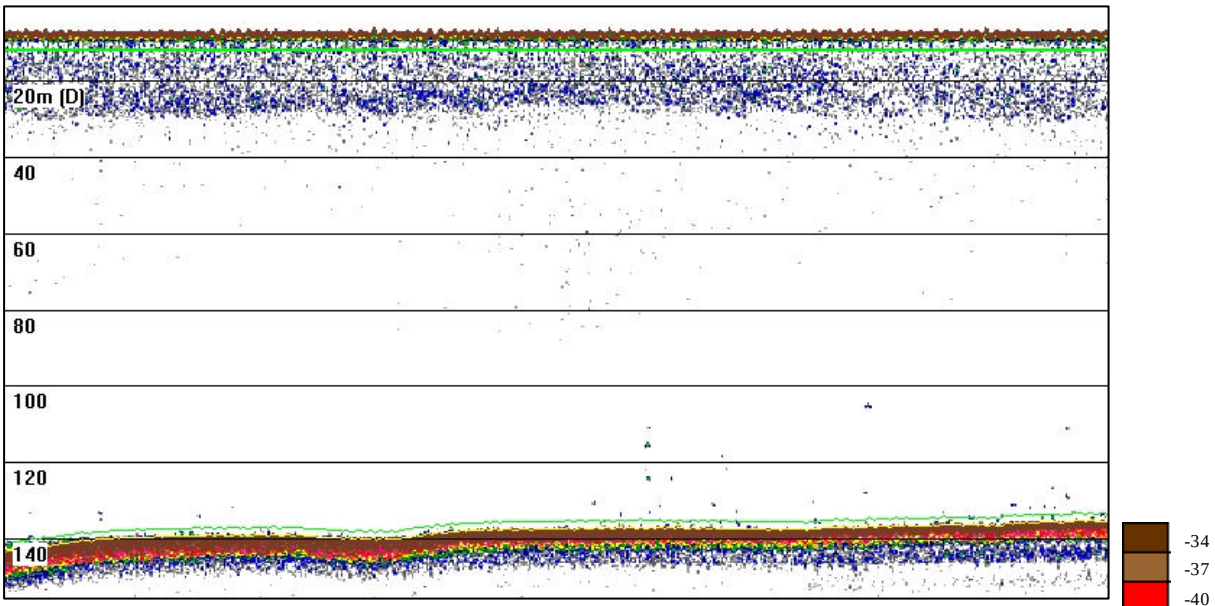

b.

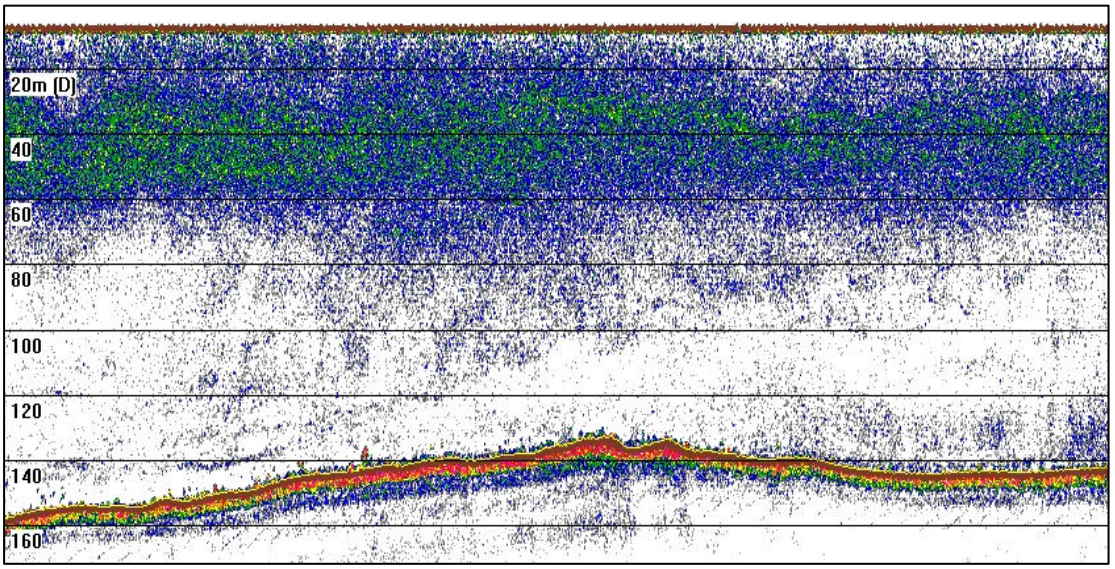

Fig 1.5: Example echograms showing variety in the strong 38 kHz layer as observed in July 2003. Water depth is shown down the y-axis of each. Water depth is displayed on the left of each echogram. Backscatter intensity (S_v) is shown by use of colour, with the legend showing decibel (dB) values (in 3 dB steps) for each colour used in the display. The strong red line near the bottom of each represents the sea-bed. These echograms were recorded at a ship speed of approximately 10 knots.

***a.** Start 2151 GMT, 59°17.96N, 0°11.06E, ship's heading 269°*
***b.** Start 1531 GMT, 60°48.08N , 0°02.02E, ship's heading 269°*

a.

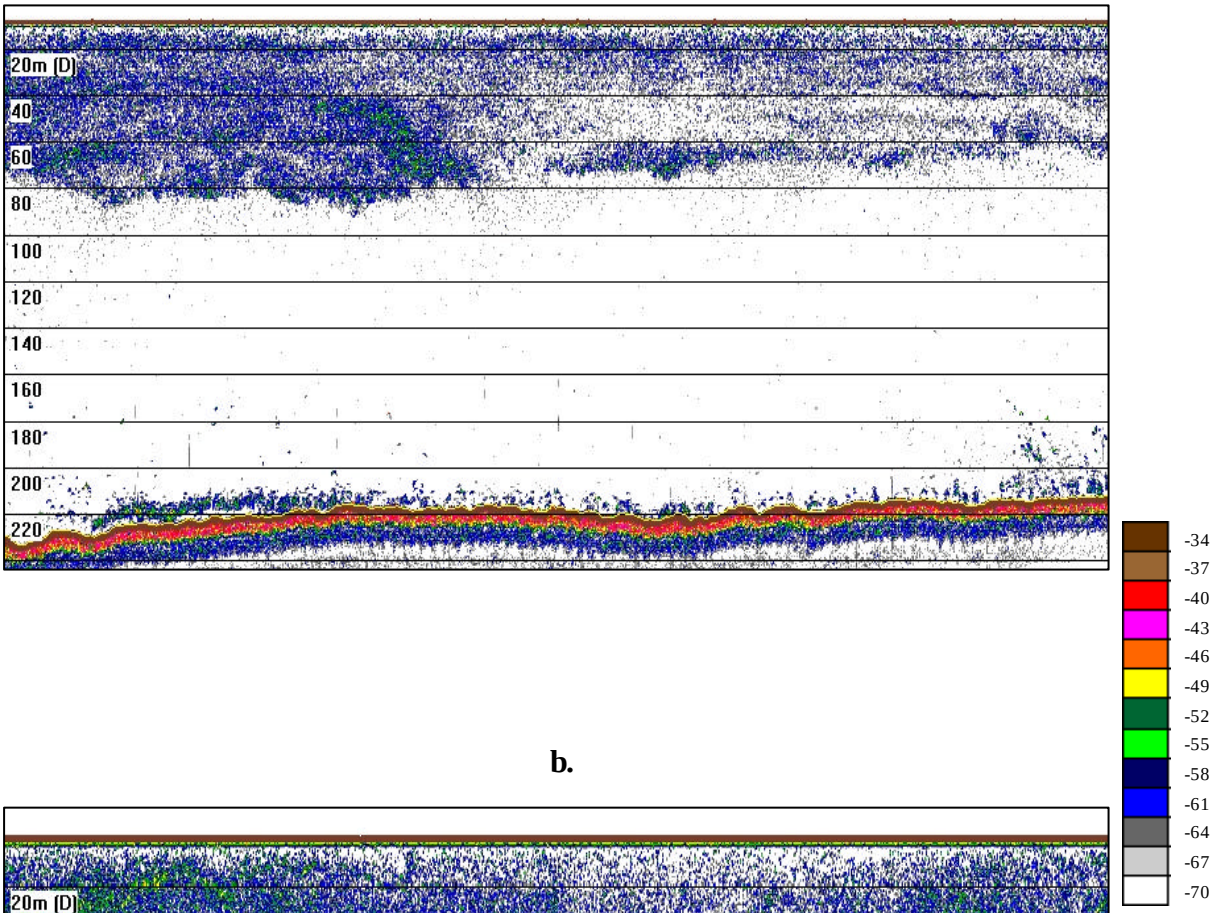

b.

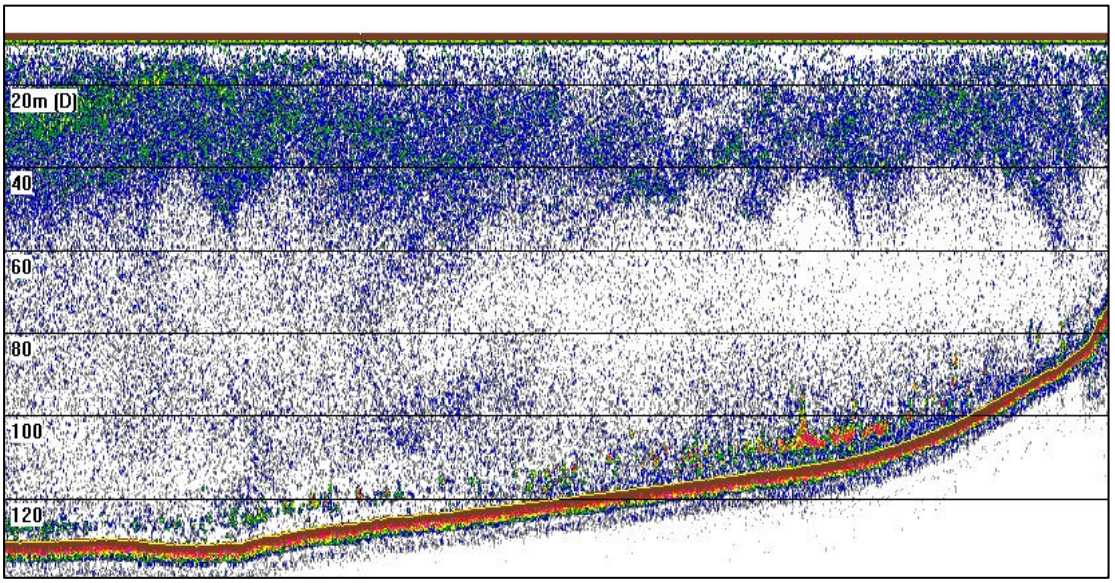

Fig 1.6: Example echograms showing variety in the strong 38 kHz layer as observed in July 2003. Water depth is shown down the y-axis of each. Water depth is displayed on the left of each echogram. Backscatter intensity (S_v) is shown by use of colour, with the legend showing decibel (dB) values (in 3 dB steps) for each colour used in the display. The strong red line near the bottom of each represents the sea-bed. These echograms were recorded at a ship speed of approximately 10 knots.

a. *Start 1859 GMT, 60°33.10N, 3°05.30W, ship's heading 95°*
b. *Start 0458 GMT, 60°02.99N, 1°30.90W, ship's heading 92°*

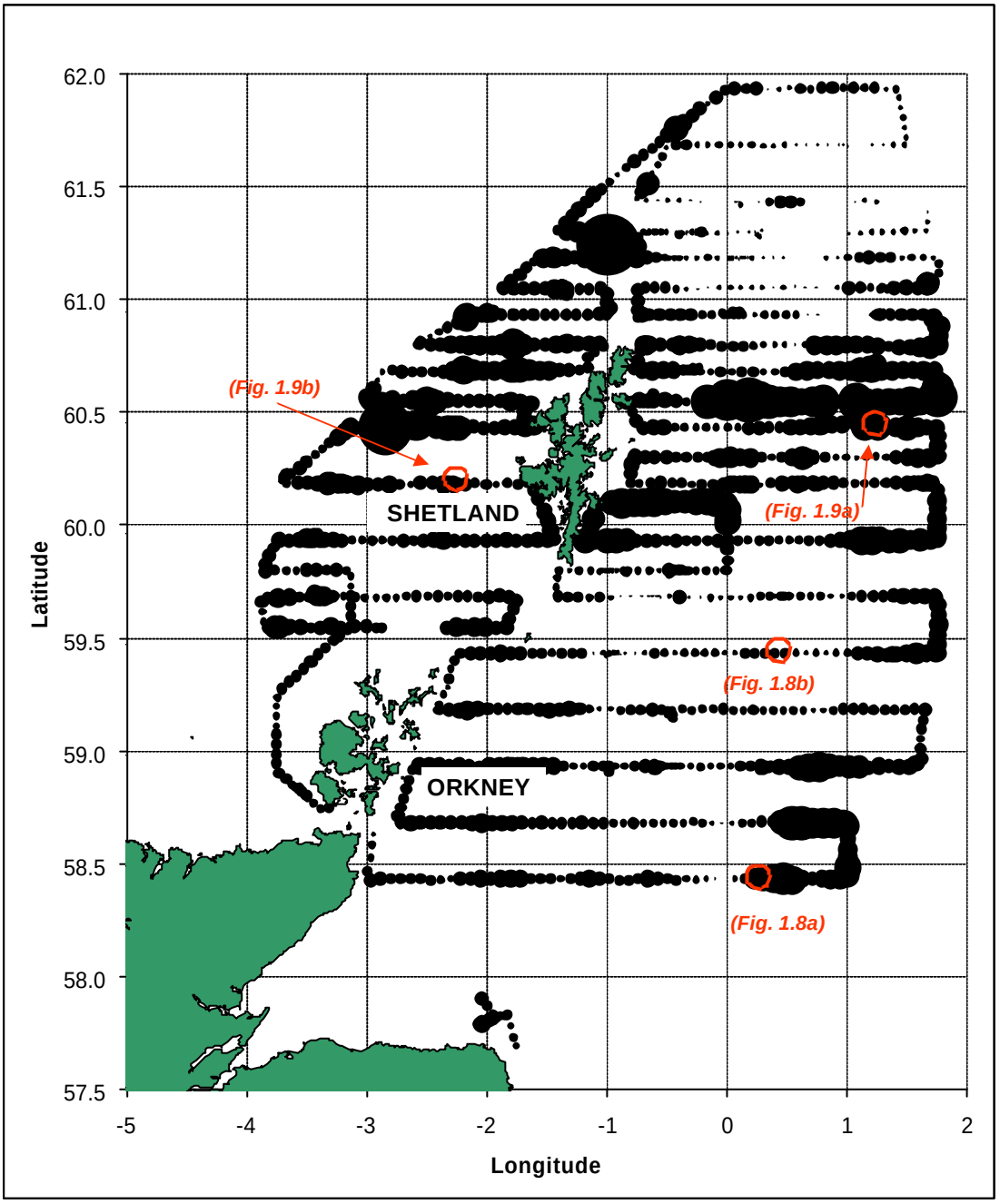

Fig 1.7: Relative acoustic density of the strong 38 kHz scattering layer in July 2004, indicated by black circles of varying sizes along the cruise track. Areas where stronger scattering was recorded are indicated by larger circles. Data were recorded during the North Sea Herring Survey, cruise 1004s. Red outline circles indicate approximate positions of the four sample echograms shown in Fig. 1.8 and Fig. 1.9.

a.

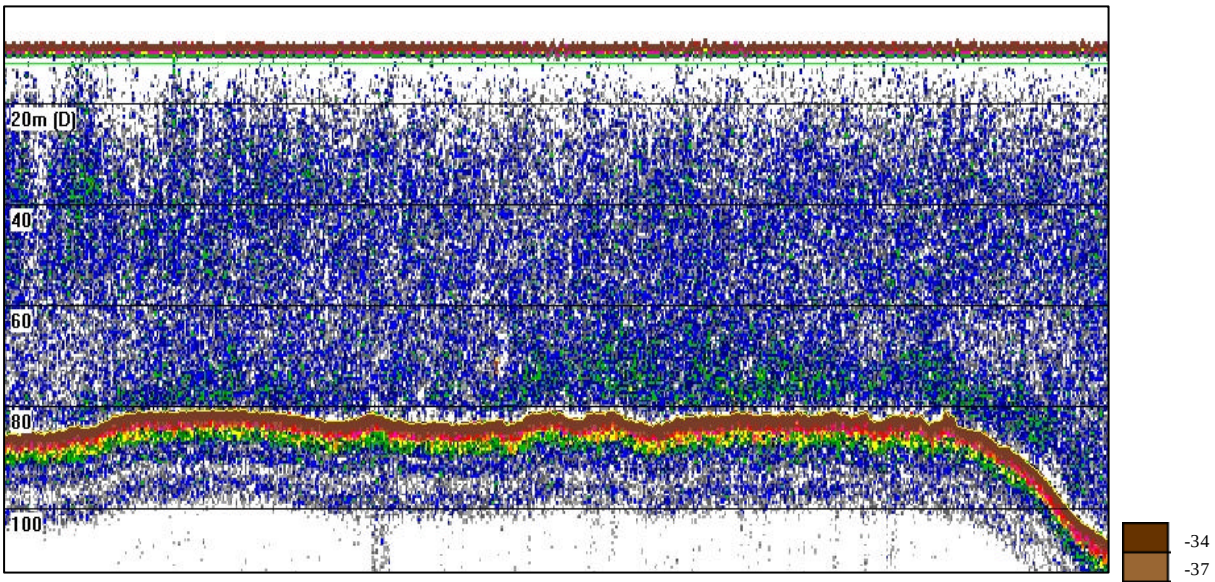

b.

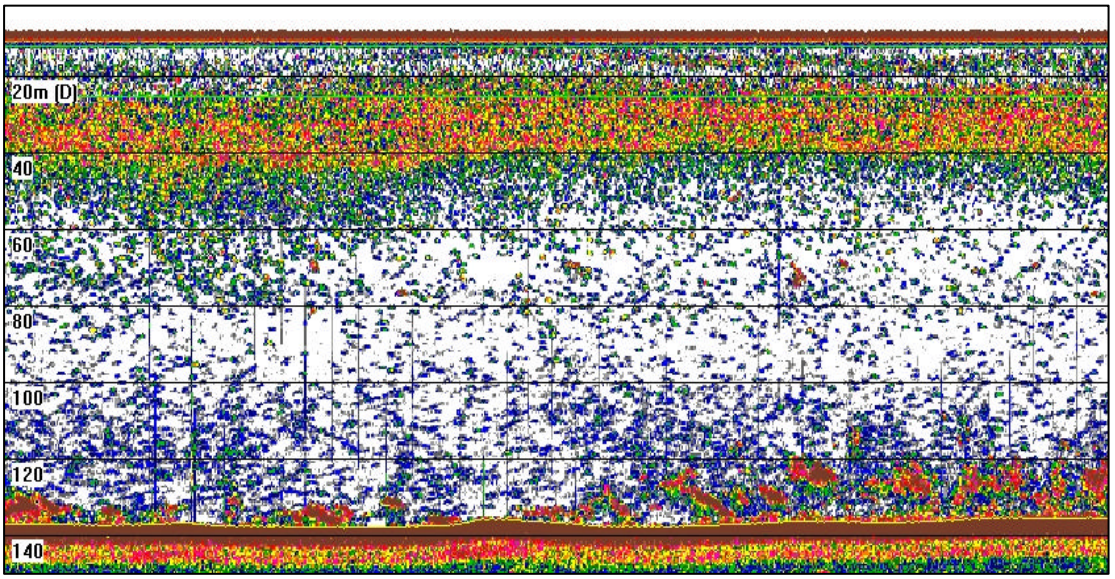

Fig 1.8: Example echograms showing variety in the strong 38 kHz layer as observed in July 2003. Water depth is shown down the y-axis of each. Water depth is displayed on the left of each echogram. Backscatter intensity (S_v) is shown by use of colour, with the legend showing decibel (dB) values (in 3 dB steps) for each colour used in the display. The strong red line near the bottom of each represents the sea-bed. These echograms were recorded at a ship speed of approximately 4 knots.

***a.** Start 0953 GMT, 58°55.79N, 0°17.46E, ship's heading 97°*
***b.** Start 1454 GMT, 59°40.99N, 0°33.77W, ship's heading 274°*

a.

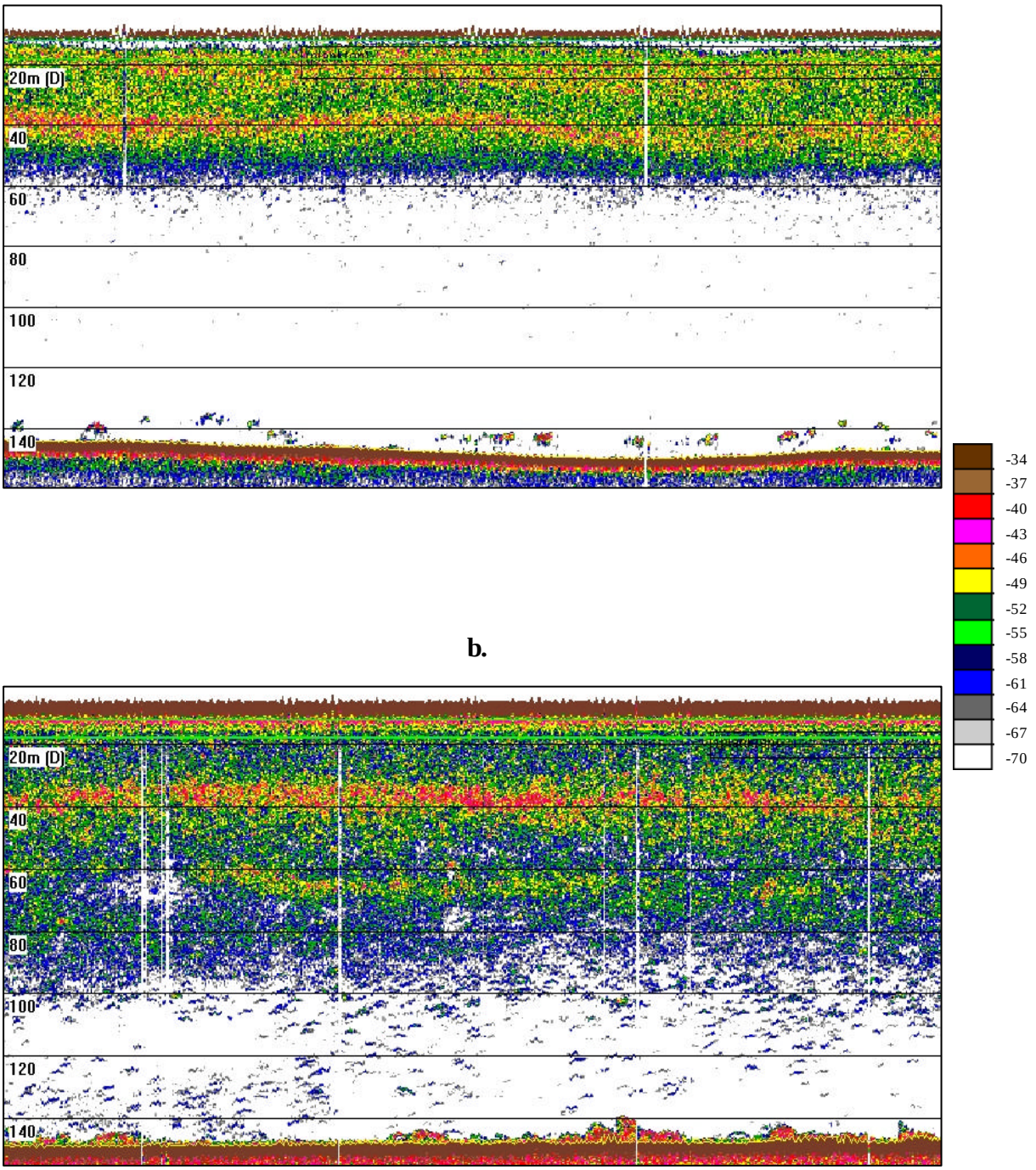

b.

Fig 1.9: Example echograms showing variety in the strong 38 kHz layer as observed in July 2003. Water depth is shown down the y-axis of each. Water depth is displayed on the left of each echogram. Backscatter intensity (S_v) is shown by use of colour, with the legend showing decibel (dB) values (in 3 dB steps) for each colour used in the display. The strong red line near the bottom of each represents the sea-bed. These echograms were recorded at a ship speed of approximately 4 knots.

***a.** Start 1306 GMT, 60°41.76N, 1°13.22E, ship's heading 37°*
***b.** Start 1615 GMT, 60°25.88N, 2°13.90W, ship's heading 175°*

(NASC) (m^2nm^{-2}) values at 7.5 minute intervals, giving an average acoustic density for the layer for each interval, and the whole process repeated for each day of the cruises.

Average acoustic density data thus obtained were plotted according to the longitude and latitude of each value, giving a graphical representation of the variability in acoustic density of the layer along the cruise tracks.

In 2003, the layer showed distinct regional differences (Fig 1.4), although it should be borne in mind that there was a time of approximately two weeks between the start and end points as was the case in 2004. Over the course of the 2003 cruise, live-viewing echograms of the layer showed many variations in consistency, depth range and acoustic density. From the start of the cruise track in the Moray Firth relatively low acoustic density was recorded (see also Fig 1.5a). An increase is evident as the ship proceeded northwards until an area of relatively high acoustic density was encountered along a single transect at approximately 61° N, to the east of the tip of Shetland (see also Fig 1.5b). Further north, as the ship headed west past 1°W, another area of high acoustic density was encountered. This decreased somewhat as the ship headed south (see also Fig 1.6a), but then increased fairly dramatically at around 60°N (see also Fig 1.6b). This area of high acoustic density appears to have been sustained almost until the ship approached the Scottish mainland near Scrabster.

Variation in acoustic density was again found in 2004 (Fig 1.7). However, the very low values recorded in the open North Sea in 2003 were not repeated (e.g. Fig 1.8a). Instead, there appears to be a slight overall increase across the whole cruise track. Live-viewing echograms displayed different characteristics at similar locations the previous year (Fig 1.8b, *cf.* Fig 1.5a). As in 2003 there is an increase to the east of Shetland, although in 2004 this is displayed slightly further south and more extensively, around 60°30N (Fig 1.9a). Following a drop in acoustic density, a similar increase is again seen as the track moves to the west of 0° longitude. There is an extensive area of high acoustic density to the north and west of Shetland, but the area thus characterised in 2003 does not display similar densities in 2004 (Fig 1.9b). Along its western edge, the cruise track followed the 200 m depth contour in each year. It is possible that some manner of geophysical process, for example upwelling of nutrients along the edge of the continental shelf, varied year-on-year causing this geographical shift in the acoustic density of the layer.

Geographic variation in acoustic density seen in 2003 and 2004, with some areas exhibiting much higher densities than others (Fig 1.4, Fig 1.7), plus differences in the morphology of the layer (e.g. Fig 1.5, Fig 1.6. Fig 1.8, Fig 1.9) suggest that its composition is not consistent across the whole of the area covered by these cruises - that is, the population composition of responsible 38 kHz scatterers varies in type and abundance in different areas. Further examples of echograms from the cruises in 2003 and 2004 can be found in Chapters 3 and 4 respectively.

Aim of this project

The goal of this project was to identify as far as possible the composition of an enhanced 38 kHz scattering layer commonly seen in the North Sea, using a combination of biological sampling and acoustic data recorded using multifrequency echosounders.

Summary of objectives and approach

The basis for this project was that ground-truthing of scattering layers be reliable. That is, the type of acoustic scatterers present in the layer needed to be sampled comprehensively. Since the scattering layer in question was thought to comprise of zooplankton, the initial objective was to identify and deploy a suitable zooplankton sampler. This objective was met by trialling a U-tow vehicle in spring 2003 (Chapter 2) and deploying it to collect biological samples in summer 2003 (Chapter 3). As a result of the analysis of acoustic and biological data collected in 2003, it became necessary to identify and deploy a sampler which was capable of catching larger and perhaps more mobile organisms, in particular juvenile fish. This was done in summer 2004, with a Methot Isaacs-Kidd Trawl (MIKT) net (Chapter 4).

Use of a new Matlab routine which implements the inverse problem using previously collected acoustic data was necessary for this study. A visit was made to IRD in Brest, France, in order to help with the testing and verification of such a routine, and contact was maintained throughout this study. IRD were supplied with acoustic data and the results of biological analysis of samples gathered during the two summer cruises mentioned above. Part of the author's role involved working in collaboration with IRD to improve extant inverse modelling procedures in order that their output better reflected the species composition biologically sampled. Finished code was then supplied by IRD, and was used in this study (Chapters 3 and 4). Work on improving this inverse modelling procedure is ongoing at the time of writing.

Chapter 2

General Methods

Plankton sampling trials

In order to attempt to identify the cause of scattering seen on echograms, biological sampling was a requirement of this study. Biological samples, generally used to ground-truth echograms in this context, require an appropriate sampler to be towed at the identified depth to sample the zooplankton community. Samples are then analysed with a view to finding what was responsible for scattering seen on echograms.

The main sampling vehicle requirement was that it should not interfere with other ship activities. The sampler also needed to be reasonably straightforward to operate, thus saving on manpower, and it needed to be reliable in that it sampled effectively in the expected size range of scatterering targets. Initially, this meant that a sampler had to be found which would reliably sample zooplankton with a typical size range of approximately 0.2 to 5 mm. This size range would be expected to include copepods, small crustaceans, gastropods etc.

The Auto-Recording Instrumented Environmental Sampler (ARIES) (Fig. 2.1a) has long been considered a reliable sampling platform. However, it is relatively large, contains sophisticated systems which require specialist knowledge, and deployment can only take place at ship speeds of 3-4 knots. Because normal survey speed is 10 knots, and data collection for this project was scheduled to take place during such a survey, ARIES itself could not be used as it would encroach on ship's time and require manpower beyond that available.

With this in mind, it was decided that if another, simpler candidate vehicle collected samples which reflected a similar species composition to those collected by ARIES, then it would be used on the scheduled data collection cruise to provide a biological dataset for this study.

The Undulating Towed Vehicle (U-tow) (Fig. 2.1b) was identified as potentially suitable, and trials were performed in March 2003 where its performance was compared directly with that of an ARIES sampling vehicle. The U-tow has previously been shown to sample zooplankton communities effectively when compared to a WP2 net (Cook and Hays, 2001). The WP2 net is a commonly used plankton sampling device, taking the form of a ring-net.

ARIES collects plankton samples in small individual cod-end bags which are spooled on at

Fig. 2.1: a. The U-tow (left) and b. ARIES (right) sampling vehicles (not to scale).

set intervals (Fig. 2.2). This means that each sample is readily separable, and identifiable from data collected during the tow. U-tow, on the other hand, is a small vehicle which utilises a plankton sampling mechanism (PSM) similar to that found in the Longhurst-Hardy Plankton Recorder (LHPR) (Fig. 2.2). That mechanism employs two rollers holding 200 micron mesh. Seawater is directed between the meshes, which are wound onto a take-up spool at pre-set intervals. By noting the exact time when the take-up spool operates prior to deployment, and with knowledge of the pre-set interval and the length of mesh wound on each time, samples can be identified and separated following recovery of the vehicle. Fig. 2.3 shows ARIES and U-tow side by side in order to give an appreciation of relative vehicle size.

U-tow does not contain the sophisticated systems employed by ARIES, and so data

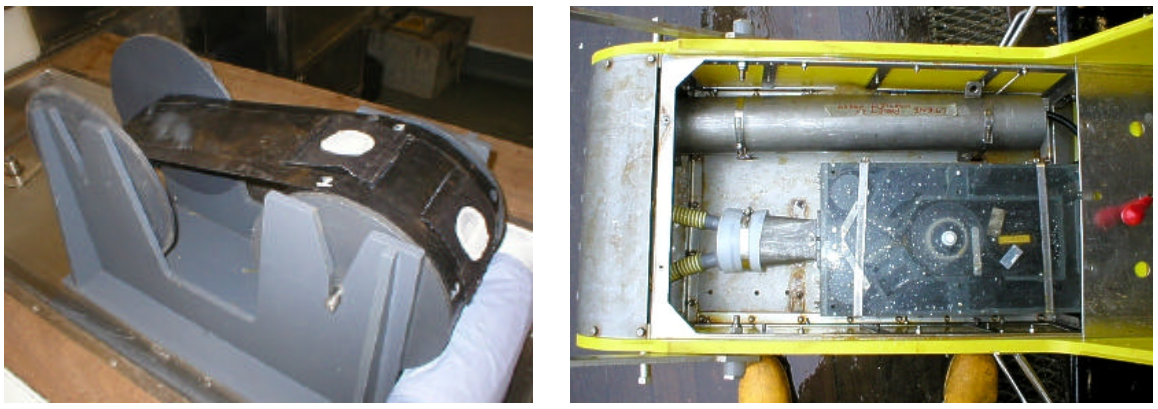

Fig. 2.2: The plankton sampling mechanisms used in ARIES (left) and U-tow (right). ARIES samples are collected in separate cod-end bags attached to a belt which is wound on at specified intervals or depths, whilst U-tow's mechanism uses two continuous rolls of mesh between which animals are trapped before being wound onto a collection roller at specified intervals.

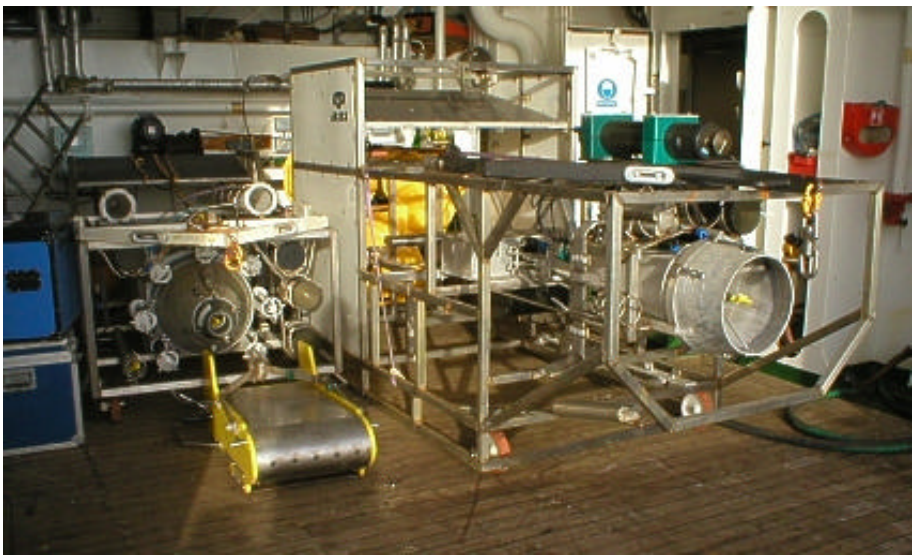

Fig 2.3: Sampling vehicles on the side-deck of FRV Scotia. On the right is the ARIES vehicle, with the U-tow on the left. Behind the U-tow is an OCEAN sampler, which was not used in this study.

concerning each tow must be logged manually.

Despite this study being concerned with acoustic methodology, data from FRV Scotia's echosounder systems was not considered during these initial sampler trials. The objective was simply to find whether the U-tow could be used as a reliable sampling vehicle.

Trial methods for plankton nets

Testing of the U-tow vehicle took place in the North Sea in March 2003 on FRV Scotia as part of the annual trials cruise. This cruise period is used to test a variety of new equipment and procedures which may then be used in later operations. Due to the need to maximise the use of ship time for a variety of tasks, there was limited time available to verify the effectiveness of U-tow.

Fig. 2.4: Deployment of U-tow from the side-deck of FRV Scotia using the plankton crane.

Fig. 2.5: Mesh removed from the PSM installed in U-tow following a sampling run. On the lower right of the picture are the two rollers which hold unused mesh, while at the top left is the collection roller. Individual samples, collected during specified periods, can be identified on the mesh by a "striping" effect.

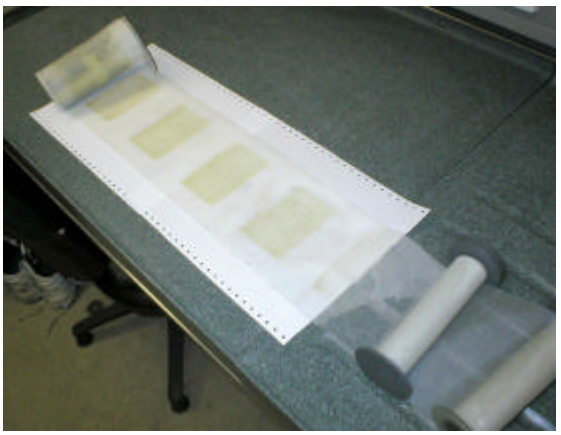

Plankton sampling operations were carried out over a two day period, which included familiarisation with operational procedures and ensuring that the U-tow, which had been in storage for some time, functioned as expected. Both the U-tow and ARIES were deployed from the side-deck of FRV Scotia, using a remotely operated crane (Fig 2.4). Live-viewing echograms were observed on board the ship, and the samplers deployed through strong 38 kHz layers.

On the first day of operations, ARIES and U-tow were deployed at the same position at various depths through the water column, one immediately after the other in order to be directed through as similar a plankton community as possible. By controlling the wire paid out, the vehicles were made to sample as close to horizontally as possible at the required

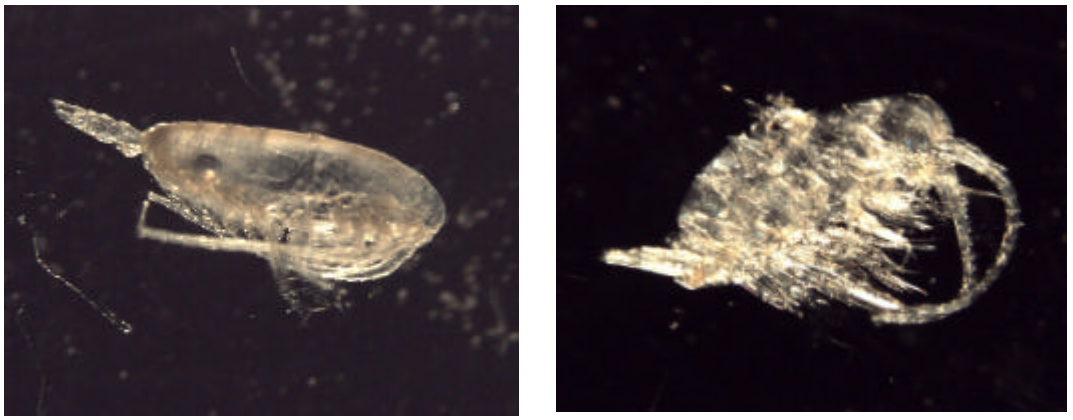

Fig. 2.6: C6 stage (adult) female Calanus finmarchicus copepods as found in samples from ARIES (left) and U-tow (right). The cod-end method of sample collection employed by ARIES allows animals to be well preserved, whilst the PSM installed in U-tow commonly distorts body shape by compressing animals between two meshes. This potentially presents identification problems during taxonomic analysis of U-tow samples. Time required for analysis is also increased.

depth. Calibrated depth sensor units (SCANMAR HC4-D: Scanmar AS, Åsgårdstrand, Norway) attached to the U-tow and ARIES operated during each deployment, enabling sampling depth to be determined to within 0.1 m at one-minute (300 m at 10 knots) intervals. The internal mechanism of each vehicle was set to sample at two minute intervals so that samples would be comparable. Tow durations were 30 minutes.

In order to simulate actual sampling conditions, U-tow was towed at normal survey speed of 10 knots, whilst ARIES was towed at its optimum operating speed of 3-4 knots. It would have been possible to tow U-tow at a similar speed to ARIES, but it was felt that this would not reflect the operating conditions under which it would be deployed on cruises where it was to be actively used for sample collection.

Indeed, there are fundamental differences between ARIES and U-tow, both physically and in the sampling methods employed. Aside from the physical size of each sampler, the sampling apertures are of considerably different diameters (U-tow = 18 mm, ARIES = 370 mm). The method of sample collection is also different, with ARIES employing a wind-on system whereby a new cod-end is moved into position for each discrete sample, whilst U-tow makes use of a plankton sampling mechanism (PSM) similar to that of a Longhurst-Hardy Plankton Recorder (LHPR). This consists of a pair of continuous 200 µm meshes being wound onto a collection roller at intervals, trapping any plankton between. Discrete samples can be identified by a "striping" effect on the meshes (Fig. 2.5). These differing sampling techniques result in varying degrees of preservation of animals, with ARIES-sampled animals being much easier to identify because they tend not to be so damaged in the mechanism (Fig. 2.6). Such differences should, however, become irrelevant if it could be shown that samples from each were similar in species composition.

On the first day of sampling, gear and deployment problems were encountered. Nevertheless, four reliable and comparable samples were recovered from each vehicle – two each at approximately 25 m and 75 m depth.

The second day of sampling yielded similar numbers of broadly comparable samples, although depths varied slightly. U-tow samples taken at 25, 40 and 60 m were compared with ARIES samples from the same area taken collected at 15, 29-48 and 70 m. Due to

procedural difficulties outlined above, it was not possible to replicate sampling runs. In Despite the apparent incompatibility of sampling depths, observation of live-viewing echograms showed that samples were taken from the same continuous scattering layer, that is in areas of scattering which had similar properties, and were thus felt to be suitable for comparison.

Samples were preserved in 4% formalin, and transported back for analysis in the laboratory.

Animals found in samples were identified in the laboratory using a binocular microscope, with copepods being separated into the following classes according to type, developmental stage and size: *Calanus finmarchicus* C6 stage adult male/female, copepodite stage 5 (C5), *C. finmarchicus* C1-C4, Calanoid nauplius, Other C6 > 1.2 mm, Other C6 < 1.2 mm, Other calanoid C1-C5 > 1.2 mm, Other calanoid C1-C5 < 1.2 mm, *Oithona spp*., Cyclopoid copepods, and Harpacticoid copepods. These categories were then added to give categories for *Copepods > 1.2 mm* and *Copepods < 1.2 mm*. Euphausiids were separated into adult, juvenile, furcilia, calyptopis and naupliar stages. Other categories included Cirripedia nauplius, Cirripedia cyprid, Decapoda juvenile, Chaetognatha, Fish larvae, Fish egg, Echinodermata larvae and hard-shelled mollusca.

The abundance of different categories of animals in each sample was calculated by dividing the number of animals in a given category and sample by the volume of water filtered for that sample. Filtered water volume was calculated as a cylinder, with the dimensions being the sampling aperture area (U-tow = 0.0005 m^2, ARIES = 0.43 m^2) and distance travelled during the sampling interval (for each two minute interval, U-tow = 617 m, ARIES = 247 m). Regression analysis was performed on animal type abundances in samples collected by U-tow and ARIES from the same layer in order to assess the similarity of species composition in samples collected by the two vehicles.

The total number of individual animals and the percentage of this total contributed by each animal type was also calculated for directly comparable U-tow and ARIES samples. These percentage values for each sampler were plotted against each other in order to provide a quick visual comparison of whether there was a similarity in species composition.

ARIES/Utow	UTOW	UTOW	UTOW	UTOW	ARIES	ARIES	ARIES	ARIES	UTOW	UTOW	UTOW	UTOW	UTOW	ARIES	ARIES	ARIES
Haul Number	09	09	09	09	10	10	10	10	12	12	12	12	12	11	11	11
Sample Number	001	002	003	004	006	007	041	056	01	02	03	04	05	005	006	014
Date sampled	010403	010403	010403	010403	010403	010403	010403	010403	020403	020403	020403	020403	020403	020403	020403	020403
Depth open (m)	25	25	75	75	19.5	23.8	70.6	74.8	25	25	60	60	40	15.3	28.9	70.6
Depth closed (m)	25	25	75	75	23.8	21.2	74.0	68.0	25	25	60	60	40	28.9	48.5	0
Calanus finmarchicus																
C6 F			1	1	3	1	5	1	3	4	1	2	2	22	105	270
C6 M							2						1	1		
C5		6	3	6	6	10	12		1		1	1	2	39	241	360
C1-C4	1	9	14	20	28	37	210	105	28	7	12	20	13	83	225	1920
Total C. finm. C5-C6		6	4	7	9	11	19	1	4	4	2	3	5	62	346	630
Total c. finmarchicus	1	15	18	27	37	48	229	106	32	11	14	23	18	145	571	2550
Calanoid nauplius			2	3		1	45	105	15	12	60	56	76	3	15	150
Other calanoid copepod																
C6 large >1.2mm		1	1	1	6	9	60	2	2	1	2	1		4	15	120
C6 small <1.2mm		2	5	4	16	6	30	30	2				1	7	30	150
C1-C5 large >1.2mm			1	1	3	14	15				1	2	1	14	105	240
C1-C5small <1.2mm	4	7	22	19	11	11	210	195	1		2	1		11	45	90
Total others >1.2mm		1	2	2	9	23	75	2	2	1	3	3	1	18	120	360
Total others<1.2mm	4	9	27	23	27	17	240	225	3		2	1	1	18	75	240
Total calanoids >1.2mm		7	6	9	18	34	94	3	6	5	5	6	6	80	466	990
Total calanoids <1.2mm	5	18	41	43	55	54	450	330	31	7	14	21	14	101	300	2160
Cyclopoid copepod	1	1					15				4	3	5	6		
Oithona spp.	1	2	2	2	4	6	30	15							15	
Harpacticoid copepod				1					1							30
Total copepod	7	28	49	55	77	94	589	348	38	12	23	30	25	187	781	3180
Cladocera - Evadne	2	8	6	1	1	13	120	240						49		150
Cirrepedia nauplii	1	27	27	35	9	39	975	255	19	10	10	17	5	8		5010
Cirrepedia cyprid	1	6	4		1	8			3	2	2	1		5		360
Euphausiid																
adult				1			1		1							
juvenile			1		1	1	1							1		3
furcilia			3		6	9	1	3	1					3		7
calyptopis			8	4	3	5	16	18	2					5		
nauplius				1		2				1	4	4		1		
Decapoda spp. juvenile	1			2		3	2	2		1				2		1
Amphipoda spp.													1	2		2
Polychaeta spp. juvenile			2	1	1	2		3			1					
Chaetognatha spp.		1	1		1	2		1			1	2	2			3
Fish Larvae spp.	2	9	2	5	1		7	8	3	1			2	1		9
Fish egg spp.			1		2		1									6
Echinoderm spp. larvae	3	11	8	1	4	4		1			2	1	1	44		
Mollusca spp.							1		1	2	3	1	1			3
TOTAL ANIMALS	**17**	**90**	**114**	**109**	**107**	**183**	**1759**	**984**	**68**	**29**	**46**	**56**	**37**	**308**	**781**	**8734**

Table 2.1: Numbers of animals found in samples from ARIES and U-tow vehicles in the North Sea in March 2003. Four comparable samples were obtained from each vehicle on the first day of sampling, with five U-tow and three ARIES samples obtained on the second day. Total animal numbers in each sample are shown at the end of each column.

ARIES/Utow	UTOW	UTOW	UTOW	UTOW	ARIES	ARIES	ARIES	ARIES	UTOW	UTOW	UTOW	UTOW	UTOW	*UTOW*	ARIES	ARIES	ARIES
Haul Number	09	09	09	09	10	10	10	10	12	12	12	12	12	*12*	11	11	11
Sample Number	001	002	003	004	006	007	041	056	01	02	03	04	05	*03-05*	005	006	014
Water volume filtered	8.6	8.6	8.6	8.6	106.2	106.2	106.2	106.2	8.6	8.6	8.6	8.6	8.6	*8.6*	106.2	106.2	106.2
Depth open (m)	25	25	75	75	19.5	23.8	70.6	74.8	25	25	60	60	40	*40-60*	15.3	28.9	70.6
Calanus finmarchicus																	
C6 F			1.2E-01	1.2E-01	2.8E-02	9.4E-03	4.7E-02	9.4E-03	3.5E-01	4.6E-01	1.2E-01	2.3E-01	2.3E-01	*1.9E-01*	2.1E-01	9.9E-01	2.5E+00
C6 M							1.9E-02						1.2E-01	*3.9E-02*	9.4E-03		
C5		6.9E-01	3.5E-01	6.9E-01	5.6E-02	9.4E-02	1.1E-01		1.2E-01		1.2E-01	1.2E-01	2.3E-01	*1.5E-01*	3.7E-01	2.3E+00	3.4E+00
C1-C4	1.2E-01	1.0E+00	1.6E+00	2.3E+00	2.6E-01	3.5E-01	2.0E+00	9.9E-01	3.2E+00	8.1E-01	1.4E+00	2.3E+00	1.5E+00	*1.7E+00*	7.8E-01	2.1E+00	1.8E+01
Total C. finm. C5-C6		6.9E-01	4.6E-01	8.1E-01	8.5E-02	1.0E-01	1.8E-01	9.4E-03	4.6E-01	4.6E-01	2.3E-01	3.5E-01	5.8E-01	*3.9E-01*	5.8E-01	3.3E+00	5.9E+00
Total c. finmarchicus	1.2E-01	1.7E+00	2.1E+00	3.1E+00	3.5E-01	4.5E-01	2.2E+00	1.0E+00	3.7E+00	1.3E+00	1.6E+00	2.7E+00	2.1E+00	*2.1E+00*	1.4E+00	5.4E+00	2.4E+01
Calanoid nauplius			2.3E-01	3.5E-01		9.4E-03	4.2E-01	9.9E-01	1.7E+00	1.4E+00	6.9E+00	6.5E+00	8.8E+00	*7.4E+00*	2.8E-02	1.4E-01	1.4E+00
Other calanoid copepod																	
C6 large >1.2mm		1.2E-01	1.2E-01	1.2E-01	5.6E-02	8.5E-02	5.6E-01	1.9E-02	2.3E-01	1.2E-01	2.3E-01	1.2E-01		*1.2E-01*	3.8E-02	1.4E-01	1.1E+00
C6 small <1.2mm		2.3E-01	5.8E-01	4.6E-01	1.5E-01	5.6E-02	2.8E-01	2.8E-01	2.3E-01				1.2E-01	*3.9E-02*	6.6E-02	2.8E-01	1.4E+00
C1-C5 large >1.2mm			1.2E-01	1.2E-01	2.8E-02	1.3E-01	1.4E-01				1.2E-01	2.3E-01	1.2E-01	*1.5E-01*	1.3E-01	9.9E-01	2.3E+00
C1-C5small <1.2mm	4.6E-01	8.1E-01	2.5E+00	2.2E+00	1.0E-01	1.0E-01	2.0E+00	1.8E+00	1.2E-01		2.3E-01	1.2E-01		*1.2E-01*	1.0E-01	4.2E-01	8.5E-01
Total others >1.2mm		1.2E-01	2.3E-01	2.3E-01	8.5E-02	2.2E-01	7.1E-01	1.9E-02	2.3E-01	1.2E-01	3.5E-01	3.5E-01	1.2E-01	*2.7E-01*	1.7E-01	1.1E+00	3.4E+00
Total others<1.2mm	4.6E-01	1.0E+00	3.1E+00	2.7E+00	2.5E-01	1.6E-01	2.3E+00	2.1E+00	3.5E-01		2.3E-01	1.2E-01	1.2E-01	*1.5E-01*	1.7E-01	7.1E-01	2.3E+00
Total calanoids >1.2mm		8.1E-01	6.9E-01	1.0E+00	1.7E-01	3.2E-01	8.9E-01	2.8E-02	6.9E-01	5.8E-01	5.8E-01	6.9E-01	6.9E-01	*6.6E-01*	7.5E-01	4.4E+00	9.3E+00
Total calanoids <1.2mm	5.8E-01	2.1E+00	4.7E+00	5.0E+00	5.2E-01	5.1E-01	4.2E+00	3.1E+00	3.6E+00	8.1E-01	1.6E+00	2.4E+00	1.6E+00	*1.9E+00*	9.5E-01	2.8E+00	2.0E+01
Cyclopoid copepod	1.2E-01	1.2E-01					1.4E-01				4.6E-01	3.5E-01	5.8E-01	*4.6E-01*	5.6E-02		
Oithona spp.	1.2E-01	2.3E-01	2.3E-01	2.3E-01	3.8E-02	5.6E-02	2.8E-01	1.4E-01								1.4E-01	
Harpacticoid copepod				1.2E-01					1.2E-01								2.8E-01
Total copepod	8.1E-01	3.2E+00	5.7E+00	6.4E+00	7.3E-01	8.9E-01	5.5E+00	3.3E+00	4.4E+00	1.4E+00	2.7E+00	3.5E+00	2.9E+00	*3.0E+00*	1.8E+00	7.4E+00	3.0E+01
Cladocera - Evadne	2.3E-01	9.3E-01	6.9E-01	1.2E-01	9.4E-03	1.2E-01	1.1E+00	2.3E+00							4.6E-01		1.4E+00
Cirrepedia nauplii	1.2E-01	3.1E+00	3.1E+00	4.1E+00	8.5E-02	3.7E-01	9.2E+00	2.4E+00	2.2E+00	1.2E+00	1.2E+00	2.0E+00	5.8E-01	*1.2E+00*	7.5E-02		4.7E+01
Cirrepedia cyprid	1.2E-01	6.9E-01	4.6E-01		9.4E-03	7.5E-02			3.5E-01	2.3E-01	2.3E-01	1.2E-01		*1.2E-01*	4.7E-02		3.4E+00
Euphausiid																	
adult				1.2E-01			9.4E-03		1.2E-01								
juvenile			1.2E-01		9.4E-03	9.4E-03	9.4E-03								9.4E-03		2.8E-02
furcilia			3.5E-01		5.6E-02	8.5E-02	9.4E-03	2.8E-02	1.2E-01						2.8E-02		6.6E-02
calyptopis			9.3E-01	4.6E-01	2.8E-02	4.7E-02	1.5E-01	1.7E-01	2.3E-01						4.7E-02		
nauplius				1.2E-01		1.9E-02				1.2E-01	4.6E-01	4.6E-01		*3.1E-01*	9.4E-03		
Decapoda spp. juvenile	1.2E-01			2.3E-01		2.8E-02	1.9E-02	1.9E-02		1.2E-01					1.9E-02		9.4E-03
Amphipoda spp.													1.2E-01	*3.9E-02*	1.9E-02		1.9E-02
Polychaeta spp. juvenile			2.3E-01	1.2E-01	9.4E-03	1.9E-02		2.8E-02			1.2E-01			*3.9E-02*			
Chaetognatha spp.		1.2E-01	1.2E-01		9.4E-03	1.9E-02		9.4E-03			1.2E-01	2.3E-01	2.3E-01	*1.9E-01*			2.8E-02
Fish Larvae spp.	2.3E-01	1.0E+00	2.3E-01	5.8E-01	9.4E-03		6.6E-02	7.5E-02	3.5E-01	1.2E-01			2.3E-01	*7.7E-02*	9.4E-03		8.5E-02
Fish egg spp.			1.2E-01		1.9E-02		9.4E-03										5.6E-02
Echinoderm spp. larvae	3.5E-01	1.3E+00	9.3E-01	1.2E-01	3.8E-02	3.8E-02		9.4E-03			2.3E-01	1.2E-01	1.2E-01	*1.5E-01*	4.1E-01		
Mollusca spp.							9.4E-03		1.2E-01	2.3E-01	3.5E-01	1.2E-01	1.2E-01	*1.9E-01*			2.8E-02
TOTAL Abundance m3	2.0	10.4	13.2	12.6	1.0	1.7	16.6	9.3	7.9	3.4	5.3	6.5	4.3	*5.4*	2.9	7.4	82.2

Table 2.2: Abundance (number of individuals per cubic metre of water) of animals found in samples from ARIES and U-tow vehicles in the North Sea in March 2003. Water volume filtered was calculated as a cylinder, with the dimensions being the area of the sampling aperture multiplied by the distance of the tow in each case. Abundance of each type was then calculated by dividing the number of sampled individuals by this volume.

Copepod	U-Tow	ARIES
Total calanoids>1.2mm	21.29	9.34
Total calanoids<1.2mm	33.49	33.38
Cyclopoid	0.43	4.3
Oithona spp.	1.6	1.46
Harpacticoid	0.06	0.24
Euphausiid		
adult	0.01	0.24
juvenile	0.25	0.11
furcilia	1.54	0.45
calyptopis	1.3	1.58
nauplius	0.19	1.72
Other types		
Cladocera-Evadne	7.84	3.35
Cirrepedia nauplius	23.88	23.26
Cirrepedia cyprid	1.62	3.46
Decapoda juvenile	0.35	1.25
Amphipoda spp.	0.11	0.45
Polychaete juv	0.29	0.52
Chaetognatha spp.	0.27	1.63
Fish larvae spp.	0.34	5.07
Fish egg spp.	0.25	0.11
Echinoderm larvae spp.	3.13	5.69
Mollusca spp.	0.01	1.84
Total abundance m $^{-3}$	41.38	50.73

Table 2.3: Animal abundances (number of individuals of each type per cubic metre of water) totalled for all U-Tow and all ARIES hauls under consideration. Calanoid copepods of similar sizes were considered together due to their acoustic properties being similar.

Results of sampler comparison

From the first day's sampling, it was possible to directly compare two U-tow samples taken at approximately 25 m depth with two ARIES samples taken between 19.5 m and 23.8 m depth. Similarly, from the second day, two U-tow samples from 25 m, two from 60 m and one from 75 m were compared with three ARIES samples from between 15.3 m and 28.9 m, 28.9 m and 48.5 m and from 70.6 m to the surface. These were found to be the only samples which could be directly compared between the two vehicles, in that they came from similar depths of the same scattering layer and were therefore more likely to have sampled the same population.

Animals found in both sets of samples were of similar types, although ARIES samples contained animal numbers up to an order of magnitude higher than U-tow samples (Table 2.1). ARIES sample 014 contained many more animals than the "equivalent" U-tow sample,

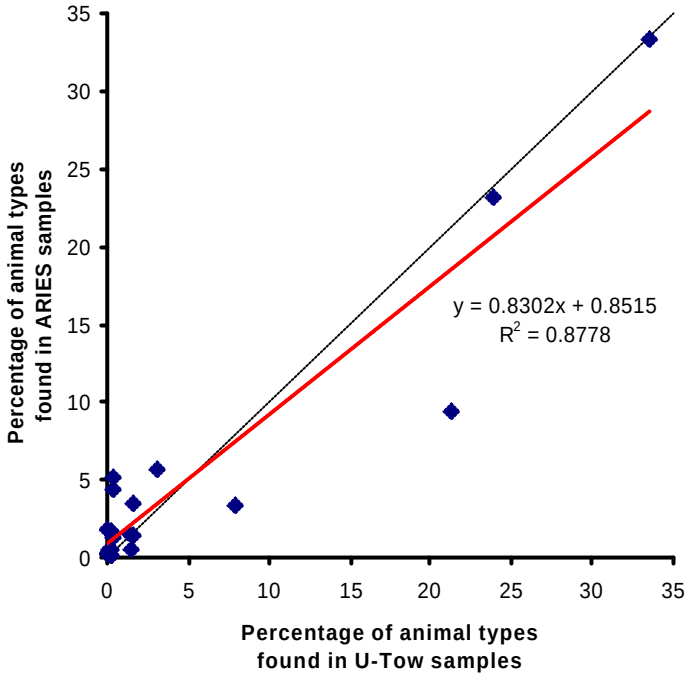

Fig 2.7: Comparison of total animal abundances (number of individuals of each type per cubic metre of water) totalled for all U-Tow and all ARIES hauls under consideration, as shown in Table 2.3. Each data point represents a different animal type. The regression line and equation are shown in red, with 1:1 relationship represented by a dotted line.

but it should be noted that this sample came from the end of a tow, where ARIES was being hauled directly to the surface thus encountering more organisms in its path. It is also the case that ARIES, with its larger sampling aperture, will filter a larger volume of water and can therefore be expected to sample more animals.

With this in mind, the abundance of each animal type in each sample was calculated according to the estimated volume of water filtered (Table 2.2). Abundance values from all U-Tow hauls and all ARIES hauls under consideration were then added together (Table 2.3), and plotted graphically (Fig. 2.7). For this purpose, all calanoid type copepods were added together to give two categories of "Calanoid copepods > 1.2 mm" and "Calanoid copepods < 1.2 mm". This grouping was considered adequate as acoustic analysis of later samples would require the consideration of such animals according to parameters such as size and general morphology which are similar across species.

	First Day		Second Day		Both Days	
	U-tow	ARIES	U-tow	ARIES	U-tow	ARIES
	4 samples	4 samples	3 samples	5 samples	7 samples	9 samples
	% of total individual animals		*% of total individual animals*		*% of total individual animals*	
Calanus finmarchicus						
C6 F	0.45	0.93	7.89	5.79	4.41	3.12
C6 M		0.03	0.11	0.90	0.07	0.45
C5	3.70	2.94	15.88	2.71	9.41	3.20
C1-C4	11.63	17.25	25.91	32.90	21.58	22.26
Total C. finm. C5-C6	4.15	3.90	23.88	9.40	13.89	6.78
Total c. finmarchicus	15.78	21.15	49.80	42.30	35.47	29.04
Calanoid nauplius	1.13	3.44			1.72	0.56
Other calanoid copepod						
C6 large >1.2mm	0.73	3.53	1.53	2.09	2.53	1.41
C6 small <1.2mm	2.57	5.75	2.61	1.39	4.18	1.98
C1-C5 large >1.2mm	0.45	2.83	6.91	1.86	4.87	1.15
C1-C5small <1.2mm	17.01	12.01	3.45	1.27	7.73	9.14
Total others >1.2mm	1.18	6.36	8.44	3.95	7.40	2.56
Total others<1.2mm	19.58	17.76	6.07	2.66	11.91	11.12
Total calanoids >1.2mm	5.33	10.26	32.33	13.35	21.29	9.34
Total calanoids <1.2mm	31.21	35.01	31.98	35.56	33.49	33.38
Cyclopoid copepod	1.75	0.21	0.65	6.85	0.43	4.30
Oithona spp.	2.92	2.56	0.64		1.60	1.46
Harpacticoid copepod	0.23		0.11	0.25	0.06	0.24
Total copepod	41.44	48.04	65.71	55.99	56.88	48.72
Cladocera - Evadne	6.71	9.81	5.88		7.84	3.35
Cirrepedia nauplii	22.92	27.77	19.99	23.59	23.88	23.26
Cirrepedia cyprid	4.01	1.33	1.92	2.91	1.62	3.46
Euphausiid						
Euphausiid adult	0.23	0.01		0.25	0.01	0.24
Euphausiid juvenile	0.22	0.38	0.12		0.25	0.11
Euphausiid furcilia	0.66	2.72	0.35	0.25	1.54	0.45
Euphausiid calyptopis	2.67	2.07	0.54	0.49	1.30	1.58
Euphausiid nauplius	0.23	0.27	0.11	3.21	0.19	1.72
Decapoda spp. juvenile	1.93	0.49	0.22	0.57	0.35	1.25
Amphipoda spp.			0.22	0.90	0.11	0.45
Polychaeta spp. juvenile	0.67	0.58		0.36	0.29	0.52
Chaetognatha spp.	0.50	0.53	0.01	2.76	0.27	1.63
Fish Larvae spp.	7.03	0.54	0.14	3.11	0.34	5.07
Fish egg spp.	0.22	0.48	0.02		0.25	0.11
Echinoderm spp. larvae	9.45	1.51	4.76	1.92	3.13	5.69
Mollusca spp.		0.01	0.01	3.68	0.01	1.84
TOTAL PERCENTAGE	100	100	100	100	100	100

Table 2.5: Percentages of total number of animals found in samples from ARIES and U-tow vehicles in the North Sea in March 2003. Four comparable samples were obtained from each vehicle on the first day of sampling, with five U-tow and three ARIES samples obtained on the second day. Total animal numbers in each sample are shown at the end of each column.

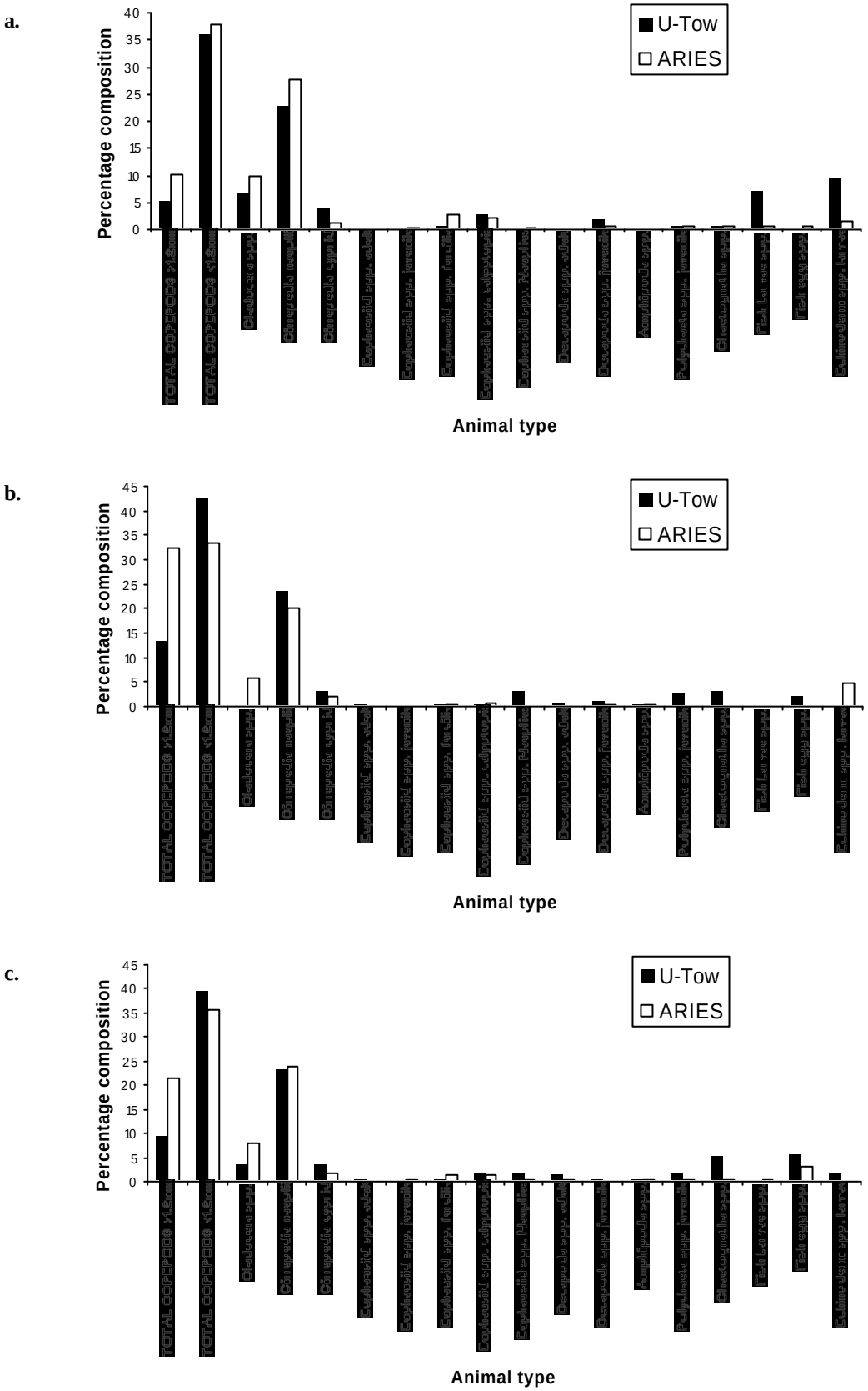

Fig. 2.8: Sample species compositions expressed as a percentage of total animal numbers in samples recovered from U-tow and ARIES vehicles in North Sea trials in March 2003. a. Day one samples, b. Day two samples, and c. Average over both days.

The resulting regression equation $y = 0.83x + 0.85$ strongly suggests a similarity in the animal abundances sampled by the two vehicles, with the R^2 value of 0.88 suggesting a good fit of data to the line..

The number of animals of each type sampled were expressed as a percentage of the total animals caught in each haul (Table 2.5) and these percentage species compositions plotted as bar charts. Comparisons were made between U-tow and ARIES sampled percentage species compositions from first day hauls, second day hauls and the average of both days (Fig. 2.8 a, b & c).

Percentage compositions were found to be broadly similar for most animal types, as can be seen from the average values (Fig. 2.8c). Numbers of calanoid copepods greater in length than 1.2 mm, however, seemed to vary. In the first day's samples, ARIES samples contained 10.26%, while U-tow contained 5.33% of these animals. The second day's ARIES samples, however, contained 13.35%, with U-tow samples containing 32.33%. Averaging these values over the two days gave 9.34% from ARIES, and 21.29% from U-tow.

Sampler comparison conclusions

The exercise was carried out in order to ascertain whether U-tow could be used as a reliable platform for the biological sampling necessary to this study. Because of the nature of the study and the need to find a sampler which could be simply operated without causing unnecessary disturbance to a normal fish survey, compromises had to be made.

Ship-time is always at a premium, and so trials had to be carried out in the available time. Two days were set aside for sampler trials. Much of this time was taken up with rectifying gear problems (the U-tow had been in storage for some time and required some general maintenance). It was not possible to obtain directly comparable samples from both vehicles because of this lack of time, so it was necessary to select samples which most closely matched depth, time and position profiles. This led to a relatively small number of samples actually being analysed.

The total number of animals in samples from each vehicle was considerably different, with ARIES sampling far greater numbers. This is likely due to the sampling aperture (370 mm

diameter) being far larger than that of U-tow (18 mm diameter) and was thus not taken as an indicator of U-tow's performance. Relative abundances of animals were compared, and regression analysis performed with results showing a strong relationship between the animal abundances sampled by the two vehicles.

Along with species composition from the two vehicles, these results show that the composition of animal types sampled by ARIES and U-tow can be considered similar. All categories of animal found in samples from one vehicle were found in samples from the other over the two days. For the purposes of this study, this indicated at this stage that the U-tow would sample the zooplankton population reliably.

Forward model predictions

Following biological sampling in 2003 and 2004 (Chapter 3, Chapter 4) and using the physical measurement and abundance data collected, the forward problem (Holliday and Pieper, 1995) was solved in order to predict backscattering values for each sample at each of the recorded frequencies using Distorted Wave Born Approximation (DWBA) models (Stanton and Chu, 2000). For modelling purposes, copepods and jellyfish were considered as fluid prolate spheroids, whilst euphausiids, decapods, amphipods, cephalopods, polychaetes, chaetognaths and clione were treated as fluid bent cylinders. Density contrast (g), sound speed contrast (h) and animal orientation parameters for such zooplankton were set as outlined in Table 2.6. Swimbladder dimensions for the different juvenile fish types encountered were not easy to estimate due to the small size of individuals in samples and the lack of literature available. However, approximate swimbladder sizes were found [e.g. pipefish juveniles and adults: Kyle (1926); gurnard: Harden Jones (1951); cod: Davenport (1999)] and are shown in Table 2.7 along with the values of g, h and L/a for either swimbladder or body as appropriate. Values for g and h were taken from the literature [Stanton *et al.* (1996), Chu & Wiebe (2005); Trevorrow & Tanaka (1997); Mukai *et al.* (2000)] with more up to date values received via personal communication with D. Chu (Woods Hole Oceanographic Institute, USA) and C. Lynam (University of St Andrews, UK). Values for the ratio of length to cylindrical radius (L/a) were calculated from measurements taken.

In order to allow direct comparison with recorded acoustic data, model-output target strength

Animal type	Model	g	h	L/a	orient. (°)	R	Reference
Copepod	FPS	1.02	1.058	6.4	0,30		Stanton & Chu (2000)
Euphausiid large	FBC	1.015	1.018	13.4	20,20		Stanton & Chu (2000)
Euphausiid small	FBC	1.016	1.019	13.4	20,20		Stanton & Chu (2000)
Decapod	FBC	as large / small euphausiid					Stanton & Chu (2000)
Amphipod	FBC	1.04	1.04	14 (large) 7 (small)	0,20		Trevorrow & Tanaka (1997)
Jellyfish	FPS	1.002	0.999	1.2	0,20		C. Lynam, Univ. St Andrews, pers. comm.
Gastropod	ES	1.732	1.732		0,20	0.5	Stanton & Chu (1994)
Cephalopod	FBC	1.025	1.007	7	0,20		Mukai et al (2000)
Polychaete	FBC	1.03	1.03	28 (sm. polych.) 20 (temopteris)	0,20		D. Chu, WHOI, pers. comm.
Chaetognath	FBC	1.03	1.03	60	0,20		D. Chu, WHOI, pers. comm.
Clione	FBC	1.03	1.03	7	0,20		assumed similar to chaetognath.

Table 2.6: parameters used in scattering models for the forward problem for non-gas bearing animal types. All L/a (length / radius) values resulted from measurements made of sampled animals. Model types used were Fluid Prolate Spheroid (FPS), Fluid Bent Cylinder (FBC) and Elastic-shelled (ES). References are given for values used for density contrast ratio (g), sound speed contrast ratio (h), animal orientation (orient.) - in the form "x,y" with "x" a mean value with standard deviation "y" - and reflection coefficient (R) (for gastropod molluscs).

Fish type	Swimbladder present (Y/N)	Swimbladder length	Model	g	h	L/a	Reference
Gadoid	Y	0.25*L	GS	0.0042	0.22	4	Swimbladder: Harden Jones (1951), g & h: Medwin & Clay (1998)
Gurnard	Y	0.25*L	GS	0.0042	0.22	4	Swimbladder: Davenport (1999), g & h: Medwin & Clay (1998)
Pipefish	Y	0.06*L	GS	0.00528	0.22	4	Swimbladder: Kyle (1926), g & h: Medwin & Clay (1998)
Sandeel	N		FBC	1.03	1.03	30	D. Chu, WHOI, pers. comm.
Flatfish	N		FPS	1.03	1.03	8	D. Chu, WHOI, pers. comm.
Cyclopterus	N		FBC	1.03	1.03	3	D. Chu, WHOI, pers. comm.

Table 2.7: parameters used in scattering models for the forward problem for fish types. Fish were divided into those with and without swimbladders. For those without swimbladders, the entire animal was considered as a scatterer and either the fluid bent cylinder (FBC) or fluid prolate spheroid (FPS) model employed for the forward problem. For fish with swimbladders, the swimbladder itself as a gaseous sphere type scatterer (GS) was considered the primary scatterer and its dimensions were used in the forward problem, with the body of the fish itself being disregarded. Approximate swimbladder length is shown as a fraction of body length. All L/a (length / radius) values for swimbladders were taken from the literature. The gaseous sphere model was used for swimbladders. References are given for both swimbladder dimensions and for density contrast ratio (g) and sound speed contrast ratio (h) values used. Note the differences in g and h values for swimbladdered and non-swimbladdered fishes, explained by the difference in density and sound speed in a gas-filled swimbladder as opposed to the typical fish body.

(TS) values were converted to mean volume backscattering strength (MVBS) using the following equation:

$$MVBS_{pred} = TS + 10log_{10}(n)$$

where $MVBS_{pred}$ is the predicted mean volume backscattering strength (dB), *TS* is the target strength output of the relevant model (dB) and *n* is the calculated number of animals per cubic metre of seawater for the relevant species group.

The dominant group of sampled scatterers for each haul at each frequency was identified as that which made the greatest contribution to total $MVBS_{pred}$. Due to the nature of the forward problem, which calculates a predicted backscattering level for animals known to be present via biological sampling, those scatterer types not found in samples could not be included in this calculation.

Acoustic data collection and analysis

Acoustic data were obtained simultaneously with net samples in 2003 and 2004 (Chapter 3, Chapter 4) using a SIMRAD EK500 scientific echosounder transmitting and receiving via transducers positioned at a depth of 8.6 m on FRV Scotia's drop keel at 38 kHz (single beam, 7º beam width), 120 kHz (split-beam, 7º beam width) and 200 kHz (single beam, 7º beam width). Prior to sampling, the echosounder was calibrated using standard sphere techniques (Foote et al, 1987). Pings were transmitted every 1.5 s with a pulse duration of 1 ms for each frequency. Acoustic signals were digitised and processed by EK500 (20 log R TVG and calibration gains applied) and volume backscattering strength data (Sv in dB re. 1 m^{-1}) were logged for post-processing. SonarData Echoview software (SonarData Pty Ltd, GPO Box 1387, Hobart, Tasmania, Australia), was used in the graphical representation of acoustic data, in the form of calibrated echograms. Data from echograms were exported in a raw format for further processing. Each pixel on echograms represented an area of 7.5 m horizontally and 3.5 m vertically.

An "observed" mean volume backscatter strength ($MVBS_{obs}$) value for each haul region defined on echograms according to haul parameters was obtained via echo integration at each of the three frequencies. $MVBS_{pred}$ was compared with $MVBS_{obs}$ in each case.

Inverse model predictions

Inverse processing of acoustic data generates as output the single type of scatterer which dominates acoustic reflection in each data bin. Bearing this in mind, the area of each haul analysed in 2003 and 2004 (Chapter 3, Chapter 4) was divided into higher resolution smaller sampling volumes for this procedure in order to get an indication of the diversity of organisms present. In order to comply with the previously written code which performed inverse calculations, haul regions on echograms were divided into cells corresponding to areas of the water column 150 m in length (equating to 15 acoustic pings) and 2 m in depth. Due to the nature of the inverse method, which fits theoretical models to data, scatterer types other than those sampled – such as gas-bearing plankton - were considered as potential candidates. For each cell, the inversion process fits models to the MVBS values measured at 38, 120 and 200 kHz. The available models include Truncated Fluid-filled Sphere (Costello *et al*., 1989), DWBA Fluid-filled Prolate Spheroid (D. Chu and G. Lawson, Wood's Hole Oceanographic Institute, USA, personal communication), DWBA Fluid-filled Bent Cylinder (Stanton and Chu, 2000), High-pass Elastic Shelled (Stanton *et al*., 1998) and High-pass Gaseous Sphere (Stanton, 1989). Solution of the inverse problem provides a possible population composition which, were the forward problem to be solved for it, would have a calculated MVBS as close as possible to measured MVBS in a least squares sense. The following error norm is calculated:

$$\text{Error} = \sum [s_v^{calc}(f_i) - s_v^{meas}(f_i)]^2$$

where n is the total number of measured frequencies,
s_v (volume backscattering coefficient) is as MVBS = 10*log(s_v),
and f_i is the frequency being considered.

The model that provides the lowest error is considered as that which most closely matches the observed values. This was taken to be an indicator of dominant scatterer type in each cell, with the possibility of strong responses to different sound frequencies by different components of the insonified population being considered.

Chapter 3

The contribution made by mesozooplankton to the scattering layer

published as

Mair A.M., Fernandes P.G., LeBourges-Dhaussy A., Brierley A. (2005)

An investigation into the zooplankton composition of a prominent 38 kHz scattering layer in the North Sea.

Journal of Plankton Research 27 (7), 623-633

Introduction

The contribution made by mesozooplankton to backscatter was investigated in summer 2003 through biological sampling directed to the layer in question. The aim was to obtain samples of those organisms present as well as concurrent acoustic data. Application of forward and inverse problems to the dataset thus collected would then provide results which showed the extent to which the sampled animals could be held responsible for enhanced 38 kHz scattering.

Methods

Zooplankton sample collection

An undulating towed vehicle (U-tow) equipped with a plankton sampling mechanism (PSM) similar to that found in the Longhurst-Hardy Plankton Recorder (Longhurst *et al*., 1966) (Fig. 3.1) was deployed from the side deck of FRV Scotia during the summer 2003 North Sea Herring Survey (ICES, 2004) to collect plankton samples. The cruise track is shown in Fig. 3.2. U-tow is a small, robust-bodied vehicle that can be deployed easily at ship speeds of up to twenty knots (EnviroTech, 2003). A full description of the vehicle has been published by Cook and Hays (2001).

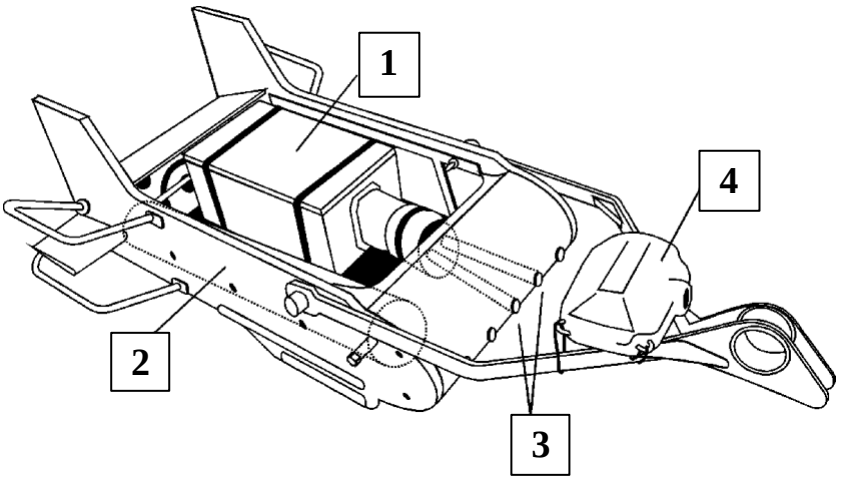

Fig. 3.1: Undulating Towed Vehicle (U-tow). The vehicle is approx. 1 m long and contains a Plankton Sampling Mechanism (PSM) unit (1) with a separate battery pack (2). Water is directed through the sampling apertures (3) and into the PSM. A SCANMAR depth unit (4) is attached in order to monitor and record sampling depth.

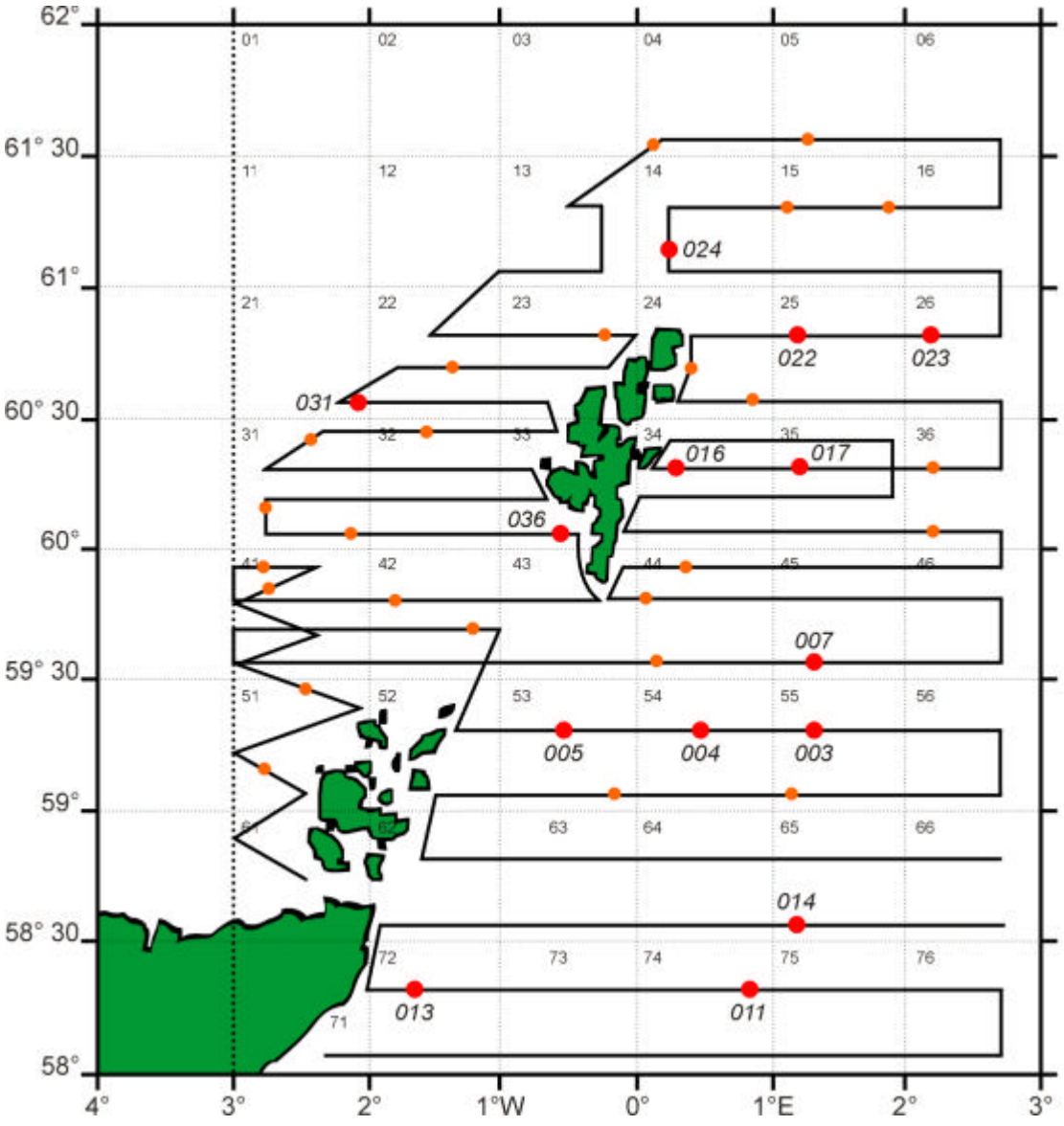

Fig. 3.2: Cruise track for FRV Scotia North Sea Herring Survey cruise 1003s. Red circles denote successful U-tow deployments which formed the basis for this analysis, and are accompanied by haul numbers. Smaller, orange circles denote failed U-tow deployments, where the sampler failed to operate correctly. ICES statistical square numbers are shown for Area IVa, which is delineated to the West by a thicker dotted line here.

Hoses were attached to two of the five 18 mm circular apertures on the fore-end of U-tow to direct water into the PSM. The PSM collected samples between two continuous 200 mm meshes, which were wound onto a collection roller every 2 minutes. Operation of the PSM was observed on-deck, and U-tow deployed immediately after the mesh was seen to wind on. Noting the time of this enabled the timing of subsequent samples to be calculated. Animals that entered the mechanism with the flow of water were trapped between the

meshes, with individual samples identifiable on recovery by a “striping” effect on the mesh. Samples were preserved in 4% formalin for identification later.

For most tows, the U-tow was deployed for multiples of 8 minutes at depths coinciding with a strong 38 kHz scattering layer observed on live-viewed echograms. A record was made of ship speed, time of deployment and recovery, depth of deployment and wire paid out for each haul. By setting the trim on the U-tow and controlling the wire paid out, the vehicle was made to sample as close to horizontally as possible at the required depth rather than undulating across a range of depths. A calibrated depth sensor unit (SCANMAR HC4-D: Scanmar AS, Åsgårdstrand, Norway) attached to the U-tow operated during each deployment, enabling sampling depth to be determined to within 0.1 m at one-minute (300 m at 10 knots) intervals (Table 3.1). Samples obtained from each tow were integrated so that each vial contained four samples collected over 8 minutes. The volume of water filtered was calculated by taking into account the size of U-tow’s sampling apertures, the ship’s speed

U-tow Haul identifier	Minimum depth (m)	Maximum depth (m)	Time of day start	Time of day end
003a	21.94	25.06	2141	2149
003b	19.56	20.31	2151	2159
004a	23.06	23.81	0615	0629
004b	39.69	41.25	0633	0647
005a	23.00	24.94	1155	1209
005b	48.19	49.06	1213	1219
005c	48.31	49.31	1220	1227
007a	19.12	25.75	1415	1429
007b	50.12	51.62	1433	1447
011a	19.88	21.62	0921	0935
0013	18.38	21.50	1716	1730
014a	25.88	27.12	1414	1428
014b	44.25	48.81	1432	1446
0016	23.06	23.88	1503	1517
017a	22.44	23.38	1740	1754
0022	45.62	47.44	1531	1545
023a	14.08	15.12	1833	1847
0024	21.06	26.62	0910	0924
0031	22.75	25.88	1859	1913
0036	29.50	30.88	0458	0512

Table 3.1: Description of U-tow hauls used in this study. All hauls came from ICES Area IVa in July 2003. Start and end times indicate timing of actual sampling rather than deployment and recovery times. A SCANMAR depth unit reported the U-tow’s depth each minute. Maximum and minimum reported depths are shown.

(which was 10 knots for all hauls) and the sampling period.

Zooplankton sample analysis

Analysis of zooplankton samples was carried out in the laboratory after the cruise, using a binocular microscope. Calanoid copepods were identified at least to genus, with *Calanus finmarchicus* to developmental stages C6 (adult) male/female and copepodite stages C4 and C5 due to their varying sizes and the effect this has on acoustic backscattering. Earlier developmental stages, along with *Acartia spp., Temora spp.* and other copepods less than 1.2 mm in length, were counted as "Small copepods <1.2mm". Other categories included Chaetognaths, Euphausiid juveniles, Decapod larvae, Cladocera, Cirripedia nauplii, Echinodermata larvae, Amphipoda and Polychaeta, although not all of these were found in all samples. Subsamples of up to 20 of the best-preserved individuals from each category were measured to 0.01mm for length and diameter (fine adjustments were made to these measurements to allow for deformation caused by the mechanics of the sampling vehicle) using an eyepiece graticule, with mean values later used for modelling. Twenty hauls were analysed in this way.

Because this study focussed on the acoustic properties of different types and sizes of scatterers, *C. finmarchicus* C5 juveniles and other copepods greater than 1.2 mm in length were considered together due to size similarities. *C. finmarchicus* adults (C6 stage) were considered separately, as were copepods <1.2 mm. Small euphausiids, polychaetes and chaetognaths were also considered separately, giving six categories of scatterer. The number of animals of each category per cubic metre of water was calculated from the number of animals caught and the volume of water filtered. Smaller animals (Cirripedia nauplii, Echinodermata larvae, early Decapoda larvae, Amphipoda and Cladocera) which were found to be few in number - typically no more than five individuals -and not strong acoustic scatterers were disregarded at this stage.

Forward model predictions

The forward problem (Holliday and Pieper, 1995) was solved in order to predict backscattering values for each sample at each of the three frequencies (38, 120 and 200 kHz) using the methods described in the "General Methods" chapter. The three categories of copepods were treated as fluid-filled prolate spheroids. Euphausiids, chaetognaths and polychaetes were treated as fluid-filled, bent cylinders.

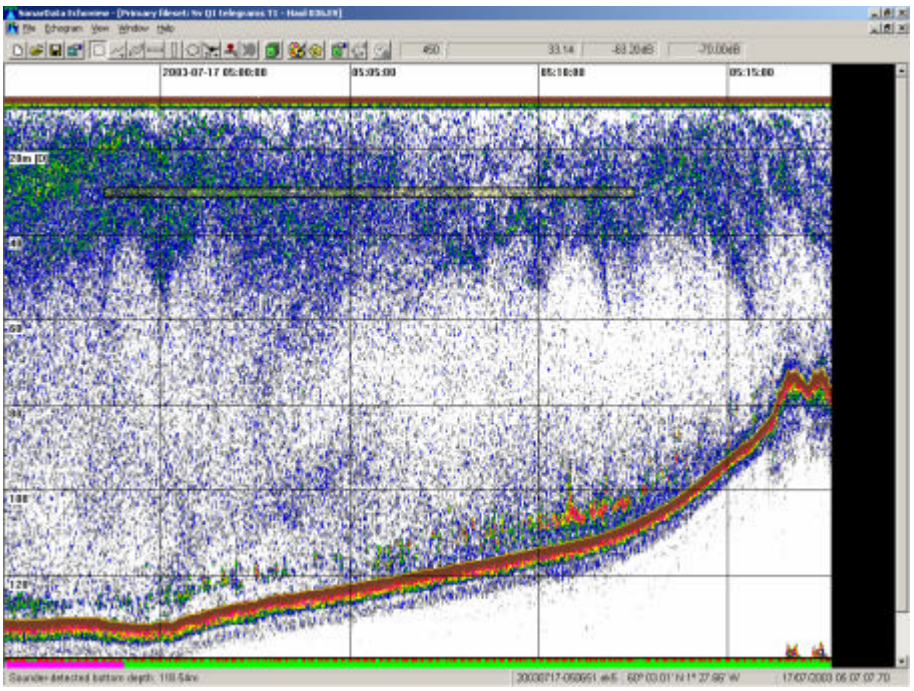

Fig 3.3: An example Echoview echogram showing the region of the haul (in this case, haul 0036) defined as a yellow box in the scattering layer. This region closely approximates the position of samples collected by U-tow in the water column during the tow.

The forward problem was solved for all six scattering categories, resulting in $MVBS_{pred}$ values for each category at all three frequencies. The resultant values were added in the linear domain to give a total $MVBS_{pred}$ firstly for cylinder and spheroid type animals separately, and then for the total of all sampled animals at the calculated abundances in each haul. The dominant group (either "spheroid" or "cylinder") of sampled scatterers for each haul at each frequency was identified as that which made the greatest contribution to total $MVBS_{pred}$. In this way, the dominant morphological type predicted by the forward problem could be related to that predicted by the inverse problem.

Acoustic data collection and analysis

Acoustic data were collected as follows. Regions of echograms corresponding to U-tow's position in the water at the time of each haul were identified using SCANMAR depth data, haul start/end times and amount of warp paid out (Fig 3.3). For example, when U-tow operated at 25 m depth it was typically 150 m behind the vessel, so a delay of 30 seconds was needed to align acoustic data with U-tow's position.

An "observed" mean volume backscatter strength ($MVBS_{obs}$) value for each defined haul region was obtained via echo integration at each of the three frequencies.

$MVBS_{pred}$ was compared with $MVBS_{obs}$ and linear regression analysis performed for each frequency. In order to gain a better understanding of whether low correlations were caused by biological samples being representative of the zooplankton community but simply not containing animals in sufficient numbers, $MVBS_{pred}$ values were calculated for sampled animal abundances multiplied by factors of 2 and 200 and then re-compared with $MVBS_{obs}$.

Inverse model predictions

The inverse problem was solved for ten of the hauls with the aim of identifying the expected dominant scatterer in each region according to scattering characteristics at the frequencies used. Echogram grids were re-defined to give a higher resolution of integration values as described in the "General Methods" chapter. The result of inverse modelling was was taken to be an indicator of dominant scatterer type in each discrete echogram cell (150 m x 2 m), allowing identification of the most likely dominant scatterer in the region of each haul analysed.

Results

Six categories of scatterers *(Calanus finmarchicus* C6 and C5, copepods <1.2mm, chaetognaths, polychaetes and euphausiids) accounted for over 95% of animals by number in all samples, and over 99% in most. Other animals found in small numbers included Cladocera, Cirripedia nauplii and fragments of gelatinous animals. Fish larvae and elastic-shelled molluscs were noticeably absent in the samples.

Solution of the forward problem for the different types, sizes and abundances of animals found in samples showed the contribution of each category of cylinder-type (Table 3.2) and spheroid-type (Table 3.3) scatterer to total $MVBS_{pred}$. These data are added and summarised in Table 3.4.

Measurements were made of a random subsample of the best-preserved animals (n=20) from each category found in each sample. Table 3.5 gives mean length with standard deviation, length to cylindrical radius ratio (L/a), and $MVBS_{pred}$ at each frequency (38, 120 and 200 kHz) data combined from all hauls. Abundance values for each category varied considerably from haul to haul.

Haul No.	Species group	Mean Length (mm)	L/a	Abundance (no. m-3)	$MVBS_{pred}$ 38 kHz (dB)	$MVBS_{pred}$ 120 kHz (dB)	$MVBS_{pred}$ 200 kHz (dB)
003a	**euph**	7.3	6.7	45.2	-93.37	-76.50	-71.91
003a	**polych**	0.8	8.0	5.2	-163.17	-143.15	-134.36
003a	**chaeto**	7.6	18.0	32.3	-110.89	-93.28	-86.71
003b	**euph**	6.9	6.7	3.2	-106.25	-89.10	-84.22
003b	**polych**	0.8	8.0	4.5	-163.66	-143.73	-134.93
003b	**chaeto**	8.4	18.0	2.6	-119.33	-102.05	-95.59
004a	**euph**	5.3	6.7	0.4	-121.94	-103.74	-97.69
004a	**polych**	1.3	8.0	685.6	-129.21	-109.34	-100.68
004a	**chaeto**	5.1	18.0	71.7	-117.63	-98.90	-91.79
004b	**euph**	7.1	6.7	1.2	-109.75	-92.75	-88.01
004b	**polych**	0.6	8.0	12.6	-166.72	-146.77	-137.94
004b	**chaeto**	6.9	18.0	5.7	-120.90	-102.98	-96.31
005a	**euph**	3.8	6.7	3.2	-121.53	-102.50	-95.31
005a	**polych**	1.2	8.0	0.4	-163.53	-143.64	-134.95
005a	**chaeto**	5.3	18.0	9.3	-125.50	-106.86	-99.82
005b	**euph**	6.1	6.7	4.1	-108.40	-90.71	-85.24
005b	**polych**	1.2	8.0	0.8	-160.57	-140.68	-131.99
005b	**chaeto**	6.6	18.0	45.4	-113.00	-94.94	-88.22
005c	**euph**	3.0	6.7	4.1	-126.68	-107.31	-99.54
005c	**polych**	1.2	8.0	0.8	-160.57	-140.68	-131.99
005c	**chaeto**	5.8	18.0	9.7	-123.00	-104.58	-97.69
007a	**euph**	0.0	6.7	0.0	0.00	0.00	0.00
007a	**polych**	1.2	8.0	53.5	-142.37	-122.49	-113.79
007a	**chaeto**	7.5	18.0	55.1	-108.90	-91.24	-84.66
007b	**euph**	8.3	6.7	11.3	-96.14	-79.99	-76.21
007b	**polych**	1.2	8.0	8.1	-150.57	-130.68	-121.99
007b	**chaeto**	9.2	18.0	17.0	-108.84	-91.88	-85.52
011a	**euph**	5.2	6.7	1.2	-117.70	-99.43	-93.31
011a	**polych**	0.6	8.0	297.8	-152.97	-133.02	-124.19
011a	**chaeto**	4.8	18.0	21.5	-124.43	-105.58	-98.35
0013	**euph**	0.0	6.7	0.0	0.00	0.00	0.00
0013	**polych**	0.0	8.0	0.0	0.00	0.00	0.00
0013	**chaeto**	6.1	18.0	1.6	-129.49	-111.21	-104.38
0014a	**euph**	6.2	6.7	10.9	-103.67	-86.04	-80.65
0014a	**polych**	2.2	8.0	20.3	-130.82	-111.14	-102.85
0014a	**chaeto**	7.4	18.0	25.1	-112.65	-94.95	-88.36
0014b	**euph**	6.6	6.7	2.8	-107.94	-90.58	-85.48
0014b	**polych**	3.6	8.0	1.6	-129.01	-109.83	-102.34
0014b	**chaeto**	9.2	18.0	0.4	-125.02	-108.07	-101.70
0016	**euph**	6.5	6.7	3.2	-107.75	-90.33	-85.15
0016	**polych**	2.1	8.0	4.9	-138.23	-118.53	-110.18
0016	**chaeto**	6.0	18.0	20.3	-118.94	-100.61	-93.77
0017a	**euph**	6.7	6.7	6.5	-103.97	-86.69	-81.66
0017a	**polych**	1.0	8.0	47.0	-147.68	-127.77	-119.02
0017a	**chaeto**	9.5	18.0	24.3	-106.49	-89.64	-83.31
0022	**euph**	6.5	6.7	13.0	-101.73	-84.31	-79.13
0022	**polych**	3.5	8.0	3.2	-126.73	-107.50	-99.96
0022	**chaeto**	8.6	18.0	42.9	-106.52	-89.32	-82.88
0023a	**euph**	4.4	6.7	1.6	-120.76	-102.04	-95.30
0023a	**polych**	0.0	8.0	0.0	0.00	0.00	0.00
0023a	**chaeto**	6.1	18.0	78.6	-112.63	-94.35	-87.52
0024	**euph**	6.1	6.7	14.6	-102.84	-85.14	-79.68
0024	**polych**	2.7	8.0	2.4	-134.71	-115.19	-107.15
0024	**chaeto**	6.7	18.0	24.3	-115.33	-97.31	-90.61
0031	**euph**	0.0	6.7	0.0	0.00	0.00	0.00
0031	**polych**	0.0	8.0	0.0	0.00	0.00	0.00
0031	**chaeto**	3.2	18.0	1.2	-147.37	-127.93	-119.98
0036	**euph**	6.7	6.7	0.8	-113.00	-95.72	-90.69
0036	**polych**	2.9	8.0	6.1	-128.87	-109.42	-101.50
0036	**chaeto**	5.9	18.0	17.8	-119.93	-123.42	-94.68

Frequency (kHz)	Total $MVBS_{pred}$ euph, poly, chaet
38	-93.37
120	-76.50
200	-71.91
38	-106.25
120	-89.10
200	-84.22
38	-117.63
120	-98.90
200	-91.79
38	-109.75
120	-92.75
200	-88.01
38	-121.53
120	-102.50
200	-95.31
38	-108.40
120	-90.71
200	-85.24
38	-123.00
120	-104.58
200	-97.68
38	-108.90
120	-91.24
200	-84.66
38	-96.13
120	-79.99
200	-76.21
38	-117.69
120	-99.43
200	-93.30
38	-129.49
120	-111.21
200	-104.38
38	-103.67
120	-86.04
200	-80.65
38	-107.94
120	-90.58
200	-85.48
38	-107.75
120	-90.33
200	-85.15
38	-103.97
120	-86.69
200	-81.65
38	-101.73
120	-84.30
200	-79.13
38	-120.76
120	-102.04
200	-95.30
38	-102.84
120	-85.14
200	-79.68
38	-147.37
120	-127.93
200	-119.98
38	-113.00
120	-95.72
200	-90.69

Table 3.2: Predicted MVBS values (dB) for sampled cylinder-type scatterers (euphausiid, polychaete and chaetognath) at the calculated abundances in each haul at 38, 120 and 200 kHz. Values are also given for one haul (003a) at two and two hundred times the sampled abundances. The total predicted MVBS for cylinder-type animals at each frequency is given.

Haul No.	Species group	Mean Length (mm)	L/a	Abundance (no. m-3)	$MVBS_{pred}$ 38 kHz (dB)	$MVBS_{pred}$ 120 kHz (dB)	$MVBS_{pred}$ 200 kHz (dB)
003a	**C6**	2.19	3.2	81.94	-105.11	-85.88	-78.54
003a	**C5**	1.99	3.2	9.68	-116.87	-97.51	-89.89
003a	**Csm**	0.35	3.2	25.81	-157.83	-137.87	-129.04
003b	**C6**	2.22	3.2	9.68	-114.04	-94.83	-87.53
003b	**C5**	1.86	3.2	0.65	-130.35	-110.91	-103.13
003b	**Csm**	0.35	3.2	31.61	-156.95	-136.99	-128.16
004a	**C6**	2.29	3.2	14.59	-111.45	-92.29	-85.10
004a	**C5**	1.98	3.2	4.05	-120.78	-101.42	-93.78
004a	**Csm**	0.35	3.2	144.25	-150.36	-130.40	-121.56
004b	**C6**	2.28	3.2	11.75	-112.50	-93.34	-86.13
004b	**C5**	1.92	3.2	10.53	-117.43	-98.03	-90.32
004b	**Csm**	0.35	3.2	71.31	-153.42	-133.46	-124.62
005a	**C6**	2.33	3.2	6.89	-114.26	-95.13	-88.01
005a	**C5**	1.93	3.2	8.91	-118.02	-98.63	-90.93
005a	**Csm**	0.35	3.2	450.16	-145.41	-125.46	-116.62
005b	**C6**	2.31	3.2	25.93	-108.73	-89.59	-82.43
005b	**C5**	1.99	3.2	21.88	-113.33	-93.97	-86.35
005b	**Csm**	0.35	3.2	674.23	-143.66	-123.70	-114.87
005c	**C6**	2.33	3.2	8.91	-113.14	-94.02	-86.89
005c	**C5**	1.80	3.2	8.10	-120.24	-100.77	-92.92
005c	**Csm**	0.35	3.2	359.00	-146.40	-126.44	-117.60
007a	**C6**	2.26	3.2	46.19	-106.79	-87.61	-80.37
007a	**C5**	2.09	3.2	17.83	-112.94	-93.65	-86.17
007a	**Csm**	0.35	3.2	61.59	-154.05	-134.10	-125.26
007b	**C6**	2.27	3.2	26.74	-109.04	-89.88	-82.65
007b	**C5**	2.04	3.2	13.78	-114.69	-95.36	-87.81
007b	**Csm**	0.35	3.2	61.59	-154.05	-134.10	-125.26
011a	**C6**	2.15	3.2	18.23	-112.11	-92.86	-85.46
011a	**C5**	1.92	3.2	2.43	-123.80	-104.40	-96.69
011a	**Csm**	0.35	3.2	47.41	-155.19	-135.23	-126.39
0013	**C6**	2.30	3.2	4.05	-116.90	-97.75	-90.58
0013	**C5**	2.04	3.2	7.29	-117.46	-98.13	-90.58
0013	**Csm**	0.52	3.2	638.57	-133.58	-113.65	-104.86
0014a	**C6**	2.26	3.2	72.93	-104.80	-85.62	-78.39
0014a	**C5**	1.91	3.2	70.50	-109.31	-89.90	-82.18
0014a	**Csm**	0.35	3.2	163.29	-149.82	-129.86	-121.02
0014b	**C6**	2.40	3.2	6.89	-113.49	-94.42	-87.41
0014b	**C5**	1.83	3.2	2.03	-125.82	-106.37	-98.55
0014b	**Csm**	0.35	3.2	127.23	-150.90	-130.94	-122.11
0016	**C6**	2.33	3.2	36.47	-107.02	-87.90	-80.77
0016	**C5**	1.95	3.2	17.83	-114.74	-95.36	-87.69
0016	**Csm**	0.58	3.2	1163.70	-128.13	-108.21	-99.44
0017a	**C6**	2.28	3.2	84.28	-103.95	-84.78	-77.58
0017a	**C5**	1.97	3.2	13.78	-115.60	-96.22	-88.58
0017a	**Csm**	0.37	3.2	27.55	-156.10	-136.14	-127.31
0022	**C6**	2.33	3.2	73.74	-103.96	-84.84	-77.71
0022	**C5**	2.10	3.2	30.79	-110.45	-91.16	-83.69
0022	**Csm**	0.72	3.2	1250.41	-122.19	-102.29	-93.58
0023a	**C6**	2.31	3.2	162.07	-100.77	-81.63	-74.47
0023a	**C5**	1.97	3.2	176.66	-104.52	-85.15	-77.50
0023a	**Csm**	0.32	3.2	1257.70	-143.29	-123.33	-114.42
0024	**C6**	2.36	3.2	116.69	-101.64	-82.54	-75.46
0024	**C5**	2.02	3.2	28.36	-111.81	-92.47	-84.89
0024	**Csm**	0.34	3.2	3126.42	-137.75	-117.79	-108.95
0031	**C6**	2.33	3.2	44.98	-106.11	-86.99	-79.86
0031	**C5**	2.13	3.2	10.13	-114.91	-95.64	-88.21
0031	**Csm**	0.34	3.2	899.92	-143.16	-123.20	-114.36
0036	**C6**	2.29	3.2	10.13	-113.03	-93.88	-86.69
0036	**C5**	1.97	3.2	9.32	-117.29	-97.92	-90.28
0036	**Csm**	0.41	3.2	552.67	-140.40	-120.45	-111.63

Frequency (kHz)	Total $MVBS_{pred}$ C6, C5 & Csm
38	-105.11
120	-85.88
200	-78.54
38	-114.04
120	-94.83
200	-87.53
38	-111.45
120	-92.29
200	-85.10
38	-112.50
120	-93.34
200	-86.13
38	-114.26
120	-95.13
200	-88.00
38	-108.73
120	-89.58
200	-82.43
38	-113.14
120	-94.02
200	-86.89
38	-106.78
120	-87.61
200	-80.37
38	-109.04
120	-89.87
200	-82.65
38	-112.11
120	-92.86
200	-85.46
38	-116.79
120	-97.60
200	-90.28
38	-104.80
120	-85.62
200	-78.39
38	-113.49
120	-94.42
200	-87.40
38	-107.02
120	-87.89
200	-80.77
38	-103.94
120	-84.78
200	-77.58
38	-103.96
120	-84.84
200	-77.71
38	-100.77
120	-81.63
200	-74.47
38	-101.64
120	-82.54
200	-75.46
38	-106.11
120	-86.98
200	-79.86
38	-113.03
120	-93.88
200	-86.69

Table 3.3: Predicted MVBS values (dB) for sampled spheroid-type scatterers (C6 = adult copepods, C5 = copepodite stage 5, Csm = small copepods <1.2mm) at the calculated abundances in each haul at 38, 120 and 200 kHz. Values are also given for one haul (003a) at two and two hundred times the sampled abundances. The total predicted MVBS for spheroid-type animals at each frequency is given.

Haul No.	Freq.	$MVBS_{pred}$ spheroid	$MVBS_{pred}$ cylinder	Total $MVBS_{pred}$	$MVBS_{obs}$
003a	**38**	-105.11	-93.37	-93.37	-65.94
	120	-85.88	-76.50	-76.50	-69.81
	200	-78.54	-71.91	-71.91	-66.56
003b	**38**	-114.04	-106.25	-106.25	-66.94
	120	-94.83	-89.10	-89.10	-76.65
	200	-87.53	-84.22	-84.22	-74.73
004a	**38**	-111.45	-117.63	-111.45	-66.21
	120	-92.29	-98.90	-92.29	-68.63
	200	-85.10	-91.79	-85.10	-65.51
004b	**38**	-112.50	-109.75	-109.75	-63.64
	120	-93.34	-92.75	-92.65	-69.58
	200	-86.13	-88.01	-86.13	-66.34
005a	**38**	-114.26	-121.53	-114.26	-70.40
	120	-95.13	-102.50	-95.13	-76.55
	200	-88.00	-95.31	-88.00	-72.70
005b	**38**	-108.73	-108.40	-108.23	-66.92
	120	-89.58	-90.71	-89.55	-74.65
	200	-82.43	-85.24	-82.43	-70.96
005c	**38**	-113.14	-123.00	-113.14	-65.02
	120	-94.02	-104.58	-94.02	-74.36
	200	-86.89	-97.68	-86.89	-70.41
007a	**38**	-106.78	0.00	-106.78	-62.84
	120	-87.61	0.00	-87.61	-69.99
	200	-80.37	0.00	-80.37	-67.06
007b	**38**	-109.04	-96.13	-96.13	-63.63
	120	-89.87	-79.99	-79.99	-70.21
	200	-82.65	-76.21	-76.21	-67.12
011a	**38**	-112.11	-117.69	-112.11	-69.16
	120	-92.86	-99.43	-92.86	-75.61
	200	-85.46	-93.30	-85.46	-74.45
0013	**38**	-116.79	-129.49	-116.79	-62.95
	120	-97.60	-111.21	-97.60	-71.40
	200	-90.28	-104.38	-90.28	-68.67
0014a	**38**	-104.80	-103.67	-103.64	-67.45
	120	-85.62	-86.04	-85.48	-72.21
	200	-78.39	-80.65	-78.38	-68.83
0014b	**38**	-113.49	-107.94	-107.94	-81.23
	120	-94.42	-90.58	-90.58	-81.09
	200	-87.40	-85.48	-85.47	-76.13
0016	**38**	-107.02	-107.75	-106.95	-62.65
	120	-87.89	-90.33	-87.89	-67.81
	200	-80.77	-85.15	-80.77	-68.92
0017a	**38**	-103.94	-103.97	-103.66	-65.92
	120	-84.78	-86.69	-84.78	-72.21
	200	-77.58	-81.65	-77.58	-72.11
0022	**38**	-103.96	-101.73	-101.73	-58.82
	120	-84.84	-84.30	-84.19	-64.41
	200	-77.71	-79.13	-77.69	-64.76
0023a	**38**	-100.77	-120.76	-100.77	-66.69
	120	-81.63	-102.04	-81.63	-69.97
	200	-74.47	-95.30	-74.47	-70.54
0024	**38**	-101.64	-102.84	-101.61	-60.41
	120	-82.54	-85.14	-82.53	-66.30
	200	-75.46	-79.68	-75.46	-67.24
0031	**38**	-106.11	-147.37	-106.11	-65.59
	120	-86.98	-127.93	-86.98	-71.19
	200	-79.86	-119.98	-79.86	-71.18
0036	**38**	-113.03	-113.00	-112.72	-60.97
	120	-93.88	-95.72	-93.87	-70.37
	200	-86.69	-90.69	-86.69	-70.73

Table 3.4: Predicted MVBS values for spheroid and cylinder type animals was added to give a total predicted MVBS ($MVBS_{pred}$) for each haul at each of the three frequencies. Also shown is the observed MVBS value ($MVBS_{obs}$), taken from echo-integration of haul regions defined in SonarData Echoview software.

Species group		Averages across all hauls					
		Mean Length (mm)	Standard deviation	L/a	38 kHz $MVBS_{pred}$ (dB)	120 kHz $MVBS_{pred}$ (dB)	200 kHz $MVBS_{pred}$ (dB)
Spheroid type	C. finmarchicus C6	2.30	0.06	3.2	-108.94	-89.79	-82.60
	C. finmarchicus C5	1.98	0.10	3.2	-116.52	-97.15	-89.51
	Copepods < 1.2 mm	0.39	0.09	3.2	-146.13	-126.18	-117.35
Cylinder type	Euphausiids	5.58	2.64	6.7	-93.17	-78.14	-73.46
	Polychaetes	1.31	1.04	8.0	-124.47	-107.68	-100.49
	Chaetognaths	7.55	2.54	18.0	-118.34	-101.46	-93.59

Table 3.5: Average predicted mean volume backscattering strength (MVBS) at 38, 120 and 200 kHz for the six scatterer types identified in samples. The animal length and MVBS data shown are average values (with standard deviation) calculated across all hauls for each of the six categories. Mean length and length to cylindrical radius ratios (L/a) were calculated from measurements of sampled animals.

As may be expected due to their greater size, adult *C. finmarchicus* were the dominant sampled scatterer among spheroid-type animals in all hauls, and contributed the highest percentage of total backscatter in twelve of the twenty hauls. In the same way, Euphausiids were generally found to be the scatterer among cylinder-types that dominated backscatter, despite the often far greater abundance of Chaetognaths and Polychaetes. Cylinder-type animals were the overall dominant sampled scatterers in four hauls at all three frequencies. In the remaining four hauls, neither type dominated. It should be noted that candidates for the dominant "sampled" scatterer included only those animal types which were found in samples and not other possibilities such as gas-bearing particles, which were not present in net samples.

$MVBS_{pred}$ was plotted against $MVBS_{obs}$ for each haul at each of the three frequencies (Fig. 3.4a, b and c), linear regression analyses performed, and R^2 values calculated. For 38 kHz, the regression equation was $y = 0.1865x - 94.425$, with $R^2 = 0.0207$; for 120 kHz, the regression equation was $y = 0.7699x - 33.658$, with $R^2 = 0.2029$; and for 200 kHz, the regression equation was $y = 0.5833x - 40.971$ with $R^2 = 0.133$. These statistics show that $MVBS_{pred}$ was lower than $MVBS_{obs}$ for all hauls at all three frequencies, with the difference more pronounced at 38 kHz. The goodness of fit at 38 kHz was also considerably lower than at the other frequencies, although this may have been influenced by an outlying data point.

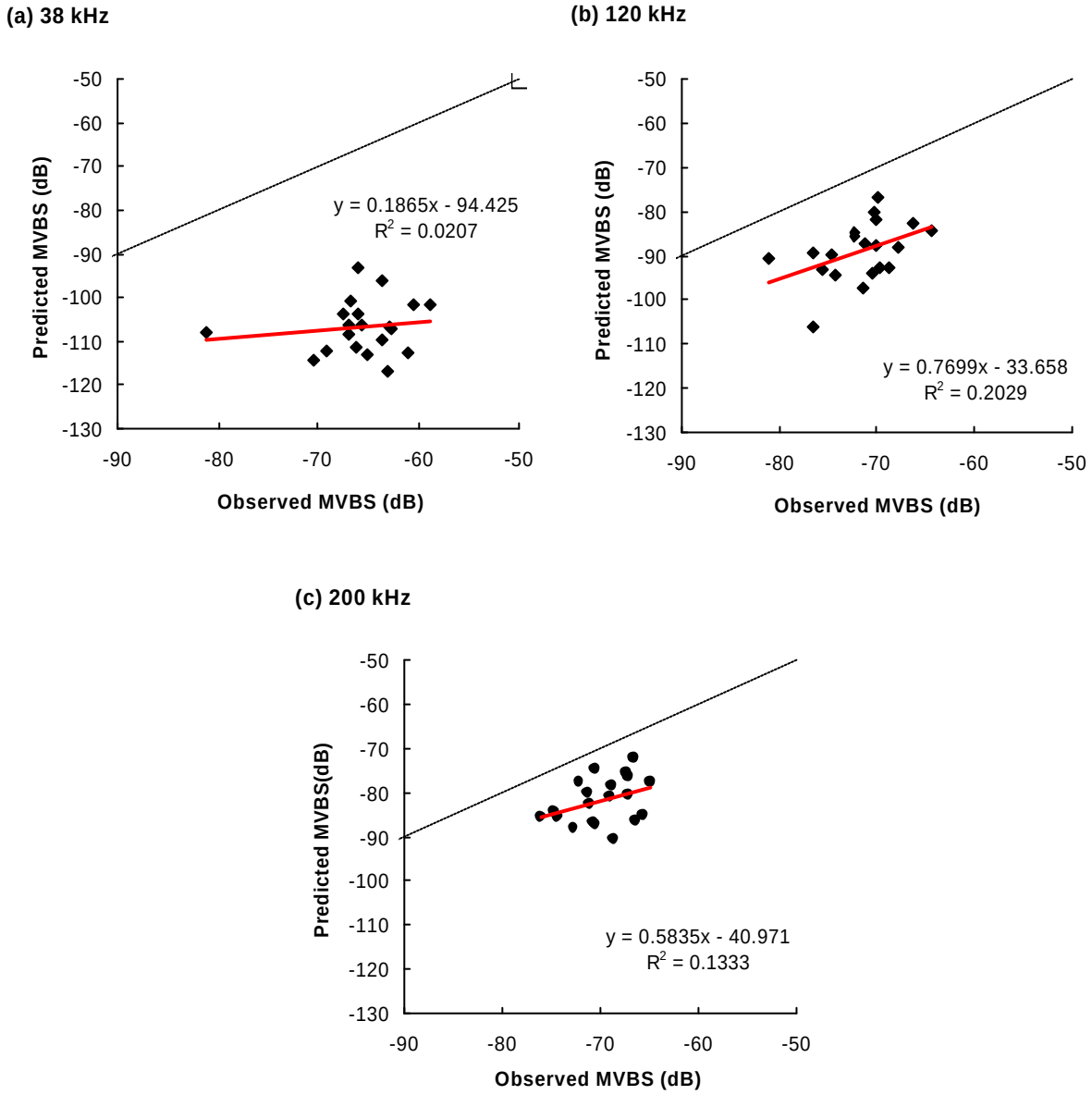

Fig. 3.4. Predicted mean volume backscattering strength (MVBS) plotted against observed MVBS at (a) 38 kHz, (b) 120 kHz and (c) 200 kHz for each of the 20 hauls under consideration. In each case, the dotted line represents a 1:1 relationship, whilst the regression line is shown in red. The regression equation and R^2 value is shown on each plot. For all hauls at all frequencies, predicted MVBS was less than observed MVBS, and considerably more so at 38 kHz.

The most noticeable difference between $MVBS_{obs}$ and $MVBS_{pred}$ is the relationship between 38 and 120 kHz (Fig. 3.5). Curves were fitted to each set of three points (at 38, 120 and 200 kHz) in Fig. 3.5 in order to aid visual interpretation of relative scattering levels. The curve for observed values has a decreasing trend between 38 and 120 kHz, whilst that for predicted values increases. Using data from one haul, the abundances of sampled cylinder-type and

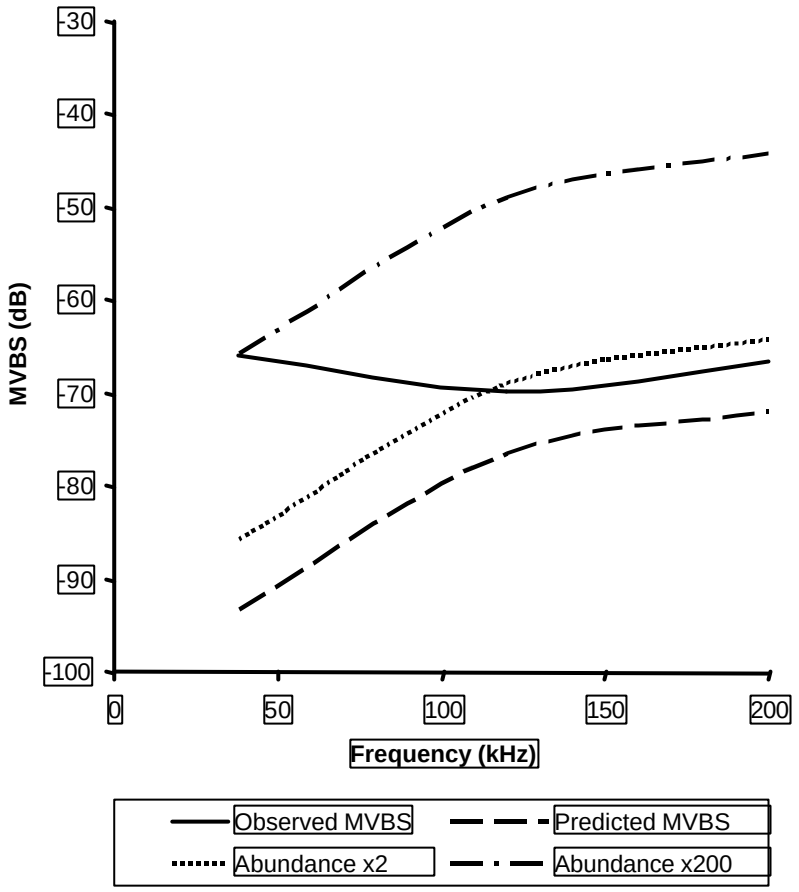

Fig. 3.5: Predicted mean volume backscattering strength ($MVBS_{pred}$) for one haul according to sampled zooplankton (dashed line), and the predicted increase in MVBS caused by 2x (dotted line) and 200x (dash-dot line) sampled animal abundance. The solid line shows observed MVBS.

spheroid-type animals were artificially doubled and scattering models re-applied. This procedure gave $MVBS_{pred}$ values which closely approached $MVBS_{obs}$ at 120 and 200 kHz. However, a 200-fold increase in abundance was required to give $MVBS_{pred}$ values close to $MVBS_{obs}$ at 38 kHz (Table 3.6a & 3.6b). Such an increase gave $MVBS_{pred}$ values at 120 and 200 kHz which were far greater (~20 dB) than $MVBS_{obs}$ at those frequencies (Fig. 3.5).

Solution of the inverse problem identified a single theoretical dominant scatterer type for each echogram cell in ten of the hauls. The inverse routine used provides a graphical display of dominant scatterers suggested for each defined echogram cell. Examples of this are given in Fig. 3.6 and Fig. 3.7. Scatterer types which dominated backscatter according to solution of both forward and inverse problems for these hauls are given in Table 3.7. The inverse method predicts the presence of scatterers with a gas inclusion in all except two hauls, where elastic-shelled scatterers are predicted. Neither type of scatterer featured in biological

a.

Haul No.	Species group	Mean Length (mm)	L/a	Abundance (no. m-3)	$MVBS_{pred}$ 38 kHz (dB)	$MVBS_{pred}$ 120 kHz (dB)	$MVBS_{pred}$ 200 kHz (dB)	Frequency (kHz)	Total $MVBS_{pred}$
Cylinder type									
Haul 003a abundance x2									
003a	**euph**	7.3	6.7	90.3	-85.84	-68.92	-64.28	**38**	-85.84
003a	**polych**	0.8	8.0	10.3	-155.57	-135.64	-126.84	**120**	-68.92
003a	**chaeto**	7.6	18.0	64.5	-103.37	-85.72	-79.14	**200**	-64.28
Haul 003a abundance x200									
003a	**euph**	7.3	6.7	9032.3	-65.84	-48.92	-44.28	**38**	-65.84
003a	**polych**	0.8	8.0	1032.3	-135.57	-115.64	-106.84	**120**	-48.92
003a	**chaeto**	7.6	18.0	6451.6	-83.37	-65.72	-59.14	**200**	-44.28
Spheroid type									
Haul 003a abundance x2									
003a	**C6**	2.2	3.2	163.88	-102.10	-82.87	-75.53	**38**	-102.10
003a	**C5**	1.9	3.2	19.36	-113.86	-94.50	-86.88	**120**	-82.87
003a	**Csm**	0.4	3.2	51.62	-154.82	-134.86	-126.03	**200**	-75.53
Haul 003a abundance x200									
003a	**C6**	2.2	3.2	16388.00	-82.10	-62.87	-55.53	**38**	-82.10
003a	**C5**	1.9	3.2	1936.00	-93.86	-74.50	-66.88	**120**	-62.87
003a	**Csm**	0.4	3.2	5162.00	-134.82	-114.86	-106.03	**200**	-55.53

b.

Haul No.	Freq.	$MVBS_{pred}$ spheroid	$MVBS_{pred}$ cylinder	Total $MVBS_{pred}$	$MVBS_{obs}$
Haul 003a abundance x2					
003a	**38**	-102.10	-85.84	-85.84	-65.94
003a	**120**	-82.87	-68.92	-68.92	-69.81
003a	**200**	-75.53	-64.28	-64.27	-66.56
Haul 003a abundance x200					
003a	**38**	-82.10	-65.84	-65.84	-65.94
003a	**120**	-62.87	-48.92	-48.92	-69.81
003a	**200**	-55.53	-44.28	-44.27	-66.56

Table 3.6: $MVBS_{pred}$ values calculated by solving the forward problem for artificial increases in sampled animal abundances (2 and 200 times) for one haul (003a). a. $MVBS_{pred}$ for cylinder and spheroid type animals calculated for increased abundances in each category, and total $MVBS_{pred}$ for all cylinder and all spheroid type scatterers. b. Total $MVBS_{pred}$ for artificially increased abundances in the haul was calculated by adding $MVBS_{pred}$ for cylinder and spheroid types. $MVBS_{obs}$ for that haul is also shown.

samples collected by the U-tow.

Although the scatterer type having the greatest influence on total backscatter can be identified separately for each frequency by solving the forward problem, the model-fitting nature of the inverse method requires data from all three frequencies and therefore outputs only a single solution for each echogram cell. In most cells the acoustic data most closely fit the model for "gaseous sphere" (approx. 0.1 – 0.4 mm) type scatterers. Two hauls (003a and

a.

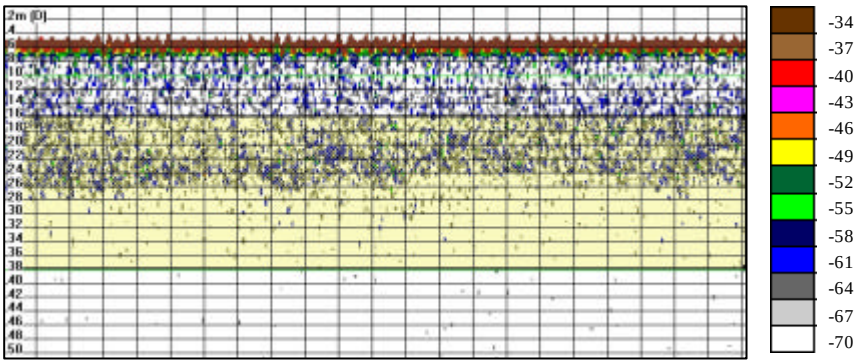

b.

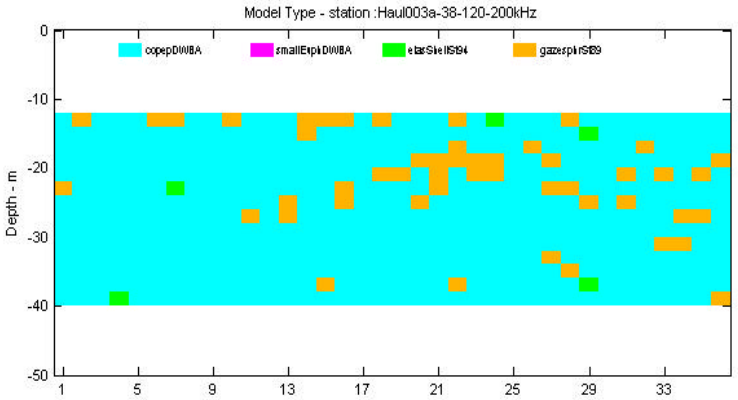

c.

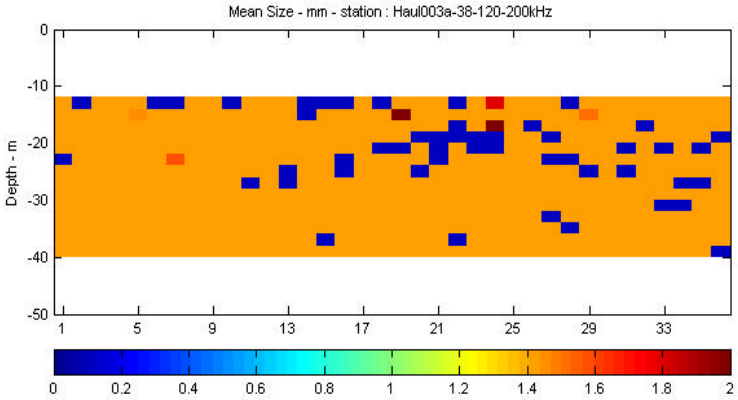

Fig. 3.6: Example graphical outputs from solutions of the inverse problems for Haul 003a. Depth is displayed on the y axis, and echogram column number on the x axis in all cases. ***a.*** *the 38 kHz echogram for the corresponding region, with the legend to the right showing the colours used to represent backscatter intensity (dB) in 3dB steps. The shaded area indicates the area sampled.* ***b.*** *the dominant predicted scatterer in each defined echogram cell, with a colour legend above.* ***c.*** *an approximate size for the types of scatterers predicted, with a colour legend along the bottom. Echogram column number is displayed on the x axis in* ***b*** *and* ***c****.*

Haul 003a covered a depth region between approx. 10 m and 40 m. Inverse problem solution suggested the most likely scatterers were fluid-filled prolate spheroids, with a size of approx. 1.4 mm. There were however, some cells which were better described by the gaseous sphere model, at a size of around 0.1 mm, and several which were best described by the elastic-shelled model at sizes between 1.4 mm and 2 mm.

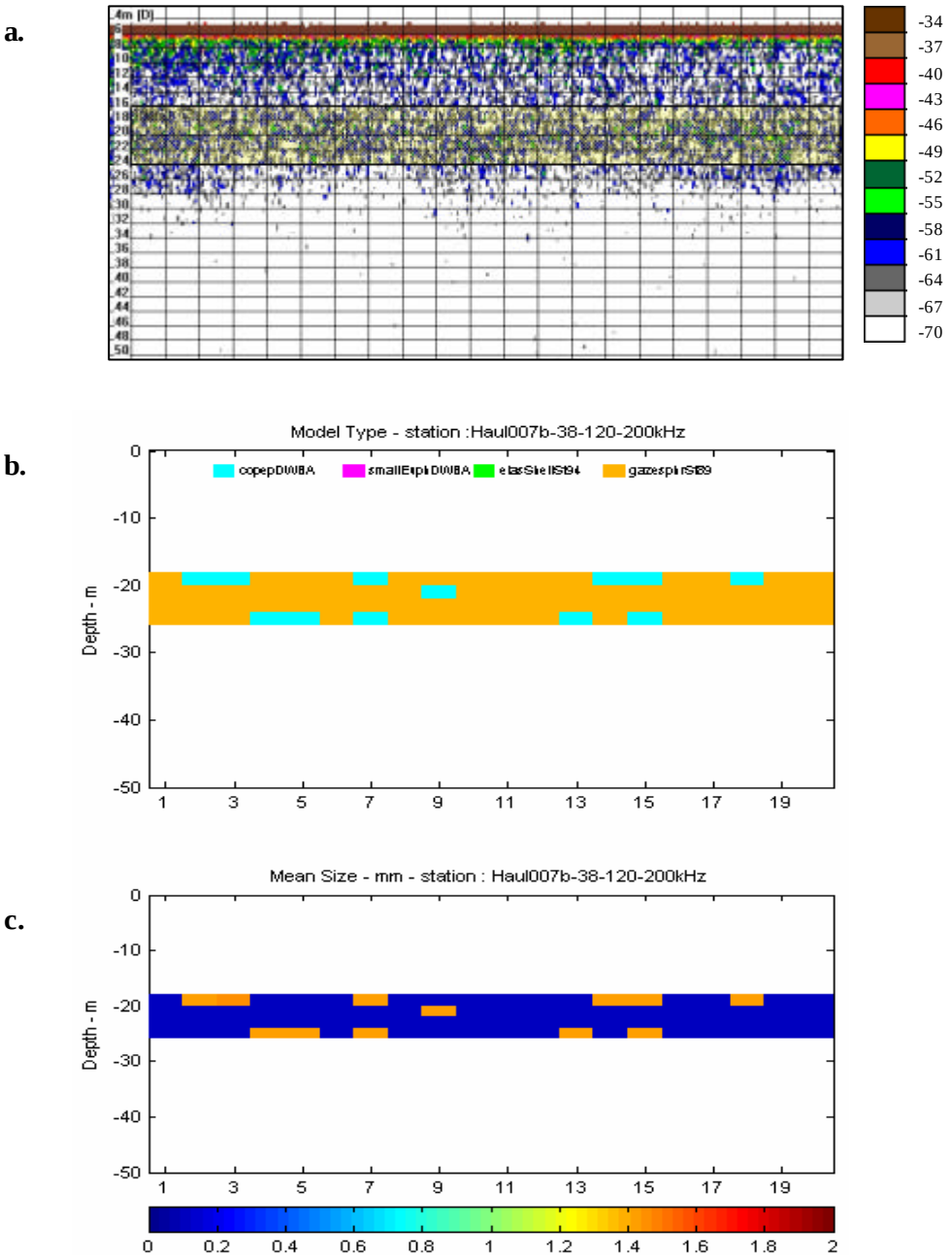

Fig. 3.7: Example graphical outputs from solutions of the inverse problems for Haul 007b. Depth is displayed on the y axis. ***a.*** *the 38 kHz echogram for the corresponding region, with the legend to the right showing the colours used to represent backscatter intensity (dB) in 3dB steps. The shaded area indicates the area sampled.* ***b.*** *the dominant predicted scatterer in each defined echogram cell, with a colour legend above.* ***c.*** *an approximate size for the types of scatterers predicted, with a colour legend along the bottom. Echogram column number is displayed on the x axis in* ***b*** *and* ***c****.*

Haul 007b covered a depth range of approx. 18 m to 26 m. Inverse problem solution predicted the dominant scatterers to be gaseous spheres of approx. 1 mm diameter, with some fluid prolate spheroid of 1.4 mm length.

Haul Number	Sampled zooplankton biovolume (mm^3 m^{-3})	Animal type dominant in catch (% of biovolume) [scatterer type]	Frequency (kHz)	Forward problem dominant scatterer at each frequency	Inverse problem dominant scatterers with approx. ESR (mm)
003a			38	cylinder	
003a	62.0	euphausiids (68%)	120	cylinder	fluid prolate spheroid (1.4), gaseous sphere (0.1)
003a			200	cylinder	
004b			38	cylinder	
004b	6.7	copepods > 1.2 mm (73%)	120	cylinder	gaseous sphere (0.1), some fluid prolate spheroid (1.4)
004b			200	spheroid	
005a			38	spheroid	
005a	4.2	copepods > 1.2 mm (58%)	120	spheroid	gaseous sphere (0.1), some fluid prolate spheroid (1.4)
005a			200	spheroid	
007a			38	spheroid	
007a	19.8	copepods > 1.2 mm (57%)	120	spheroid	gaseous sphere (0.1)
007a			200	spheroid	
007b			38	cylinder	
007b	29.4	euphausiids (46%)	120	cylinder	gaseous sphere (0.1), some fluid prolate spheroid (1.4)
007b			200	cylinder	
011a			38	spheroid	
011a	6.4	copepods > 1.2 mm (50%)	120	spheroid	gaseous sphere (0.1)
011a			200	spheroid	
0013			38	spheroid	
0013	3.5	copepods > 1.2 mm (54%)	120	spheroid	fluid prolate spheroid (1.4), elastic shelled (1.4)
0013			200	spheroid	
0014a			38	cylinder	
0014a	33.3	copepods > 1.2 mm (64%)	120	spheroid	fluid prolate spheroid (1.4), gaseous sphere (0.1)
0014a			200	spheroid	
0014b			38	cylinder	
0014b	4.6	euphausiids (47%)	120	cylinder	fluid prolate spheroid (1.4), elastic shelled (1.4)
0014b			200	cylinder	
0036			38	spheroid	
0036	7.0	copepods > 1.2 mm (44%)	120	spheroid	gaseous sphere (0.1)
0036			200	spheroid	

Table 3.7: Dominant scatterer types as identified by forward and inverse problems. For the forward problem, dominant scatterer type is given for each frequency. All three frequencies are used in arriving at solutions for the inverse problem, for which the best fit was found at the Equivalent Spherical Radius (ESR) shown in each case. The total biovolume of sampled animals in each haul and the type of animal which contributed most to this is also shown.

014a) were dominated by “fluid prolate spheroid” (approx. 1.4 mm) with some amount of “gaseous sphere” (approx 0.1 mm), and one (0014b) showed “fluid prolate spheroid” as dominant with some “elastic shelled” (approx. 1.4 mm) type.

Using physical animal measurements, and treating all animals as cylinders, biovolume for each haul was calculated. Table 3.7 provides a summary of results, showing which type of animal contributed most to each haul as a percentage of total sample biovolume calculated in this way, and also the dominant scatterer as predicted by forward and inverse problems.

Discussion

Zooplankton sampling regime

There was a large mismatch between predicted and observed backscatter at 38 kHz for most of the hauls, which is probably attributable to selective net sampling. The PSM collects samples on a continuous mesh system. In this study, it was installed in a U-tow vehicle with circular sampling apertures of 18 mm diameter, and towed at a normal survey speed of ten knots. The size of the sampling apertures immediately precludes the capture of larger animals. It may be expected that some fish larvae, also potentially strong 38 kHz scatterers, were present in the area of sampling. Cod larvae, for example, develop a swimbladder which dominates scattering by the time they are around 40 days old and 1.2 cm in length (Morrison, 1993; Chu et al, 2003) and are found in the North Sea from March to September (Beaugrad *et al.*, 2003), and the spawning times of other species such as haddock and whiting (Coull *et al.*, 1998) suggest that larvae of such species may be present. The total lack of these in any of the samples suggests that they either avoided the vehicle or were deflected away from the sampling apertures by its bow-wave. Siphonophores, another potentially strong scatterer at the frequencies under consideration (Benfield *et al.*, 2003), were also absent from the samples, although pieces of gelatinous material were occasionally found. It is possible that such animals were destroyed by the mechanism of the sampler and thus rendered unidentifiable. Larger gelatinous animals, such as *Aurelia aurita* and *Cyanea spp.*, which may have been present, and have similar anatomies to gelatinous species that have been shown to be strong acoustic targets at 38 kHz (Brierley *et al.*, 2001), were simply too large to be sampled.

Trials (described in the chapter "General Methods") which compared the performance of U-tow with the ARIES plankton sampler (Dunn *et al.*, 1993) appeared to confirm that U-tow sampled the zooplankton community effectively in that the same types of animals were found in samples from both, although the number of animals sampled by ARIES was often an order of magnitude higher. Animal abundances, when calculated by volume of water filtered, however, showed strong correlation. Similar results were found by Cook and Hays (Cook and Hays, 2001) when comparing U-tow's sampling capabilities with a WP2 net.

By artificially increasing zooplankton abundance values, the product of the forward problem, $MVBS_{pred}$, can be forced to approach $MVBS_{obs}$ more closely, with an increase of 5 to 10 dB

in $MVBS_{pred}$ resulting in a closer correlation with $MVBS_{obs}$ at 120 and 200 kHz. Such an increase is possible with a doubling of our sampled animal abundance at the same species composition, but this artificial method of moving predicted closer to observed values does not solve the difference in "curve" trend between 38 and 120 kHz. Similar manipulation of abundance results in an $MVBS_{pred}$ value at 38 kHz which is still around 20 dB lower than $MVBS_{obs}$ at that frequency. It can be said with some confidence, therefore, that simple under-sampling of the zooplankton community is not responsible for the difference between $MVBS_{pred}$ and $MVBS_{obs}$ at 38 kHz – rather, we must be failing to catch scatterers that give strong echoes at 38 kHz. These are likely to be non-crustacean zooplankton, fish or physical objects such as bubbles.

The most likely candidate scatterers that we failed to sample by net are those containing some form of gas inclusion, including small or larval fish with a developed swimbladder, siphonophores, other gas-bearing animals or some combination of these. There is a lack of published data relating larval or postlarval fish to strong 38 kHz scattering layers, but the presence of such a layer coinciding with samples containing small fish has been observed (M. Heath, FRS Marine Laboratory, Aberdeen, Scotland, personal communication). Larger, swimbladder-less fish may also have been present. It has been suggested that the presence of gas vacuoles in phytoplankton cells increases their target strength considerably at frequencies of 10-30 kHz (Selivanovsky *et al.*, 1996). Traces of phytoplankton were found in samples, but the abundance could not be measured quantitatively. Hydrodynamic wakes of animals such as squid and fish are reported to contain gas bubbles formed either by cavitation due to pressure drop or, in the case of the former, by the inclusion of phytoplankton cells containing gas in expelled jets of water (Selivanovsky and Ezersky, 1996). However, the characteristic linear traces produced by such wakes were not detected on the echograms here.

Additionally, many kinds of plankton from bacteria to large jellyfish produce exudates and excreta as by-products of feeding and metabolism. Most often these consist of sticky mucosubstances which aggregate to form marine snow. Such aggregations can be very numerous in the sea, and are quickly colonised by bacteria and microflagellates. These break down the substances and particles trapped within the matrix and add their own exudates and metabolic by-products (Kiørboe, 2001). Marine snow does not always simply sink as any gas

trapped in the matrix can result in varying degrees of buoyancy. Indeed, the aggregations may also trap bubbles rising from sediments or mixed down from surface waves. Such flocs are usually so fragile that nets are incapable of effectively sampling them. However, they must be considered as a potential source of scattering.

Elastic-shelled molluscs, identified by the inverse problem as an important scatterer type in one haul and present scatterers in two other hauls, may have been present in the water column but were not sampled. Such animals, e.g. *Limacina spp.*, appear commonly in North Sea zooplankton samples (J. Dunn, FRS Marine Laboratory, Aberdeen, Scotland, personal communication) and have a greater target strength than the types of animals which were sampled (Stanton *et al.*, 1996).

In this study, the sampling limitations of the U-tow vehicle have become apparent. Of primary concern are the small sampling apertures and the mechanics of sample collection within the PSM – resulting respectively in avoidance of the vehicle or destruction of animals on the mesh. Results show that the collected samples are not representative of the total scattering population, either due to under-sampling or an inability to sample a part of that population. The results of the forward and inverse problems show that possible under-sampling is more likely to affect our results at 120 and 200 kHz, whilst strong 38 kHz scatterers do not seem to have been sampled at all.

Forward model predictions

$MVBS_{pred}$ values were lower than $MVBS_{obs}$ in all cases. This is to be expected because net samples are unlikely to contain all scatterers sampled acoustically. $MVBS_{pred}$ approached unity with $MVBS_{obs}$ at 120 kHz more closely than at 38 or 200 kHz and with a better data fit as shown by regression analysis. This suggests that the numbers of organisms sampled are proportionally representative of those that are strong scatterers at this frequency. This appears to reinforce the proposition that 120 kHz scattering layers are strongly associated with mesozooplankton (smaller than krill), as found by in the Southern Ocean (Brierley and Watkins, 1996). Results of similar comparisons at 38 and 200 kHz were more variable, with 38 kHz $MVBS_{pred}$ in particular being considerably lower than $MVBS_{obs}$.

It should also be noted that assumptions were made when comparing $MVBS_{pred}$ and

$MVBS_{obs}$ values. It was assumed that the same population was sampled biologically and acoustically. Acoustic data recorded in the region of each haul were defined as accurately as possible according to sampler depth and distance behind the ship. At a speed of ten knots, however, the deployed sampler travelled through the water column at a distance of up to 450 m (about 1.5 minutes) behind the ship's transducers. Thus, acoustic and biological data are unlikely to have been matched exactly. It should also be noted that it is possible that rarely occurring strong scatterers represented in the acoustic data may not be biologically sampled either due to this time lag between acoustic and biological sampling, or because higher mobility may allow them to avoid the sampler. Fielding *et al.* (2004), for example, reported that a single pteropod represented 69.5% of model-predicted backscattering yet only 0.1% of sampled biovolume. This potentially large mismatch, however, was not found in this study.

Parameters used in the predictive acoustic modelling may require further investigation. In addition to problems with species composition, errors may arise due to the values for density contrast (g), sound-speed contrast (h) and animal orientation used in models. Values we have used may not be wholly appropriate for the types of zooplankton under consideration in the North Sea. There are limited published data on the subject of density and sound-speed contrast in zooplankton, none of which involve animals sourced from the North Sea (e.g. Chu and Copley, 2000; Chu and Wiebe, 2005; Kogeler *et al.*, 1987), and an acknowledged difficulty in determining *in situ* animal orientation (Foote and Stanton, 2000)

Inverse model predictions

Solution of the inverse problem for ten of the hauls showed in most cases that acoustic data most closely corresponded to expectations for gaseous spheres, with two hauls containing cells most closely matching the fluid prolate spheroid model mixed with cells matching the gaseous sphere model, and one haul most closely matching the fluid prolate spheroid model mixed with the elastic-shelled model. This would appear to confirm the suggestions above that the dominant scatterer, that was not sampled biologically, generally contained some form of gas inclusion.

Conclusion

The evidence presented here indicates that mesozooplankton, as sampled by U-tow, cannot be solely responsible for the strong 38 kHz scattering layer in the North Sea in summer. Artificial manipulation of sampled animal abundances showed that many more animals of

the types sampled were required to account for scattering at 38 kHz than at 120 or 200 kHz. Application of the inverse method suggested that some form of gaseous sphere type scatterer was present, but such scatterers were not found in samples (it is recognised that some types of zooplankton fall into this category). With this in mind, biological and acoustic sampling were repeated in the summer of 2004 with a view to further narrowing down the list of possible candidates which could be considered as responsible for the enhanced 38 kHz scattering.

Chapter 4

The contribution made by micronekton to the scattering layer

Introduction

It became clear following analysis of samples collected in summer 2003 that the U-tow did not comprehensively sample those scatterers responsible for the enhanced 38 kHz scattering layer. The most likely potential candidates were identified, by modelling, as targets containing some form of gas inclusion. Further, some candidates could be ruled out, for example larger fish (there were no typical discrete fish traces on echograms), and common zooplankton which were sampled in summer 2003 and shown not to be responsible for enhanced 38 kHz scattering

With this in mind, the biological sampling procedure was repeated in July 2004 using a Methot Isaac-Kidd Trawl (MIKT) net (Fig. 4.1) in place of the U-tow. The inverse problem solution had predicted that gaseous-type scatterers were most likely to be responsible for the observed enhanced 38 kHz scattering. The primary objective was therefore to attempt to sample larval or small fish, if present, in particular those possessing a swimbladder. In addition to 38, 120 and 200 kHz, acoustic data at 18 kHz was also collected during the 2004 cruise.

The MIKT net was chosen for similar reasons to U-tow in that it is easily operated, and therefore does not require extra manpower. It does, however, require the ship to be slowed to

Fig. 4.1: The MIKT net during deployment from the side-deck of FRV Scotia in summer 2004. The net is attached to a 1.5 m x 1.5 m metal frame, giving a mouth opening of 2.25 m^2. Animals entering the mouth of the net are directed along the length of the net (mesh size 2 mm) and trapped in the terminal cod-end (mesh size 200 micron).

Fig. 4.2: MIKT net cod-end. The re-usable cod-end is attached to the end of the net by a locking mechanism, and can be completely detached (as here) for sample collection and preservation..

3-4 knots and for this reason it was decided to deploy the MIKT immediately following fish-sampling trawl operations (that are a routine component of the herring acoustic survey). Fish sampling requires the ship to turn back from the normal survey track in order to deploy nets on fish marks identified on echograms. Following the trawl, the ship again turns to its original heading and returns to the survey track. The time taken to return to the position where normal survey conditions resume was sufficient to deploy the MIKT net and obtain a sample. In this way, disruption to survey operations was minimised.

The MIKT net (mesh size: 2 mm) is attached to a square metal frame with dimensions of approximately 1.5 m by 1.5 m (Fig. 4.1). This means that the mouth opening is approximately 2.25 m^2, considerably larger than U-tow. The main effect of this is that animals will be less able to avoid the sampler, although the relatively slow speed at which it must be towed might aid such efforts. The large mouth size is also likely to catch gelatinous animals, although more fragile animals of this type are still destroyed. For other animal types, sample preservation is excellent. Animals entering the mouth of the net are directed along the mesh and into a removable 200 µm mesh cod-end bag (Fig. 4.2). Sample size is much larger than either U-tow or ARIES. The cod-end has a capacity of several litres, and this contributes to good physical preservation of collected animals.

However, the large mouth size, small mesh size and large cod-end taken together can cause

Fig. 4.3: Sampled animals in a container of approx. 30 cm diameter after removal from the MIKT net's cod-end. This sample contained several adult pipefish as well as some small juvenile fish (e.g. upper right of picture) along with a large number of small copepods and other animals.

Methods

Sample collection

A Methot Isaac-Kidd Trawl net (MIKT) was deployed from the side deck of FRV Scotia during the summer 2004 North Sea Herring Survey to collect plankton and micronekton samples. The cruise track is shown in Fig. 4.4. Due to the necessity for ship speed to be reduced, the net was deployed immediately following fishing operations, when the ship was returning to the survey track. This facilitated the required towing speeds of 3 - 4 knots.

A manual record was made of ship speed, time and position of deployment / recovery and wire paid out for each haul. Other environmental variables were also noted for possible future reference. Sampling depth was controlled by varying the amount of wire paid out until a signal from the attached depth sensor unit (SCANMAR HC4-D: Scanmar AS, Asgardstrand, Norway) showed that the required depth had been reached. Sampling depth could thus be determined to within 0.1 m at one minute intervals.

For each tow, the MIKT was deployed for approximately twenty minutes at a depth

problems when a large concentration of jellyfish is encountered. On one occasion on this cruise, the cod-end bag filled with jellies, the quantity of which continued for some tens of centimetres up the net when held vertically. Recovery of the net can be problematic in such cases due to the weight of animals in the net. Large sample volume also leads to increased analysis time due to the number and diversity of animals that may be present (Fig. 4.3).

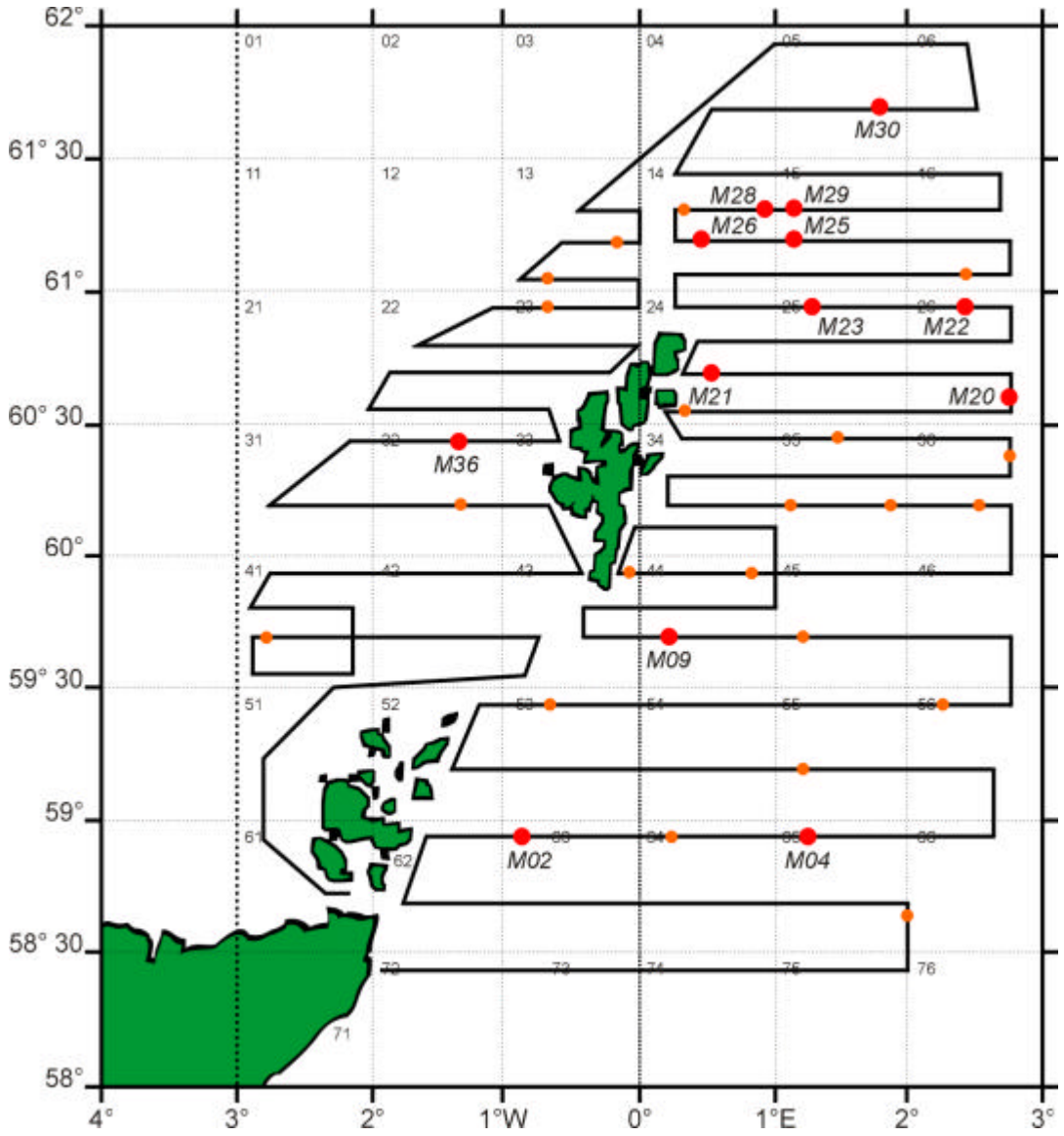

Fig. 4.4: Cruise track for FRV Scotia North Sea Herring Survey cruise 1004s. Red circles denote successful MIKT deployments which formed the basis for this analysis, and are accompanied by haul numbers. Smaller, orange circles denote failed deployments, where unforeseen circumstances prevented reliable sample collection. ICES statistical square numbers are shown for Area IVa, which is delineated to the West by a thicker dotted line here.

Haul identifier	m02	m04	m09	m20	m21	m22	m23	m25	m26	m28	m29	m30	m36
Date	3.7.04	4.7.04	6.7.04	10.7.04	10.7.04	11.7.04	11.7.04	14.7.04	14.7.04	14.7.04	15.7.04	15.7.04	18.7.04
Sea surf. Temp (ºC)	12.5	13.2	12.98	13.51	12.18	13.48	12.24	12.63	12.46	12.8	12.7	12.9	12.9
Wind Spd (kts)	11.8	9.9	17.1	23.4	17	15	32	3.6	4.5	3.1	20.3	18.2	24
Wind direction (deg)	343	322	292	36	36	350	332	154	222	238	275	274	190
Ship speed (kts)	3.8	3.5	3	3.5	3.5	3	3.5	3.4	3.6	3.5	3	3	3
Ship speed (m/h)	7037.6	6482	5556	6482	6482	5556	6482	6296.8	6667.2	6482	5556	5556	5556
ICES Sq. No.	46 E8a	46 F0a	48 E9c	50 F1c	50 E9d	50 F1a	50 F0a	51 F0c	51 E9d	51 E9b	51 F0a	52 F0d	49 E7b
Ship Heading (deg)	65	97	274	37	25.4	344	359	258	270	56	265	265	175
GPS Start	58.55N	58.55N	59.40N	60.41N	60.40N	60.55N	60.55N	61.11N	61.10N	61.17N	61.25N	61.40N	60.25N
	1.50W	0.17E	0.33E	1.13E	0.14W	1.20E	0.60E	0.09E	0.23W	0.24W	0.06E	0.58E	2.13W
GPS end	58.55N	58.55N		60.42N	60.41N	60.56N	60.56N	61.10N	61.10N	61.17N	61.20N	61.40N	60.25N
	1.48W	0.19E		1.14E	0.13W	1.20E	0.50E	0.70E	0.26W	0.22W	0.50E	0.56E	2.13W
Depth 1 (m)	**30**	**30**	**35**	**17**	**35**	**33**	**40**	**25**	**24**	**40**	**40**	**19**	**17**
Time start (GMT)	19:07	09:53	14:54	13:06	19:01	13:57	19:21	08:41	12:30	19:52	13:20	22:30	15:54
Time end (GMT)	19:29	10:16	15:16	13:23	19:21	14:12	19:41	00:00	12:55	20:15	13:47	22:53	16:15
Line out (m)	100	110	130	110	150	124	140	120	130	130	130	80	120
MIKT offset (m)	117.85	128.83	148.40	133.36	169.68	142.74	157.16	141.39	152.17	146.28	146.28	100.90	143.70
MIKT offset (min:s)	01:00.3	01:11.5	01:36.2	01:14.1	01:34.2	01:32.5	01:27.3	01:20.8	01:22.2	01:21.2	01:34.8	01:05.4	01:33.1
Adusted end time	19:30:00	10:17:12	15:17:36	13:24:14	19:22:34	14:13:32	19:42:27	0:01:21	12:56:22	20:16:21	13:48:35	22:54:05	16:16:33
Volume sampled (m3)	5008	4371	4163	3885	4613	2706	4613	4482	5744	5099	5203	4371	3954
No. samples	1	1	1	1	1	1	1	1	1	1	1	1	1

Table 4.1: Summary of data for the thirteen MIKT net hauls analysed in this study. All hauls came from the North Sea in July 2004. The first part of the table shows the date and conditions particular to each haul, with logged ship speed (knots) also converted to metres per hour. Geographical position for start and end of haul and the length of warp paid out are also shown. From this, and knowing the sampling depth of the net, a simple trigonometrical calculation allowed the net's average distance behind the transducer to be determined. With knowledge of the ship's speed, this was converted to a time value, which was used to horizontally shift defined areas of echograms which then corresponded as closely as possible to the area sampled. The volume of water sampled in each haul is also shown. This was calculated by multiplying the area of the MIKT net's mouth (2.25 m2) by the distance travelled during each haul).

coinciding with a strong 38 kHz scattering layer observed on live-viewed echograms. The MIKT used was a single-net system, and so samples inevitably included any animals at shallow depths which the gear encountered during deployment to, and recovery from, the targetted depth. Wire was paid out as quickly as possible to reach the required depth in order to minimise the catch of such animals, which could not reliably be related to acoustic data

due to the absence of acoustic data from near-surface depths. At the end of each tow, the MIKT was recovered as quickly as possible for the same reason.

Animals entering the mouth of the MIKT are directed along the net and into a terminal 200 µm mesh cod-end bag. On recovery, samples were washed out and preserved in 4% formalin for later analysis in the laboratory.

The volume of water filtered during each tow was calculated by taking into account the area of the MIKT net's mouth, the ship speed and the sampling period.

The MIKT net was deployed thirty-six times in total during the cruise. However, some of the samples thus collected had to be disregarded for various reasons including a lack of, or unusable, concurrent acoustic data, failure of the net and failure of the depth sensor. Thirteen hauls provided samples which could be reliably related to acoustic data. Parameters for these are summarised in Table 4.1.

Sample analysis

Analysis of samples was carried out in the laboratory after the cruise. All large animals (including fish larvae and juveniles, large decapods, large euphausiids and amphipods over 5mm) were removed from samples for enumeration and measuring. Fish were identified at least to family, and the approximate swimbladder size in those fish which possessed one was calculated. Other conspicuous animals such as juvenile cephalopods, large euphausiids and decapods were also removed, counted and measured at this stage. The remaining animals were then sub-sampled in order to count and measure smaller organisms such as copepods, small euphausiids, gastropod molluscs, etc. The percentage of total animal numbers contributed by each animal type was calculated.

Copepods were divided into several categories, although size and morphological characteristics of some of these are similar. Categories included: *Calanus finmarchicus:* C6 adult, copepodite stage C5 and copepodite stages 1-4; *Euchaeta spp.* C5-6; *Eucalanus spp.* C5-6; *Metridia spp.; Oithona spp.;* small calanoid copepods < 1.2 mm; and Cyclopoid *spp.* Euphausiids and decapods were separated into "large" and "small" categories, with the former including animals over 10 mm in length measured from the front of the eye to the tip

of the telson. Amphipods were also separated in this way. Jellyfish were separated into two categories of “large” and “small” where relevant, but this was only necessary when more than one species was present with obvious size differences. Gastropod molluscs were similarly separated into “large” and “small” categories.

Dividing the number of individuals in each category by the volume of water sampled in that haul as calculated above gave an abundance figure describing the number of animals per cubic metre of sampled water. An approximate biovolume (mm^3/m^3) for each category was then calculated using mean animal measurements and these abundance values. Most animal types were treated as full cylinders for this purpose, with the exception of copepods and amphipods which were treated as prolate spheroids, gastropod molluscs which were treated as spheres, and juvenile flatfish which were treated as prolate spheroids. The percentage contribution to sample biovolume made by each animal type was also calculated.

Forward model predictions

The forward problem was used to predict backscattering values for each sample at each of the four sound frequencies, 18, 38, 120 and 200 kHz. By this method, expected backscattering for each animal type was calculated according to physical measurements and abundance.

Larval and juvenile fish were split into two categories of scatterer: those with and those lacking a swimbladder. Fish without swimbladders were treated as fluid bent cylinders (or fluid prolate spheroid in the case of flatfish) with whole-body measurements taken into consideration. Because a gaseous inclusion will strongly dominate scattering from an individual, those fish types which possessed a swimbladder were modelled as gaseous spheres having an equivalent spherical radius (ESR) to the approximate swimbladder volume. The rest of the body of such fishes was disregarded at this stage due to the scattering dominance of the swimbladder (McCartney and Stubbs, 1971; Foote, 1980; Chu *et al.*, 2003).

Model output target strengths (TS) were converted to MVBS (dB) on the basis of numerical densities sampled. The resultant values for each animal type were added in the linear domain to give a total $MVBS_{pred}$ for each haul. The dominant type of sampled scatterer was

identified as that which made the greatest contribution to total $MVBS_{pred}$.

Acoustic data collection and analysis

Acoustic data were collected according to methods described in the "General Methods" chapter. Regions of echograms corresponding to the MIKT net's position in the water at the

	Haul Identifier	M02	M04	M09	M20	M21	M22	M23	M25	M26	M28	M29	M30	M36
Calanus finmarchicus	**C6(adult)**	4.99	1.78		1.35			7.63	0.53	0.49	0.76	0.08	2.48	4.65
	copepodite C5	2.35	5.34	9.94	1.76	0.75	0.48	9.44	1.33	6.97	13.22	0.32	21.48	5.01
	copepodite C1 - C4	1.61	15.71	7.95	0.83	1.50	0.95	4.02	1.86	0.56	5.72	0.28	13.79	1.43
							0.95							
Other calanoid	**Euchaeta spp. C56**							0.20	1.73	0.05	0.11			
	Eucalanus						0.95			0.02	0.11	0.04	0.09	8.58
	C1-C5 small <1.2mm	**81.43**	14.53	15.90	**47.01**		0.48	**53.23**	**88.23**	**87.20**	**79.65**	**98.37**	**54.99**	18.60
	Metridia spp.					**73.50**	**58.42**		0.07	0.12				
	Oithona spp.		1.05							0.15				
Euphausiid	**large**	1.83E-03						0.20	0.13				0.00	2.15
	small	1.17	0.18					1.41	0.40	0.02	0.22		5.39	1.07
Decapoda	**large**	1.61		4.22	0.10	1.50			1.40					17.89
	small	1.61	0.27	**35.78**	0.21	0.75	0.17	9.04	1.93	0.15				13.95
	small crab					5.25	8.59							
Amphipoda	**large**													0.36
	small		0.09		18.68	0.01						0.20		0.36
Worms	**Polychaeta**	0.15	**48.29**		0.10			0.60						
	Temopteris worms	0.04	0.14		0.10			0.40						1.79
Chaetognatha	**Chaetognatha spp.**	0.44	0.98	9.94	1.35	0.75		0.20		0.07	0.22		0.18	
Gelatinous	**Hydrozoan spp.**	0.35		14.41	6.75	3.00	1.91	7.63						4.47E-03
	Small hydrozoans	2.16					13.84							**22.18**
													5.39	
Fish	**Gadoid large**	0.02	4.57E-03	0.07	0.02			0.11	0.26	0.01	2.25E-04	1.69E-04	8.84E-04	0.05
	Gadoid small	0.07	0.02		0.05	0.13	0.02	0.76	1.47	0.02	2.25E-04	1.69E-04	8.84E-04	0.26
	Sandeel	0.07	0.01	0.22	0.29	0.73	0.30	0.21	2.22E-03	1.62E-03	2.25E-04	1.69E-04		0.21
						0.37	0.42							
	Flatfish juv.	0.14	0.01	1.14	0.01			0.51	2.22E-03					0.12
	Cyclopterus spp.	0.07	1.14E-03			0.33	0.03				2.25E-04			0.04
	Gurnard spp.				1.73E-03			0.01		4.05E-04				0.05
	Pipefish adult					0.01	0.01		4.44E-03	4.05E-03	2.25E-04	3.38E-04		0.16
	Pipefish juv/larvae	1.83E-03		0.02	1.73E-03			0.18	0.04	0.06	0.01	4.40E-03	3.54E-03	4.47E-03
						0.12	0.05							
Echinodermata			0.01									0.69		
Mollusca	**Limacina spp. large**		0.32							0.02				
	Limacina spp. small	0.59	11.15		2.59		0.01	1.00	0.60	4.08				0.72
	Cephalopod juvenile													0.01
	Clione				0.10	0.03								

Table 4.2: The percentage of total animal numbers contributed by each animal type from each haul. The animal type which contributed the highest percentage is highlighted in bold in each case. Most samples were dominated numerically by small copepods. However, hauls M04, M09 and M36 were dominated by polychaetes, small decapods and small hydrozoans respectively.

time of each haul were identified using SCANMAR depth data, haul start/end times and amount of warp paid out. For example, when the MIKT net was towed at 25 m depth it was found to be 140 m behind the vessel, so a delay of 1 minute 21 seconds was needed to align acoustic data with the MIKT net's position. Distance behind the ship varied considerably from haul to haul (Table 4.1).

An "observed" mean volume backscatter strength ($MVBS_{obs}$) value for each defined haul region was obtained via echo integration at each of the four frequencies.

$MVBS_{pred}$ was compared with $MVBS_{obs}$ and plots made of the relationship at each frequency. Regression analyses were performed at all frequencies, and R^2 values calculated. Plots were also made of $MVBS_{pred}$ against $MVBS_{obs}$ for hauls which contained adult pipefish (M25, M26, M28, M29), and for one of those hauls (M29) where a relatively close relationship between $MVBS_{pred}$ and $MVBS_{obs}$ was found.

Inverse model predictions

Acoustic data collected from the regions of the analysed hauls was inversely modelled in order to predict the dominant scatterers in each. Data at 18, 38, 120 and 200 kHz were used, and modelling parameters set as described in the previous chapter "General Methods".

Results

Sample analysis

Initial coarse shipboard examination of MIKT net samples showed that fish larvae and gastropod molluscs were present. Jellyfish were also to be found in some of the samples.

The percentage composition of each haul by animal type is given in Table 4.2. Small copepods < 1.2 mm (including *Metridia spp.*) were generally the most abundant animal type, except in hauls M04, M09 and M36 which were numerically dominated by small polychaetes, small decapods and small jellyfish respectively. Measurements of animal length and cylindrical radius were made from subsamples (n=20) of each animal type found in each sample, allowing calculation of biovolume ($mm^3\ m^{-3}$). Each animal type's contribution to total sample biovolume per metre cubed of sampled water could then be estimated. Table 4.3 shows an example of the results of these calculations for one haul (M02). Due to the

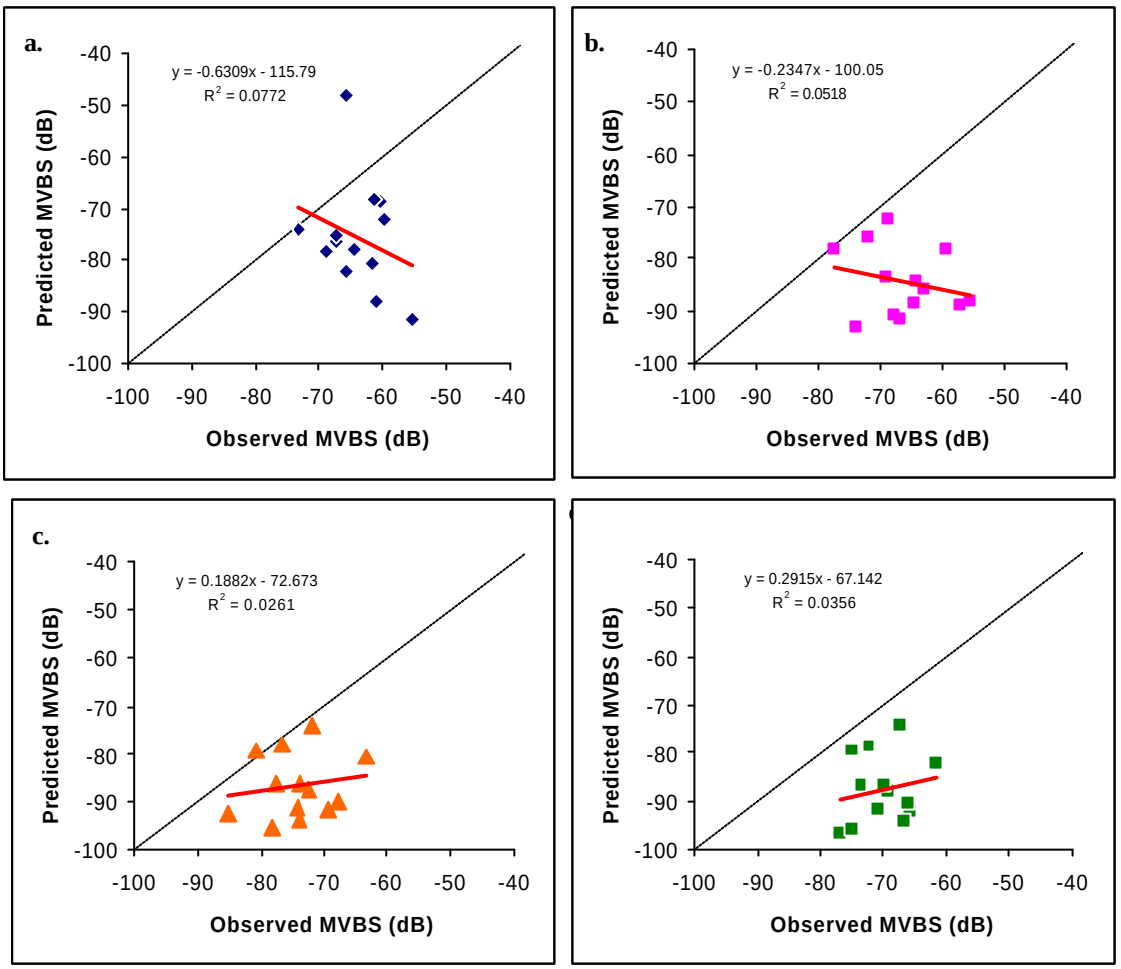

*Fig. 4.5: Predicted MVBS plotted against observed MVBS for each haul at each of the four sound frequencies (**a**. 18 kHz, **b.** 38 kHz, **c.** 120 kHz, **d.** 200 kHz) used in the study. In each case, the dotted line represents a 1:1 relationship, whilst the regression line is shown in red. The regression line equation and R^2 value is shown on each plot. One haul showed a far greater predicted than observed MVBS at 18 kHz - this was found to correspond to the maximum Sv found via echo-integration of acoustic data. Most predicted values were less than observed values at all frequencies and for all hauls.*

differing sizes of various animal types, that which is numerically dominant will not necessarily contribute most to sample biovolume. For example, in haul M02 small copepods contributed 81.43% to animal numbers, but only 1.17% of sample biovolume, due to the presence of some much larger jellyfish. The percentage of total biovolume contributed by each sampled animal type is given in Table 4.4. The biovolume of most hauls was dominated by gelatinous hydrozoans, with several dominated by small copepods and one by adult pipefish.

1004s MIKT sample analysis		Haul M02				
		Mean length (mm)	Abundance (no. m^{-3})	Biovolume (mm^3/m^3)	%age of total biovolume m^{-3}	%age of total no. of animals
Calanus finmarchicus	C6 (adult)	2.31	0.54	2.74	2.09	4.99
	copepodite C5	2.03	0.26	0.88	0.67	2.35
	copepodite C1 - C4	1.68	0.18	0.34	0.26	1.61
Other calanoid	Euchaeta spp. C5-6	0.75	8.86	1.53	1.17	81.43
	Eucalanus					
	C1-C5 small <1.2mm					
	Metridia spp.					
	Oithona spp.					
Euphausiid	large	10.00	0.00	0.01	0.01	0.00
	small	7.13	0.13	3.23	2.47	1.17
Decapoda	large	3.75	0.18	0.65	0.49	1.61
	small	2.33	0.18	0.16	0.12	1.61
	small crab					
Amphipoda	large					
	small					
Worms	Polychaeta	3.90	0.02	0.07	0.05	0.15
	Temopteris worms	9.00	0.00	0.20	0.16	0.04
Chaetognatha	Chaetognatha spp.	14.50	0.05	10.22	7.80	0.44
Gelatinous	Hydrozoan spp.	7.05	0.04	46.98	35.83	0.35
	Small hydrozoans	4.05	0.23	54.55	41.61	2.16
Fish	Gadoid large	17.00	0.00	0.19	0.15	0.02
	Gadoid small	11.10	0.01	0.22	0.17	0.07
	Sandeel	18.44	0.00	0.04	0.03	0.07
	Flatfish juv.	24.70	1.58E-02	4.98	3.80	0.14
	Cyclopterus spp.	12.20	0.01	4.05	3.09	0.07
	Gurnard spp.					
	Pipefish adult					
	Pipefish juv/larvae	33.00	0.00	0.04	0.03	0.00
Echinodermata	Larvae					
Mollusca	Limacina spp. large					
	Limacina spp. small	0.49	0.06	0.03	0.02	0.59
	Cephalopod juvenile					
	CLIONE					
			Abundance	Biovolume		
	TOTALS		10.76	131.11		

Table 4.3: An example of results obtained for mean length, abundance and biovolume for one haul (M02). The percentage contributed by each animal type to biovolume and total animal numbers was also calculated for each haul. Mean length was determined by measuring subsamples of each animal type found in a particular sample, and averaging the measurements. For biovolume calculations, copepods and amphipods were treated as prolate spheroids, Limacina molluscs were treated as spheres and all other animal types were treated as cylinders. Not all animal types were found in all hauls.

	Haul Identifier	M02	M04	M09	M20	M21	M22	M23	M25	M26	M28	M29	M30	M36
Calanus finmarchicus	**C6(adult)**	10.45	10.45		1.95	0.73	0.01	2.06	1.44	2.94	3.45	1.43	8.80	0.43
	copepodite C5	0.67	22.13	0.10	1.88	1.08	0.01	1.77	2.59	26.48	**35.11**	4.41	**57.61**	0.30
	copepodite C1 - C4	0.26	19.72	0.03	0.37			0.33	2.08	0.94	9.07	1.68	22.16	0.04
Other calanoid	**Euchaeta spp. C5&6**						0.02	0.10	7.17	0.15	0.41			
	Eucalanus						0.01			0.53	5.68	1.45	0.98	5.69
	C1-C5 small <1.2mm	1.17	2.43	0.01	3.16	2.31	0.03	0.46	6.92	16.19	14.96	**68.15**	8.78	0.06
	Metridia spp.								0.08	0.12				
	Oithona spp.		0.06							0.03				
Euphausiid	**large**	0.01						1.23	1.12				0.05	0.23
	small	2.47	3.25			25.65		0.76	0.05	0.04	0.16		0.81	0.04
Decapoda	**large**	0.49		1.56	0.79	0.42	0.02		2.54					0.43
	small	0.12	0.18	1.04	0.20	2.84	0.07	1.56	2.24	0.22				0.21
	small crab													
Amphipoda	**large**					0.18								0.08
	small		0.01		0.17							0.06		0.00
Worms	**Polychaeta**	0.05	6.00		0.06			0.11						
	Temopteris worms	0.16	0.15		0.46	1.95		0.26						0.06
Chaetognatha	**Chaetognatha spp.**	7.80	**30.61**	1.44	8.41	**36.03**	0.03	0.57		2.80E-03	0.31		0.37	
Gelatinous	**Hydrozoan spp.**	**35.83**		**94.87**	**78.62**		**96.52**	**86.34**						**84.40**
	Small hydrozoans	41.61												3.06
Fish	**Gadoid large**	0.15	1.46	0.24	1.62	8.55	0.03	1.44	32.46	2.11	0.22	0.38	0.39	0.57
	Gadoid small	0.17	0.36		1.07	3.56	0.05	1.22	26.98	0.95	0.05	0.15	0.03	1.35
	Sandeel	0.03	0.42	0.01	0.82	2.10	2.10E-03	0.36	0.04	0.05	1.76E-03	3.86E-03		0.03
	Flatfish juv.	3.80	0.42	0.57	0.04	6.98	0.01	1.35	0.01					0.87
	Cyclopterus spp.	3.09	0.40								0.01			0.16
	Gurnard spp.				0.01	0.16	3.99E-04	0.03		0.02				0.05
	Pipefish adult								14.22	**48.48**	0.57	21.27		0.15
	Pipefish juv/larvae	0.03		9.65E-04	0.01	0.07	3.21	0.04	0.02	0.09	30.01	0.03	0.01	0.00
Echinodermata												0.98		
Mollusca	**Limacina spp. large**		0.54				1.90E-03			0.05				
	Limacina spp. small	0.02	1.41		0.21		4.41E-04	0.01	0.03	0.61				0.00
	Cephalopod juvenile					7.40								1.79
	Clione				0.15									

Table 4.4: The percentage of total sampled biovolume contributed by each animal type from each haul. The animal type which contributed the highest percentage is highlighted in bold in each case. Most samples were dominated numerically by small copepods. However, gelatinous animals dominated biovolume in most cases, except hauls M28 and M30 (C5 stage Calanus finmarchicus), M29 (small calanoid copepods), and M26 (adult pipefish).

1004s MIKT sample analysis		Haul M02					
		Mean length (mm)	Abundance (no. m^{-3})	$MVBS_{pred}$ 18 kHz (dB)	$MVBS_{pred}$ 38 kHz (dB)	$MVBS_{pred}$ 120 kHz (dB)	$MVBS_{pred}$ 200 kHz (dB)
Calanus finmarchicus	**C6 F**	2.31	5.43E-01	-150.21	-137.30	-118.10	-110.81
	C5	2.03	2.56E-01	-156.84	-143.91	-124.54	-116.87
	C1 - C4	1.68	1.76E-01	-163.40	-150.45	-130.88	-122.83
Other calanoid	**Euchaeta spp. C5-6**	0.75	8.86E+00	-167.38	-154.41	-134.51	-125.80
	Eucalanus						
	C1-C5 small <1.2mm						
	Metridia spp.						
	Oithona spp.						
Euphausiid	**large**	10.00	2.00E-04	-160.40	-147.89	-131.45	-125.67
	small	7.13	1.28E-01	-144.10	-131.36	-113.65	-107.26
Decapoda	**large**	3.75	1.76E-01	-159.40	-146.49	-127.27	-119.65
	small	2.33	1.76E-01	-171.79	-158.84	-139.16	-130.85
	small crab						
Amphipoda	**large**						
	small						
Worms	**Polychaeta**	3.90	1.60E-02	-177.09	-164.18	-144.95	-137.27
	Temopteris worms	9.00	3.99E-03	-155.58	-142.95	-125.85	-119.36
Chaetognatha	**Chaetognatha spp.**	14.50	4.79E-02	-139.56	-127.43	-111.60	-105.26
Gelatinous	**Hydrozoan spp.**	7.05	3.83E-02	-141.25	-129.44	-126.27	-123.24
	Small hydrozoans	4.05	2.35E-01	-147.59	-134.99	-119.67	-122.03
Fish	**Gadoid large (sb)**	17.00	1.80E-03	-88.09	-93.10	-94.52	-95.43
	Gadoid small (sb)	11.10	7.39E-03	**-76.45**	**-89.02**	**-91.65**	**-92.20**
	Sandeel (no sb)	18.44	1.80E-03	-147.71	-136.00	-120.72	-114.68
	Flatfish juv. (no sb)	24.70	1.58E-02	-108.18	-97.79	-93.53	-92.67
	Cyclopterus spp. (no sb)	12.20	7.99E-03	-128.84	-116.62	-102.33	-100.52
	Gurnard spp. (sb)						
	Pipefish adult (sb)						
	Pipefish larva/juv. (sb)	33.00	2.00E-04	-96.60	-97.03	-97.68	-98.66
Echinodermata	**larvae**						
Mollusca	**Limacina large**	0.49	6.39E-02	-161.23	-148.25	-128.29	-119.58
	Limacina small						
	Squid juv.						
	CLIONE						
	TOTAL MVBSpred		**M02**	-76.45	-89.02	-91.64	-92.07

Table 4.5: An example of results obtained for predicted mean volume backscatter ($MVBS_{pred}$) for each animal type in one haul (M02). Fish with a swimbladder (sb) were modelled as gaseous spheres according to approximate swimbladder size, whilst those without swimbladder (no sb) were modelled as fluid-filled cylinders according to fork length.. MVBS was calculated for each sampled animal type and abundance via the forward problem using models described in the text. These logarithmic decibel values were then added in the linear domain for each frequency and the result logged to give a total MVBSpred at each of the four sound frequencies 18, 38, 120 and 200 kHz. The dominant sampled scatterer in this haul was "Gadoid small". MVBS values for this type are shown in bold.

		Mean length (mm)	S.D.	18 kHz $MVBS_{pred}$ (dB)	38 kHz $MVBS_{pred}$ (dB)	120 kHz $MVBS_{pred}$ (dB)	200 kHz $MVBS_{pred}$ (dB)
Calanus finmarchicus	**C6(adult)**	2.33	0.06	-155.58	-142.67	-123.48	-116.21
	copepodite C5	2.06	0.05	-155.51	-142.58	-123.23	-115.61
	copepodite C1 - C4	1.60	0.12	-161.65	-148.71	-129.10	-120.98
Other calanoid	**Euchaeta spp. C5-6**	2.51	0.43	-160.00	-147.10	-128.07	-121.13
	Eucalanus	3.71	1.14	-149.66	-136.87	-119.12	-115.01
	C1-C5 small <1.2mm	0.77	0.04	-172.06	-159.08	-139.19	-142.43
	Metridia spp.	1.55	0.36	-175.68	-162.73	-143.11	-134.95
	Oithona spp.	0.60	0.18	-187.59	-174.61	-154.69	-145.93
Euphausiid	**large**	12.41	6.81	-147.14	-134.93	-119.13	-114.68
	small	5.20	2.95	-159.49	-146.68	-128.15	-121.01
Decapoda	**large**	6.35	3.32	-154.05	-141.30	-123.21	-116.40
	small	3.51	0.91	-162.78	-149.86	-130.57	-138.88
	small crab						
Amphipoda	**large**	6.68	4.77	-164.67	-152.42	-140.70	-137.38
	small	0.86	0.26	-183.76	-170.78	-150.90	-142.20
Worms	**Polychaeta**	2.94	1.27	-177.23	-164.30	-144.81	-136.75
	Temopteris worms	7.21	4.06	-157.00	-144.31	-126.37	-119.47
Chaetognatha	**Chaetognatha spp.**	9.42	4.46	-158.72	-146.17	-128.81	-121.91
Gelatinous	**Hydrozoan spp.**	19.08	25.90	-134.04	-126.52	-120.80	-118.79
	Small hydrozoans	2.71	1.90	-158.13	-145.36	-127.96	-125.21
Fish	**Gadoid large**	27.22	6.20	-89.45	-91.42	-93.01	-94.80
	Gadoid small	15.23	5.31	-79.35	-89.98	-92.10	-93.21
	Sandeel	15.99	5.49	-145.79	-136.04	-121.69	-116.09
	Flatfish juv.	16.70	6.65	-127.04	-115.49	-104.90	-105.79
	Cyclopterus spp.	9.47	2.57	-141.14	-128.70	-113.54	-111.97
	Gurnard spp.	18.03	3.43	-86.97	-87.89	-90.51	-92.18
	Pipefish adult	276.25	63.95	-87.13	-86.81	-85.48	-84.72
	Pipefish juv/larvae	20.86	6.27	-91.09	-92.43	-92.97	-93.44
Echinodermata	**Echinoderm larv.**	1.85	1.88	-159.97	-147.07	-128.10	-121.45
Mollusca	**Limacina spp. large**	1.38	1.14	-149.73	-136.75	-116.84	-108.38
	Limacina spp. small	0.36	0.08	-166.13	-153.15	-133.19	-124.43
	Cephalopod juvenile	10.75	5.30	-143.75	-131.67	-120.44	-119.67
	Clione	1.05		-185.60	-172.63	-152.72	-143.99

Table 4.6: Mean length of different animal types with standard deviation (S.D.) across the thirteen hauls under consideration. Average $MVBS_{pred}$ values are given for each type at each of the four sound frequencies (18, 38, 120 and 200 kHz).

Forward model predictions

Using the measurements made during sample analysis, predicted MVBS was calculated for each animal type in each haul. An example of the results - again for haul M02 - is shown in Table 4.5. In this case, the dominant sound scatterer among sampled animals was the swimbladdered fish type "gadoid small". It may be noted that this type was neither

Haul	Forward Problem dominant sampled scatterer with mean body length and approximate swimbladder ESR (mm)				Inverse Problem predicted dominant scatterer with approximate ESR (mm)
	Sound frequency (kHz)				
	18	38	120	200	
M02	Gadoid juv (11.1, 1.75)	Gadoid juv (11.1, 1.75)	Gadoid juv (11.1, 1.75)	Gadoid juv (11.1, 1.75)	G.S. (0.1 - 4)
M04	Gadoid juv (22.7, 1.38)	Gadoid juv (22.7, 1.38)	Gadoid juv (22.7, 1.38)	Gadoid juv (22.7, 1.38)	G.S. (0.1), F.P.S. (3), E.S. (0.1)
M09	Gadoid juv (20.0, 3.15)	Gadoid juv (20.0, 3.15)	Gadoid juv (20.0, 3.15)	Gadoid juv (20.0, 3.15)	E.S. (0.1), some G.S. (0.1 - 4)
M20	Gadoid juv (14.9, 2.35)	Gadoid juv (14.9, 2.35)	Gadoid juv (14.9, 2.35)	Gadoid juv (14.9, 2.35)	G.S. (0.1)
M21	Gadoid juv (10.9, 1.72)	Gadoid juv (10.9, 1.72)	Gadoid juv (10.9, 1.72)	Gadoid juv (10.9, 1.72)	G.S. (0.1 + 1.5), some E.S. (1)
M22	Gadoid juv (14.9, 2.35)	Gadoid juv (14.9, 2.35)	Gadoid juv (14.9, 2.35)	Gadoid juv (14.9, 2.35)	G.S. (0.1 - 4)), E.S. (0.1)
M23	Gadoid juv (11.4, 1.79)	Gadoid juv (11.4, 1.79)	Gadoid juv (11.4, 1.79)	Gadoid juv (11.4, 1.79)	G.S. (0.1 - 4)
M25	Gadoid juv (11.9, 1.87)	Gadoid juv (11.9, 1.87)	Gadoid juv (11.9, 1.87)	Gadoid juv (11.9, 1.87)	G.S. (0.1 - 3)
M26	Gadoid juv (12.5, 1.97)	Pipefish ad. (300, 5.67)	Pipefish ad. (300, 5.67)	Pipefish ad. (300, 5.67)	G.S. (0.1 - 4), some E.S. (1)
M28	Pipefish ad. (200, 3.78)	Pipefish ad. (200, 3.78)	Pipefish ad. (200, 3.78)	Pipefish ad. (200, 3.78)	G.S. (0.1 - 4)
M29	Pipefish ad. (350, 6.61)	Pipefish ad. (350, 6.61)	Pipefish ad. (350, 6.61)	Pipefish ad. (350, 6.61)	G.S. (0.1 - 4), E.S. 0.1)
M30	Gadoid juv. (12.0, 1.89)	Pipefish juv. (23.5, 0.89)	Pipefish juv. (23.5, 0.89)	Pipefish juv. (23.5, 0.89)	G.S. (0.1 - 4), some E.S. (0.1)
M36	Gadoid juv. (13.1, 2.06)	Gurnard juv. (20.2, 3.18)	Gurnard juv. (20.2, 3.18)	Gurnard juv. (20.2, 3.18)	G.S. (0.1 - 1.5)

Table 4.7: Type of sampled scatterers found to contribute most to backscatter at each sound frequency in the region of each MIKT haul through solution of the forward problem ("juv" = juvenile, "ad" = adult). The mean body length of this dominant scatterer type for each sample is shown in brackets, as is the approximate swimbladder equivalent speherical radius (ESR). Dominant scatterers for each haul predicted by solution of the inverse problem utilising data from all four frequencies are shown with an approximate ESR (mm). All hauls were dominated by some combination of gaseous sphere (G.S.) and elastic-shelled (E.S.) scatterers. Some areas of haul M04 were dominated by fluid prolate spheroid (F.P.S.) types.

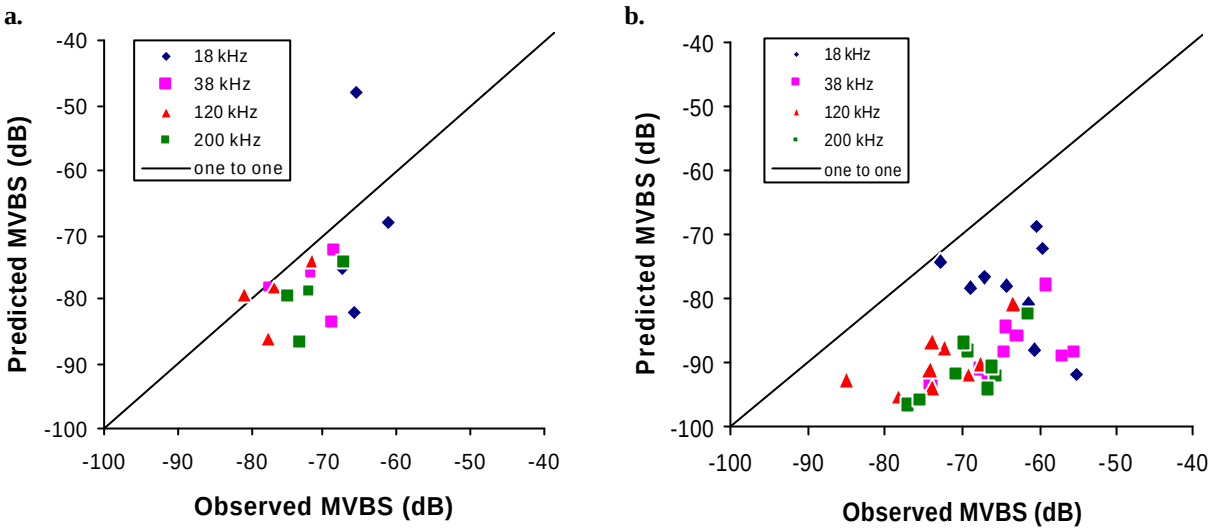

*Fig. 4.6: $MVBS_{pred}$ plotted against $MVBS_{obs}$ for **a**. those hauls (M25, M26, M28 and M29) which contained adult pipefish, and **b.** those hauls which did not contain adult pipefish. Predicted MVBS from hauls containing adult pipefish approached observed MVBS more closely in general. Nevertheless, predicted MVBS was still lower than observed MVBS in most cases. For one haul (M25), predicted MVBS was greater than observed MVBS by approximately 17.5 dB at 18 kHz.*

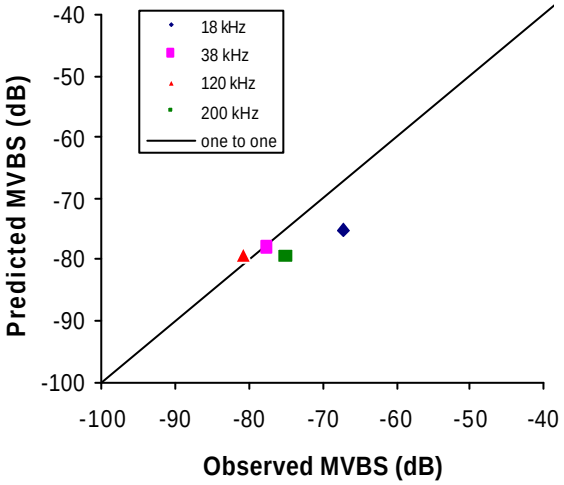

Fig. 4.7: $MVBS_{pred}$ plotted against $MVBS_{obs}$ for haul M29. Predicted MVBS from this haul was the most closely related to observed MVBS. The forward problem dominant sampled scatterers in this haul were adult pipefish averaging 350 mm in length. Predicted MVBS approached observed MVBS to within approximately 2 dB at 38 and 120 kHz.

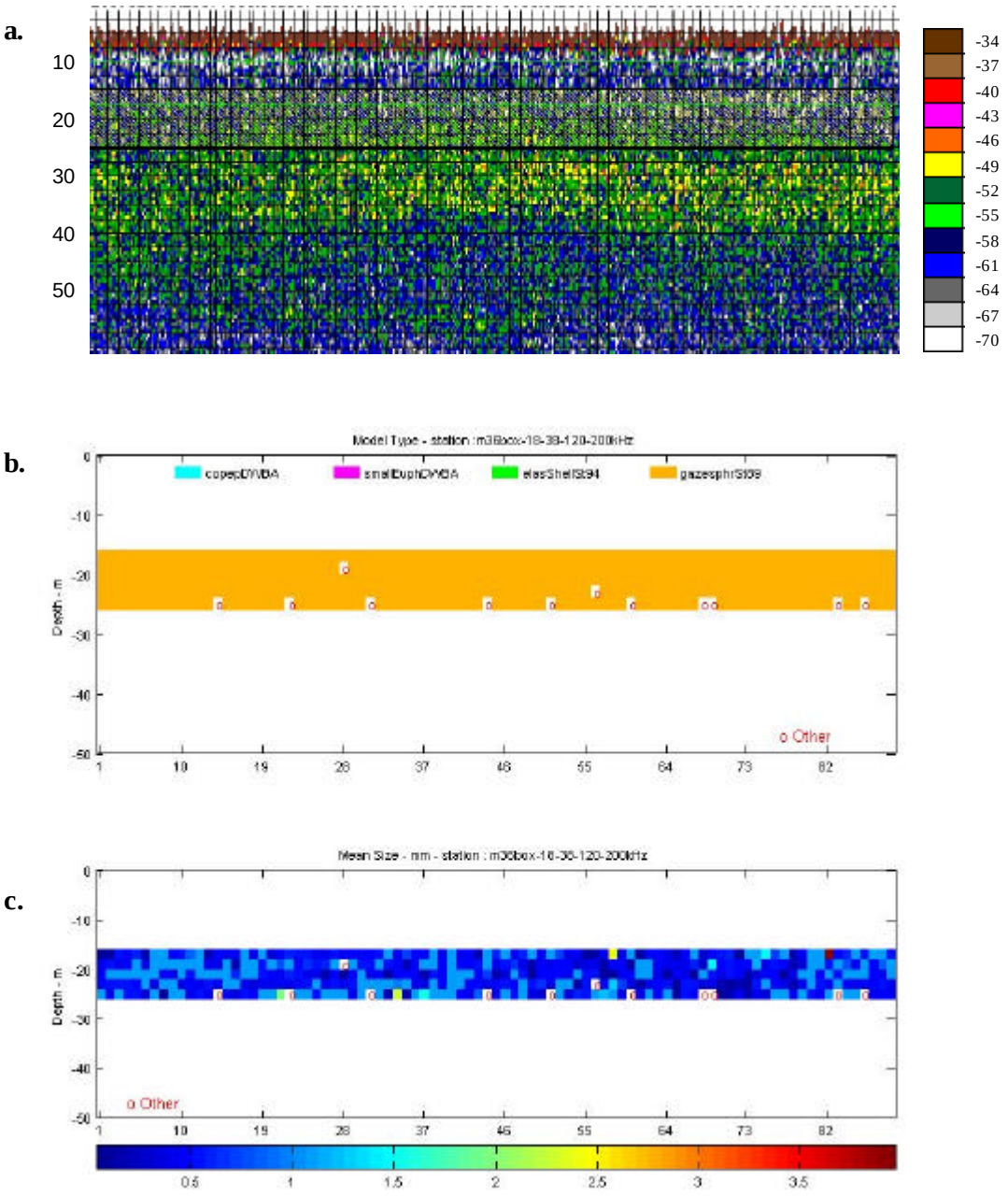

Fig. 4.8: Example graphical output showing theoretical scatterers predicted by solution of the inverse problem for haul M36. ***a.*** *the 38 kHz echogram for the corresponding region, with the legend to the right showing the colours used to represent backscatter intensity (dB) in 3dB steps, and water depth on the y-axis. The shaded area indicates the area sampled.* ***b.*** *shows that gaseous sphere type (yellow) scatterers were found to be dominant in almost all cases here.* ***c.*** *approximate sizes for the types of scatterers predicted, with a colour legend along the bottom. Several echogram cells could not be fit to model curves, and are displayed as "o" (other).*

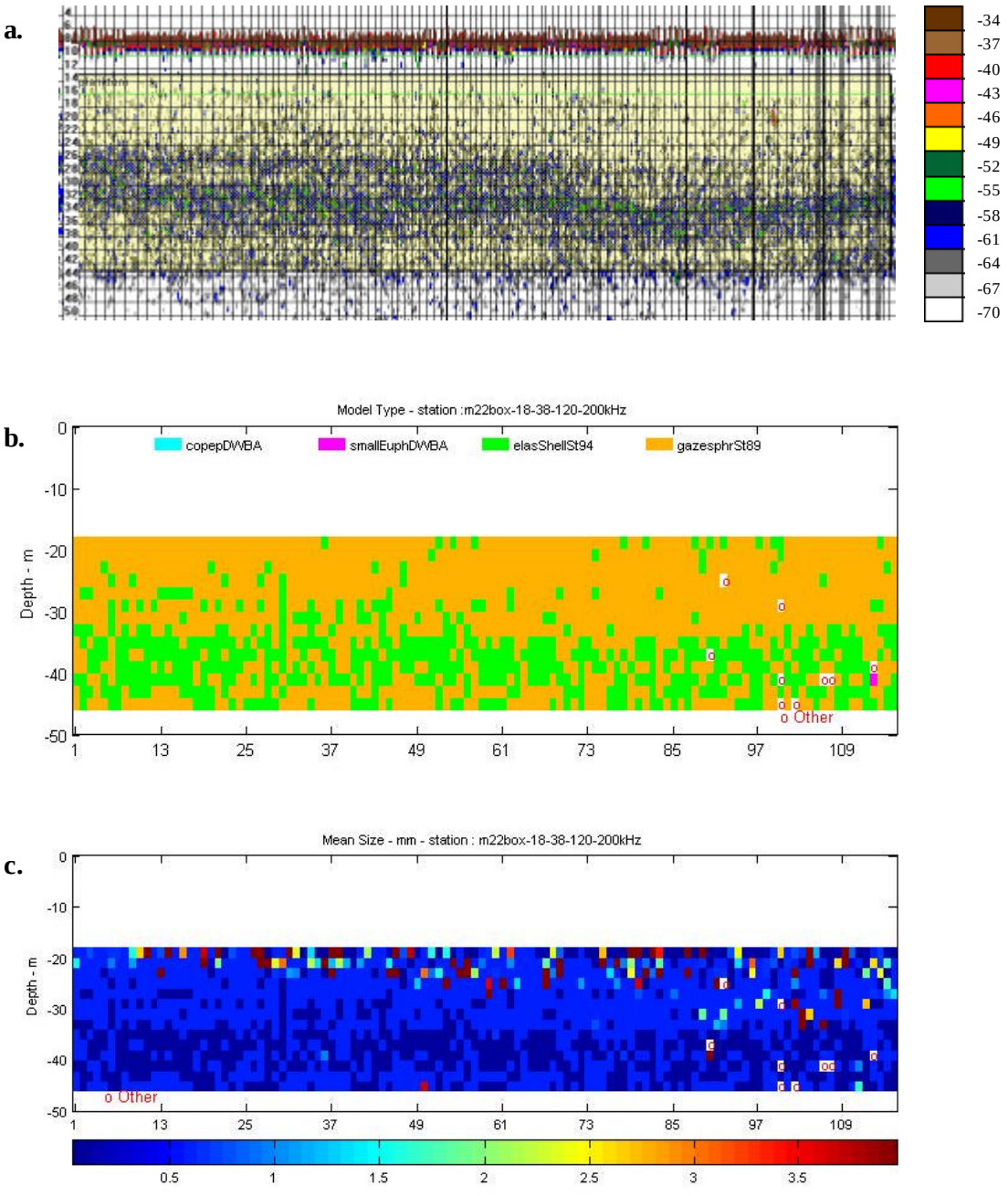

Fig. 4.9: Example graphical output showing theoretical scatterers predicted by solution of the inverse problem for haul M22. ***a.*** *the 38 kHz echogram for the corresponding region, with the legend to the right showing the colours used to represent backscatter intensity (dB) in 3dB steps, and water depth on the y-axis.* ***b.*** *shows that gaseous sphere (yellow) and elastic-shelled type (green) scatterers were found to be dominant in almost all cells.* ***c.*** *approximate sizes for the types of scatterers predicted, with a colour legend along the bottom. Several echogram cells at the lower right could not be fit to model curves, and are displayed as "o" (other).*

numerically dominant nor a high contributor to biovolume in this haul. Mean length of sampled animals (with standard deviation) and average $MVBS_{pred}$ for each frequency across all thirteen hauls is given in Table 4.6.

In all hauls, the dominant sampled scatterer type at all frequencies was found to be fish with swimbladders. The category of fish varied between juvenile gadoid (five-bearded rockling *Ciliata mustela* in most samples), adult pipefish *Syngnathus sp.* and juvenile gurnard *Trigla sp*. Table 4.7 shows dominant sampled scatterer, with mean length, at 18, 38, 120 and 200 kHz for all thirteen hauls. Adult pipefish were found to be the dominant scatterer at all frequencies in two of the four hauls in which they were found (M26, M28 and M29). In a third haul (M26) they were dominant at all frequencies except 18 kHz (Gadoid juv.). In the fourth (M25), adult pipefish $MVBS_{pred}$ was only marginally less than gadoid juvenile

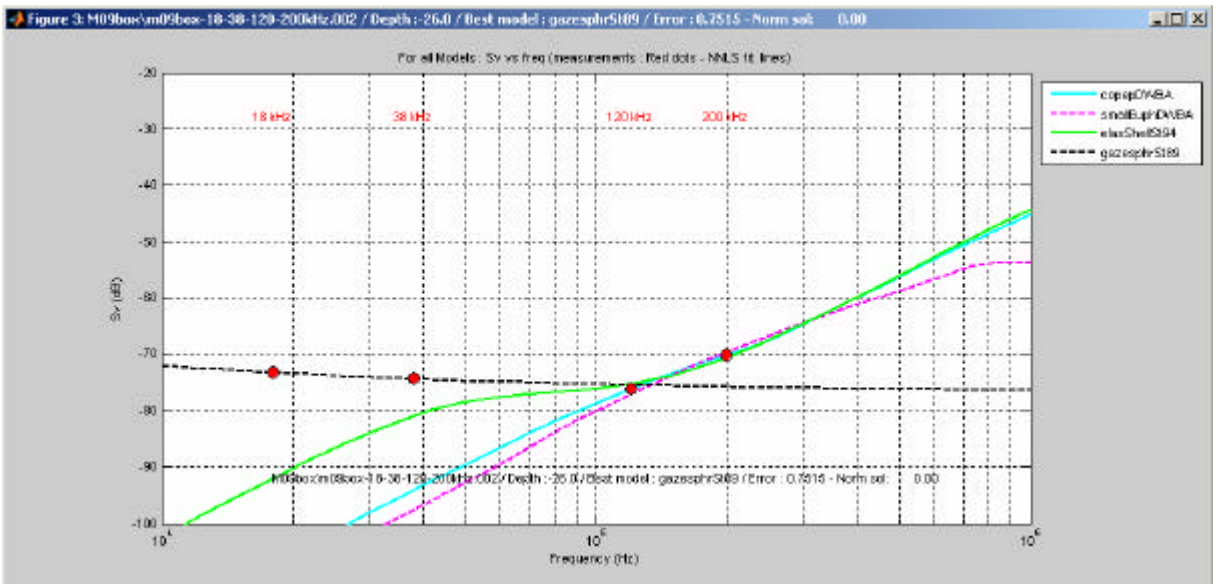

Fig. 4.10: An example of graphical ouput given by the Matlab inverse problem solving routine for a single echogram cell in haul M09. The red dots represent the observed backscatter values at each of the four frequencies, identified at the top of the plot. Curves represent the four model types under consideration in the range of the recorded frequencies. The legend identifies these curves by colour. In many echogram cells, as here, observed MVBS values at 18 and 38 kHz most closely fit the curve for gaseous sphere type scatterers, whilst 120 and 200 kHz MVBS values were more ambiguous, appearing to also closely match models for other types. This would seem to indicate the presence of a mixture of scatterer types. In this cell, the overall dominant scatterer was predicted as gaseous sphere type by the routine, which provides a single output.

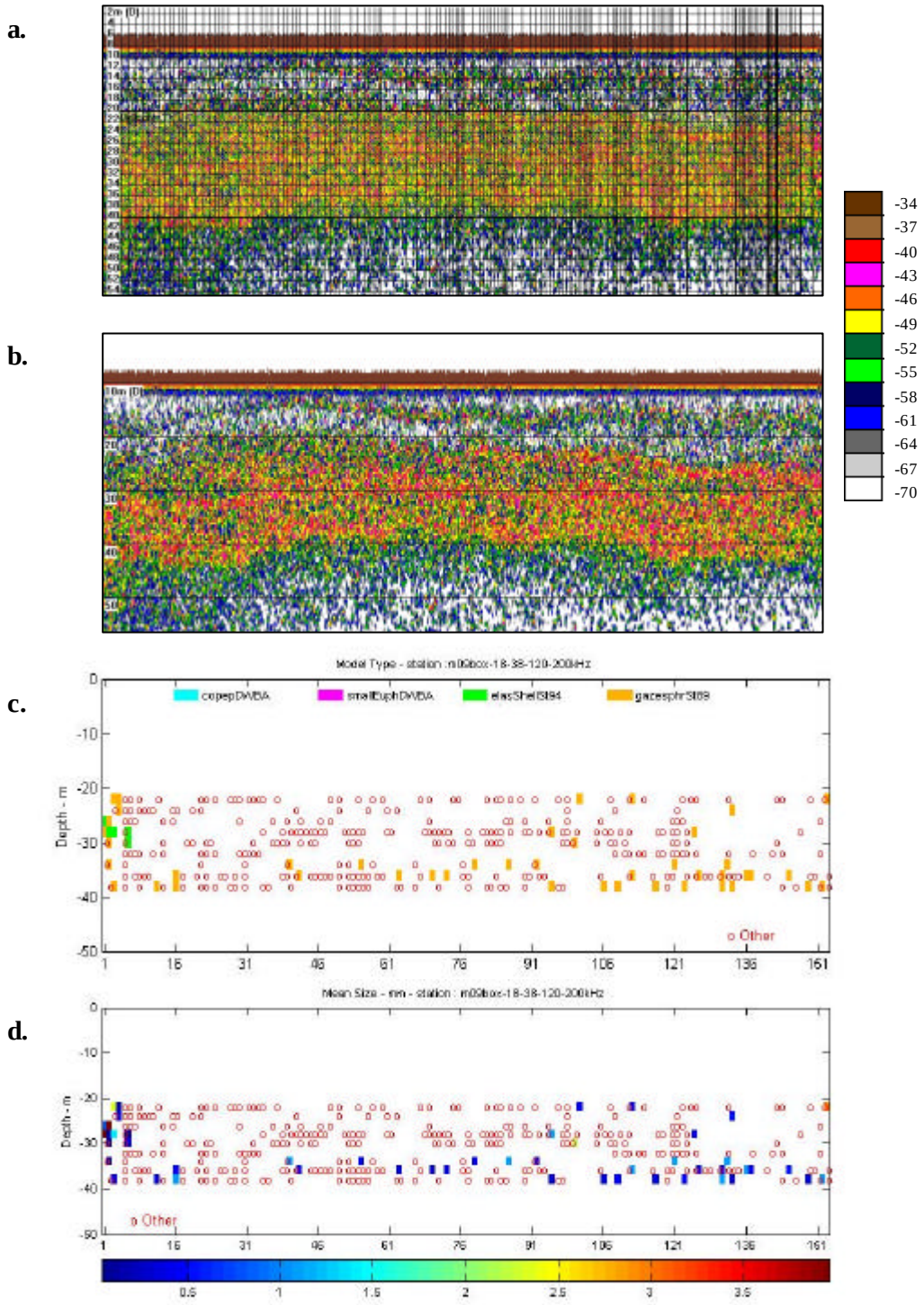

Fig. 4.11: Inverse problem solutions for haul M09 using all four frequencies (18, 38, 120 and 200 kHz). ***a.*** *the 38 kHz echogram for the corresponding region, with the legend to the right showing the colours used to represent backscatter intensity (dB) in 3dB steps, and water depth on the y-axis. The region of the haul is shown by a yellow shaded box.* ***b.*** *the same echogram with gridlines and haul region removed, for clarity.* ***c.*** *in most cells, the routine was unable to match acoustic data to any of the model curves, although some cells were identified as corresponding closely to gaseous sphere type, with several predicted as elastic-shelled.* ***b.*** *Predicted sizes of scatterers, where identified.*

a.

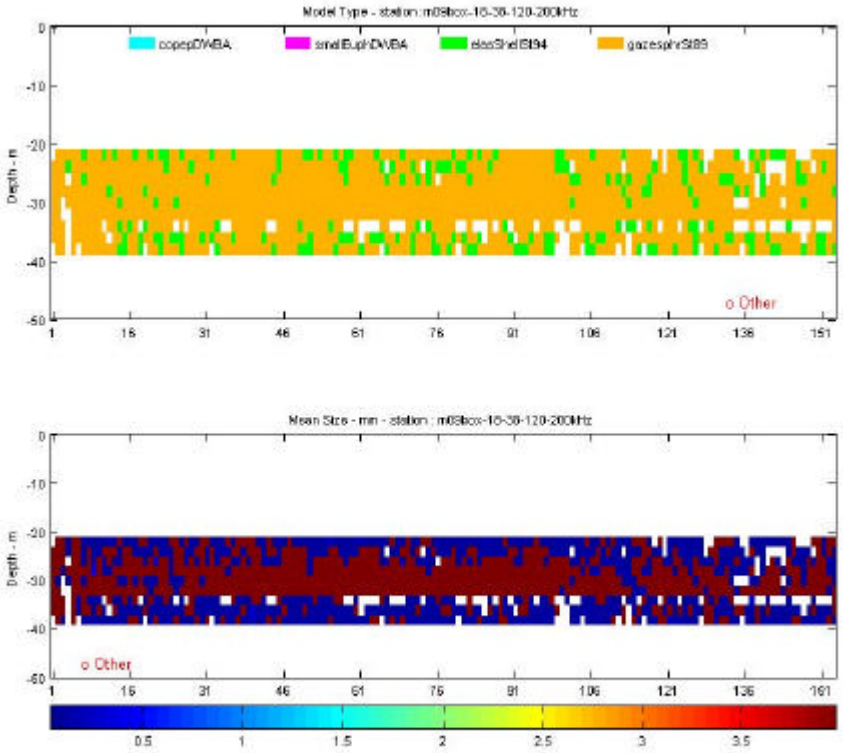

b.

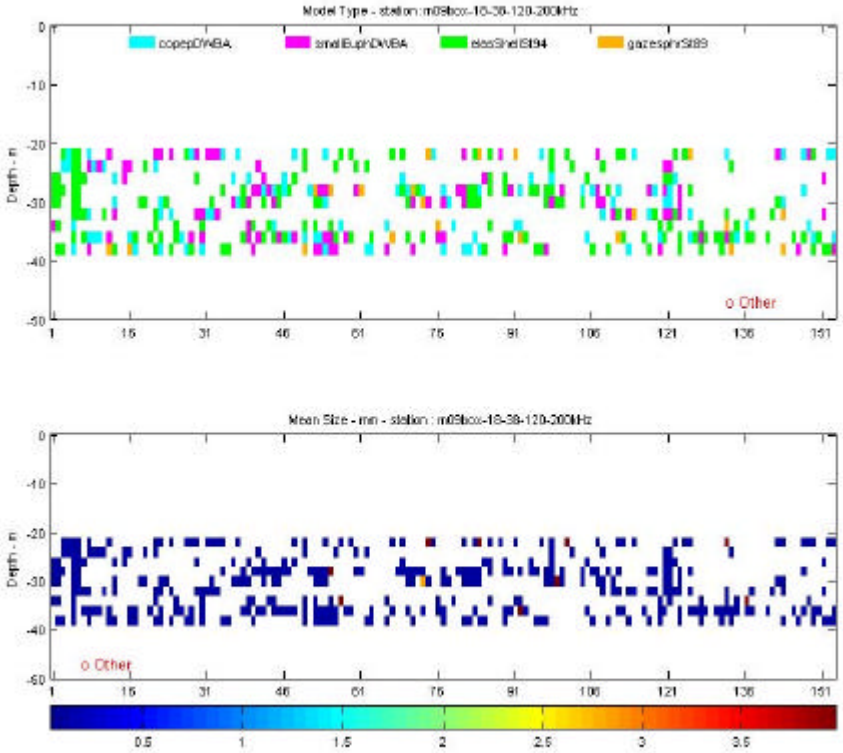

*Fig. 4.12: Inverse problem solutions for haul M09 at **a.** 18 and 38 kHz and **b.** 120 and 200 kHz. (Refer to Fig. 4.11 for echogram.) At the lower frequencies, gaseous sphere and elastic-shelled types are predicted as dominant. At the higher frequencies, however, fluid prolate spheroids, fluid bent cylinders and elastic-shelled share dominance among those cells whose data at these frequencies could be fit to models.*

$MVBS_{pred}$. A particularly high abundance of gadoid juveniles was found in this haul, resulting in an unusually high 18 kHz $MVBS_{pred}$ value.

Overall $MVBS_{pred}$ was lower than recorded $MVBS_{obs}$ for almost all hauls at all frequencies (Fig. 4.5). Two exceptions arose. For haul M25, $MVBS_{pred}$ at 18 kHz (-48.06 dB, dominated by a high abundance of gadoid juveniles) was considerably higher than $MVBS_{obs}$ (-65.65 dB), and for haul M29, $MVBS_{pred}$ at 120 kHz was -79.24 dB whilst $MVBS_{obs}$ was -80.96 dB. The large departure from a one-to-one relationship between $MVBS_{pred}$ and $MVBS_{obs}$ at 38 kHz observed with U-tow samples was not seen here in such marked fashion (Fig. 4.5 a, b, c, d). Considering all hauls, regression analyses indicated a negative overall relationship between $MVBS_{pred}$ and $MVBS_{obs}$ at 18 and 38 kHz, with a relatively weak positive relationship at 120 and 200 kHz. However, data points were well spread and R^2 values indicated that, in each case, data was not well fitted to the regression equation.

Although $MVBS_{pred}$ values from hauls containing adult pipefish (M25, M26, M28, M29) were lower than $MVBS_{obs}$, they tended to approach a 1:1 relationship more closely than other hauls (Fig. 4.6). One haul in particular (M29) had $MVBS_{pred}$ values which were much closer to $MVBS_{obs}$ than any other haul (Fig 4.7). The most abundant animal type in this haul was "small copepod < 1.2mm" (98.37%), which also contributed most to biovolume (68.15%). The haul, however, also contained two adult pipefish of average length 350 mm (3.4×10^{-4} % of animal abundance, 21.3% of biovolume) which dominated the scattering at all frequencies.

Inverse model predictions

The inverse problem was solved using acoustic data from the regions of all hauls as before. The theoretical dominant scatterers in most hauls were thus identified as being of gaseous sphere type. Hauls M21, M22, M26, M29 and M30 showed some areas of the region dominated by the elastic-shelled type (gastropods), and in one haul (M09) the dominant theoretical scatterer was elastic-shelled, with some gaseous sphere present. Haul M04 also showed some fluid prolate spheroid types (copepods). Examples of the graphical output obtained are given in Fig. 4.8 and Fig. 4.9.

From observation of the interim graphical displays produced by the Matlab inverse routine, it was noticeable that in many cases the lower frequencies appeared to fit the gaseous sphere

model, whilst the higher frequencies better fitted another. An example of the graphical output given by the routine for a single echogram cell from haul M09 is given in Fig. 4.10. (The input data in this case came from one of the cells shown on the extreme left in Fig. 4.11, identified as a gaseous sphere.) In order to further investigate this, and bearing in mind that a loss of resolving power in solving the inverse problem would result, acoustic data from one haul (M09) recorded at firstly 18 and 38 kHz and secondly 120 and 200 kHz were inverted separately. The predicted scatterers using all four frequencies are shown in Fig. 4.11. In this case, the routine was unable to assign many of the cells, although some were output as dominated by gaseous sphere, with several as elastic-shelled. Following separation of the acoustic data into the two "low" and two "high" frequencies, inverse solutions showed that at the lower frequencies gaseous sphere type scatterers (4 mm) were predicted as dominant, with many cells also dominated by elastic-shelled types (0.1 mm) (Fig. 4.12a). At the higher frequencies, however, gaseous spheres were seldom predicted. Instead, fluid prolate spheroids (representing copepods), fluid bent cylinders (representing mainly euphausiids) and elastic-shelled (gastropods, mostly at the smallest size of 0.1 mm) shared dominance across the region (Fig. 4.12b). Those gaseous sphere types which were predicted in a small number of cells in this case were approximately 4 mm ESR. Data from many cells could not be fit to any models at these two frequencies alone.

It may be noted that, in this haul (M09), the dominant sampled animals by number of individuals (approximately 35%) were small decapods (Table 4.2), nearly 95% of sampled biovolume was accounted for by hydrozoans (Table 4.4), and solution of the forward problem indicated swimbladder-bearing juvenile gadoid fish to be the dominant sampled scatterer (Table 4.7).

Discussion

It was hoped that deployment of the MIKT net would produce samples containing animals which were not sampled by the U-tow, allowing them to be included in $MVBS_{pred}$ calculations with the ultimate aim of finding a closer relationship between $MVBS_{pred}$ and $MVBS_{obs}$. Indeed, the MIKT net sampled juvenile and relatively small adult fish possessing swimbladders (e.g. juvenile gadoids, gurnards and pipefish, and adult pipefish). Jellyfish were also sampled in several cases. These types of animal either avoided or were destroyed by the U-tow. Elastic-shelled gastropod molluscs (*Limacina spp.*), also absent from U-tow

samples, were found in abundance in some of the MIKT net samples. However, once again, no evidence of siphonophores was found. This may mean that none were present, but in any case it is expected that they would not have been well preserved in this type of net. Neither does the net technology permit sampling of flocculent material which, as mentioned previously, may contain gas inclusions as a result of metabolic breakdown of materials by bacteria and microflagellates.

$MVBS_{pred}$ was generally found to approach $MVBS_{obs}$ more closely than was the case with U-tow samples at all frequencies. Regression analyses showed weak relationships between $MVBS_{pred}$ and $MVBS_{obs}$ at all frequencies, but also a certain amount of dispersal of data away from the regression equation. Swimbladder-bearing fish made a major contribution towards backscattering at all frequencies. $MVBS_{pred}$ from those hauls which contained adult pipefish generally approached $MVBS_{obs}$ more closely than was the case in other hauls.

In one haul (M25), $MVBS_{pred}$ (-48.06 dB) was found to be much greater than $MVBS_{obs}$ (-65.65 dB). Further investigation showed that the maximum S_v for the region of this haul was -46.34 dB. It may be concluded that the scatterer responsible for this maximum value was actually sampled, whilst the echo-integration process providing $MVBS_{obs}$ smoothed the single large S_v value resulting in a lower averaged value. This smoothing effect was not repeated in calculations of $MVBS_{pred}$ since $MVBS_{pred}$ is not an average, but rather the sum of predicted backscatter. $MVBS_{pred}$ was also found to be marginally greater than $MVBS_{obs}$ at 120 kHz for haul M29. This difference may be due either to a similar averaging process or to approximation in model parameters. Although this haul contained only two pipefish, they were the largest sampled during the cruise (mean length of 2 individuals was 350 mm). Had the number of usable samples been larger, it may have been possible to obtain more detailed results regarding the contribution made by such animals to backscattering.

Solution of the inverse problem gave the expected predictions that gaseous-type scatterers were dominant in most cases. It was of interest that separating the data into “low” and “high” frequencies produced different results in each case than when all four were combined. This may provide an indication of the complexity of the composition of the layer, and suggests that the use of data from all four frequencies at once is perhaps too coarse a method of identifying all the types of animals present. Conversely, it must be borne in mind that less

points may be fit to a curve more easily, perhaps giving false results. It has certainly become apparent that in a mixed layer, some difficulty is encountered when attempting to correctly fit data from multiple frequencies to model curves. Due to the varying scattering properties of different animal types at different frequencies, it is unlikely that any one will exhibit acoustic dominance at all frequencies employed, ranging in this case from 18 to 200 kHz. Thus, an overlap will occur when attempting to resolve to one dominant scatterer model. A solution may be to collect data at more frequencies than used in this study. There is the further possibility of allowing solution of the inverse problem to provide more options than a single fit to a preferred model curve, which disregards acoustic data points which do not actually fit that curve. The current procedure may identify an acoustically dominant scatterer which is neither dominant by number of individuals nor by biovolume in the area under consideration, which limits its application value.

Consideration may be given to the fact that the inverse routine utilised in this study is still being developed, with future work perhaps taking account of these points. It should also be noted that similar assumptions and potential problems concerning model parameters and biological versus acoustical sampling as mentioned in the last chapter must be taken into consideration.

Conclusions

Solution of the forward problem for samples collected with the MIKT net produced predicted mean volume backscattering strength values which, in some cases, approached observed values far more closely than for samples collected with the U-tow. This suggests that animals which were not sampled by the U-tow, but which were by the MIKT net, contribute significantly to backscattering from the layer in question. In particular, small or juvenile fish containing gas-filled swimbladders (which dominated predicted backscattering) can be considered as major contributors.

It is, however, still the case that $MVBS_{pred}$ is considerably less than $MVBS_{obs}$ in most cases. Therefore it has to be concluded that scatterers sampled with the MIKT net, although making a large contribution to scattering observed from the enhanced 38 kHz layer, are not fully responsible for it. The most likely remaining candidates would appear to be:

1. fish possessing swimbladders which were not sampled;
2. other gas-bearing organisms such as siphonophora;
3. gas bubbles produced metabolically by organisms such as bacteria or phytoplankton.

Future studies should include methodology which takes account of these possibilities, and be designed with the ability to sample such potential scatterers. It is anticipated that further sampling with the MIKT net may provide samples containing fish, but this type of gear is not suitable when considering other potential scattering candidates mentioned above. Some type of optical device would perhaps be best suited to such a sampling exercise.

The evidence presented suggests that a single type of vehicle is not sufficient to comprehensively sample whatever scatterers are present in this layer. The MIKT net appears to be capable of effectively sampling organisms in a size range of approximately 0.5 - 20 mm, and also catches adult pipefish. It remains that such animals may not be sampled in representative numbers, as there is every possibility that patches of them which are detected acoustically are not encountered by the net.

Due to mesh size, smaller animals may be more effectively sampled by a vehicle such as ARIES, whilst those animal types which cannot be properly sampled by such net-based systems may be effectively sampled by an optical system. The latter may also aid in understanding the abundance of flocculent material, or marine snow, which is present in the layer.

Chapter 5

General Discussion

The nature of the layer

The 38 kHz layer has been shown to be composed partly of zooplankton species, as had been informally thought. Indeed, copepods were numerically most abundant even in most MIKT net samples in this study (Table 4.2), although they were certainly not dominantly responsible for any enhanced sound scattering (e.g. Table 4.4). The relatively high numbers of these animals do offer some justification for the layer's traditional designation as "zooplankton". It is only when considering the acoustic properties of the layer that less numerous animals, such as larval fish possessing swimbladders, are dominant (Table 4.6).

One of the remarkable features of samples collected during July 2004 was the unexpected abundance of snake pipefish (e.g. Fig. 4.3). As well as adults of the species, commonly found to be egg-bearing, many larval individuals were found in samples (Fig 5.1). These animals were found to account for a significant part of enhanced 38 kHz scattering due to the presence of a gas-bearing swimbladder (Fig 5.2). There has been a remarkable increase in these animals in the North Sea and nearby areas over recent years, and adults are known to consume calanoid copepods (Ryer and Orth, 1987). It is therefore not unreasonable to expect that they will be present in the layer which has been shown here to often be largely composed of copepods. Harris *et al* (2007) report on greatly increased numbers of pipefish

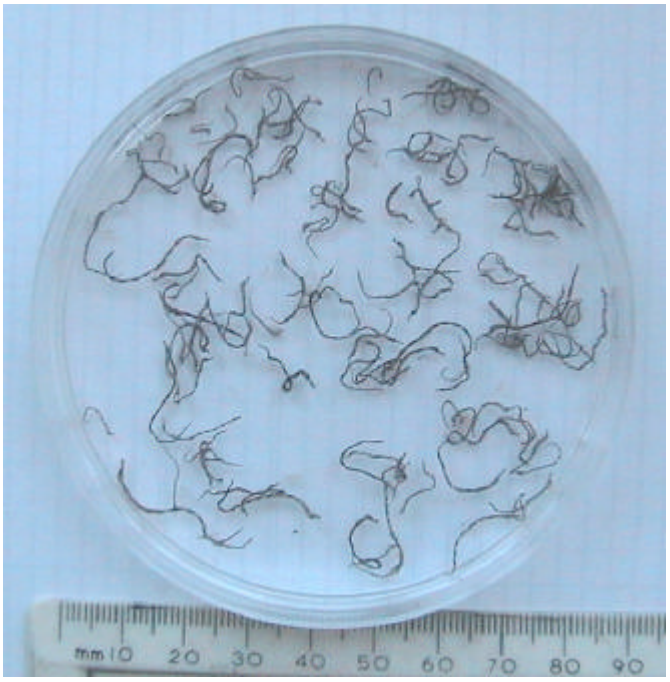

Fig. 5.1: Larval snake pipefish separated from one MIKT net sample during July 2004, cruise 1004s. Such animals were found to be abundant in many of the samples from this cruise.

in the North Sea since 2003 and the possible consequences for seabird populations more used to a diet of sandeel. The German part of the 2006 ICES-coordinated International Bottom Trawl Survey also found large numbers of snake pipefish in MIKT net samples from the North Sea (Wegner and Ulleweit, 2006). Widening the geographical location, greatly increased numbers of this species have been found off the West coast of the UK in recent years, particularly in late spring and summer (Lindley *et al.,* 2006, Kirby *et al.*, 2006). Informal reports of enhanced pipefish stocks are numerous amongst sea-anglers around the coast of the UK, although commercial inshore fishermen operating in the Moray Firth area have not generally noticed any difference (A. Wiseman, skipper "Silver Fern" FR416, G. Lyon, skipper "Charisma" BF296, and others, pers. comm.). This is possibly due to either the mesh size of commercial fishing nets being too large to retain such animals in noticeable quantity, or lack of commercial value and therefore interest. The author personally noted the presence of occasional pipefish mixed through commercial catches several times during summer 2006. Harris *et al* (2006) note the possible deleterious effect of increased pipefish and decreasing sandeel populations on seabirds, and similar effects on commercial fish stocks are a distinct possibility. Although the nutrient content of pipefish remains unmeasured, their relatively bony and indigestible bodies would seem to offer as poor a food alternative to larger fish species as they do to seabirds. Monitoring of pipefish populations therefore becomes more important in predicting future commercial fish stocks, and it would consequently be of great benefit were their acoustic properties and actual contribution to the 38 kHz layer to be better defined.

Without analysis of available historical acoustic and biological data collected during summer in years prior to 2003 in the North Sea, any increased contribution made by snake pipefish to

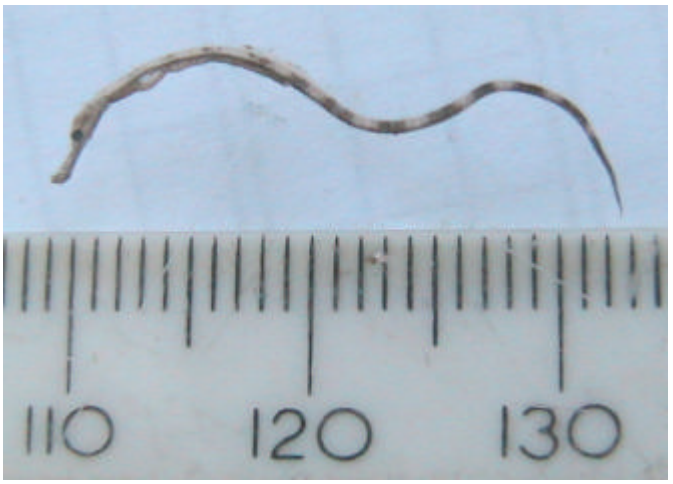

Fig 5.2: An individual larval snake pipefish found in one of the MIKT net samples during July 2004, cruise 1004s. The developing swimbladder can be clearly seen at the anterior ventral part of the body, just behind the head. The scale displays millimetres.

38 kHz scattering in recent years can only be postulated. Although some very small fish larvae were collected by the Utow during trials (Table 2.4), none of these were pipefish. Not unexpectedly, biological samples collected as part of the current study in July 2003 contained no adult or juvenile pipefish - possibly due to their size (Fig. 5.2) and the nature of the sampling vehicle (other larval fish were also absent). The species is, however, shown to have been an important constituent of the layer in July 2004 although a higher abundance would have been required to fully account for enhanced 38 kHz scattering. It may be that greater numbers were actually present and were not comprehensively sampled by the MIKT net. Current results do not, therefore, support the hypothesis that pipefish are the responsible layer component - $MVBS_{pred}$ calculated from samples which contained adult pipefish approached $MVBS_{obs}$ more closely than samples without, but did not account for $MVBS_{obs}$.

Directions for future studies

Sampling protocol

Sampling procedures utilised in this study were robust in design, given the knowledge-base available. As the 38 kHz layer was informally thought to consist primarily of zooplankton, a vehicle was initially identified to reliably sample that community. Progression was made following analysis, and a vehicle more suitable for sampling larval and small fish was employed for the second sampling season. This produced more impressive results, with $MVBS_{pred}$ approaching $MVBS_{obs}$ more closely at all frequencies, but still did not sample all of the candidates identified as potential strong 38 kHz scatterers.

For this reason, it seems clear that any vehicle employing only a single sampling method is not sufficient to comprehensively sample all candidates for strong 38 kHz scattering which may be present in the layer. It is possible that the MIKT net representatively sampled larval and post-larval fish, and adults of certain species, but generally not in numbers great enough to account for observed scattering levels. In addition, the lack of other common animals such as siphonophores in samples does not necessarily indicate that they were not present. Because of the nature of their anatomy, these animals will be destroyed by all but the most sensitive, or non-invasive, biological sampling devices. Gas bubbles suspended in the water column as component parts of phytoplankton aggregations or marine snow present similar problems. The optimum platform for enumerating such scatterers would appear be some form of video or holographic camera. Several video-based systems are currently in use (Lenz

et al, 1995; Davis *et al*, 1996; Daly *et al*, 2001), and are reported as effective. Until recently holographic systems were cumbersome and required highly specialised operation and analysis techniques, mainly due to their reliance on specialised photographic film (Foster and Watson, 1997). Technological progression is such that a much smaller underwater holographic camera has recently been developed which can be deployed as part of the equipment load of the ARIES sampling vehicle (J. Dunn, FRS Marine Laboratory, Aberdeen, pers. comm.). The "eHoloCam" can operate at depths up to 1500 m, is capable of recording high resolution digital holographic images of a water column 400 mm long by 10 mm diameter, and has been successfully trialled by FRS and the University of Aberdeen on FRV Scotia (P. Fernandes, FRS Marine Laboratory, Aberdeen, pers. comm.). Unfortunately, operational problems prevented an extensive dataset from being collected during these initial trials, but it must be considered as a potentially highly valuable tool for future *in situ* studies of the planktonic community.

In summary, it would appear that a full identification of the scattering components contained within the layer is only approachable by the deployment of several types of sampler on areas of the layer exhibiting similar scattering properties. Theoretically a single vehicle such as ARIES could produce the most reliable results by sampling an area with several different mechanisms simultaneously. However, due to its size, such a vehicle may also be more subject to factors such as avoidance.

Model parameters

Of necessity, model parameters used in this study were taken from available literature with more recent values obtained by personal communication with researchers currently working in this field. The methodology required to obtain model parameter values such as g (density contrast between organism's body and sea water), h (sound speed contrast) and animal orientation in the water column is beyond the scope of this study but commonly involves some degree of estimation or calculation involving tethered - and thus stressed - or dead animals in artificial conditions (e.g. Chu and Copley, 2000; Chu *et al* 1992). However, studies are ongoing and understanding of parameters such as natural animal orientation is advancing steadily (e.g. Demer and Conti, 2005).

It is recognised that the values used in this study were the most accurate available but it must also be considered that, in many cases, parameters calculated for different species of animals

from different geographical areas were used. Although animals used in these calculations have similar morphologies, their body composition may vary somewhat from those found in the North Sea due to varying environmental conditions and life histories.

As progress is made in accurately defining these parameters for various types and species of animal, more accurate model outputs will follow. Because forward and inverse problems both utilise these parameters, improved values should affect both solutions positively.

The estimation of the size and shape of swimbladder found in sampled fish presented some problems during this study. Such information is necessary for entry as parameters in the solution of the forward problem. It was impractical to dissect each individual under a microscope, and so estimated morphologies and volumes were used. The literature in this area was found to be somewhat lacking for anything other than the most common commercial species - few of which were found in samples, even in larval form. For example, reference to the morphology of the snake pipefish swimbladder was found only in an eighty year old textbook (Kyle, 1926). This lack of reference material presents a possible opportunity for future research, particularly bearing in mind the need for an improved database of model parameters.

Chlorophyll relationship

As zooplankton graze primarily on phytoplankton it may be expected that, if the strong 38 kHz scattering layer was primarily composed of zooplankton, areas of high 38 kHz scattering would show a relationship to phytoplankton concentration. Scott *et al* (2001), for example, estimated zooplankton biomass from acoustic backscatter intensity recorded by acoustic Doppler current profilers operating at 300 kHz and found a strong correlation with remotely sensed surface chlorophyll concentrations in the Gulf of Mexico. Alternatively, it has also been suggested in the present study that gas inclusions contained within phytoplankton or other flocculent masses may bear a degree of responsibility for enhanced 38 kHz scattering. In this case a positive relationship may also be expected.

Phytoplankton concentration can be indirectly measured by use of a fluorometer. This instrument detects and quantifies the natural fluorescence produced by the photosynthetic pigment *chlorophyll a* which is present in phytoplankton. Greater fluorescence indicates a

higher level of active photosynthesis, thus providing an indirect measure of local phytoplankton biomass (e.g. Maxwell & Johnson, 2000; Heath, 1988). There is some debate as to whether fluorescence is a reliable indicator of phytoplankton abundance (e.g. Westberry & Siegel, 2003), and indeed a number of assumptions are made when attempting to quantify phytoplankton by converting fluorescence data. Factors ranging from temporal to oceanographic variations affect the rate of photosynthesis, as does nutrient availability (Falkowski & Kolber, 1995).

FRV Scotia has on-board systems which measure fluorescence, temperature, depth and salinity of surrounding water whilst the ship is underway. These systems were running throughout the cruises during which biological and acoustic data were collected for this study, that is cruise 1003s in July 2003 and cruise 1004s in July 2004. Unfortunately, fluorescence data from cruise 1004s were unusable due to suspected biofouling of the system. This did not become apparent until analysis was attempted following the cruise. However, data from cruise 1003s were available although not for the whole time during which biological and acoustic data were collected. As the fluorometer had not been calibrated, these data could not be reliably utilised in the present study.

There are several possibilities for direction of future studies. Timesets of Sea-viewing Wide Field-of-view Sensor (SeaWIFS) satellite data are available to researchers, allowing a closer analysis of chlorophyll concentrations according to sea-surface colour (e.g. Scott *et al*, 2001). Such data has been employed, for example, in the study of trophic mechanisms involving phytoplankton off British Columbia (Ware & Thomson, 2005). It may also be beneficial to obtain profiles of chlorophyll concentrations at depths through the water column by use of a dipping mechanism. Such dips would ideally be performed contemporaneously at locations where high 38 kHz scattering is observed, allowing for closer comparison with acoustic data gathered at various depths.

Further studies of variability of plankton patchiness may benefit from spectral analysis. First employed by Mackas and Boyd (1979) for the investigation of spatial correlation between phytoplankton and zooplankton at a range of scales, this has now become a standard analysis tool for such data. Many studies (e.g. Weber *et* al, 1986; Piontkovski *et al.*, 1995) found that phytoplankton exhibited a flatter spectrum than zooplankton, and this has become the

accepted view (Martin, 2003). Martin and Srokosz (2002) attempted to improve upon existing models used to explain plankton spectra by introducing multiple zooplankton size "compartments". Consequently, they suggest that the gradient of zooplankton spectra may vary according to organism size and, in conflict with convention, that it appears to be flatter than the phytoplankton gradient. This higher-resolution methodology suggested by Martin and Srokosz (2002) would appear to provide an ideal basis for spectral analysis were a strong dataset collected in similar circumstances to the current study.

Conclusion

This study did not ultimately define the full composition of the enhanced 38 kHz layer, despite employing various methodologies in an attempt to do so in the allocated time. It has been shown that the layer is composed, at least in part, of zooplankters of types native to the North Sea and larval and post-larval fish both with and without swimbladders. In addition, adult fish of certain species – in particular, snake pipefish - appear to make a significant contribution to total 38 kHz scattering. Allowing for natural environmental stochasticity, the composition of the layer is likely to vary in different areas of the North Sea, whilst retaining such core elements in differing proportions. The enhanced 38 kHz scattering found close to the 200 m depth contour to the west of Orkney and Shetland certainly merits further investigation, for example, as does the possible persistence of enhanced scattering to the east of Shetland (Fig. 1.4, Fig 1.7). The exact nature of any relationship between the layer and phytoplankton abundance is as yet unclear and also requires further study.

In conclusion, there remains an unsampled, unidentified scatterer that is partly responsible for enhanced 38 kHz scattering levels in the North Sea. The most likely candidates are those organisms or features which contain some form of gas inclusion, the detection of which may allow a fuller description of the composition of the layer. The contribution of identified scatterers has been examined and the most likely remaining candidate 38 kHz scatterers have been suggested. It is anticipated that this will facilitate continuing research by providing strong previous knowledge and suggestions for the direction of future studies.

References

Anderson C.I.H., Horne J.K., Boyle J. **(2007)** *Classifying multi-frequency fisheries acoustic data using a robust probabilistic classification technique*. J. Acoust. Soc. Am. **121** *EL230-237*

Anderson V.C. **(1950)** *Sound scattering from a fluid sphere.* J. Acoust. Soc. Am. **22** *426-431*

Beaugrand G., Brander K.M., Lindley J. A., Suoissi S., Reid P.C. **(2003)** *Plankton effect on cod recruitment in the North Sea.* Nature **426** *661 – 664*

Benfield, M.C., Schwehm C.J., Fredericks R.J., Squyres G., Keenan S.F. and Trevorrow M.V. **(2003)** *ZOOVIS: A high-resolution digital still camera system for measurement of fine-scale zooplankton distributions.* In, P. Strutton, and L. Seuront (eds.) Scales in Aquatic Ecology: Measurement, Analysis and Simulation. CRC Press.

Benfield M.C., Davis C.S., Gallager S.M. **(2000)** *Estimating the in-situ orientation of Calanus finmarchicus on Georges Bank using the Video Plankton Recorder*. Plankton Biology and Ecology **47** *30-33*

Brierley A.S., Ward P., Watkins J.L., Goss C. **(1998)** *Acoustic discrimination of Southern Ocean zooplankton.* Deep Sea Research II **45** *1155-1173*

Brierley A.S., Axelsen B.E., Buecher E., Sparks C.A.J., Boyer H., Gibbons M.J. **(2001)** *Acoustic observations of jellyfish in the Namibian Benguela.* Marine Ecology Progress Series **210** *55-66*

Brierley A.S, Fernandes P.G., Brandon M.A., Armstrong F., Millard N.W., McPhail S.D., Stevenson P., Pebody M., Perrett J., Squires M., Bone D.G., Griffiths G. **(2002)** *Antarctic Krill Under Sea Ice: Elevated Abundance in a Narrow Band Just South of Ice Edge*. Science **295** *1890-1892*

Brodeur R.D., Seki M.P., Pakhomov E.A., Suntsov A.V. **(2005)** *Micronekton—what are they and why are they important?* Nor. Pac. Mar. Sci. Org. Pices Press **13** *7-11*

Chu D., Copley N. **(2000)** *Inference of material properties of zooplankton from acoustic and resistivity measurements.* ICES J. Mar. Sci. **57** *1128-1142*

Chu D., Wiebe P.H. **(2005)** *Measurements of sound-speed and density contrasts of zooplankton in Antarctic waters.* ICES J. Mar. Sci. **62** (4), *818-831*

Chu D., Foote K.G., Stanton T.K. **(1993)** *Further analysis of target strength measurements of Antarctic krill at 38kHz and 120kHz: Comparison with deformed cylinder model and inference of orientation distribution.* J. Acoust. Soc. Am. **93** *2985-2988*

Chu D., Stanton T.K., Wiebe P.H. **(1992*)*** *Frequency dependence of sound backscattering from live individual zooplankton*. ICES J. Mar. Sci. **49** *97-106*

Chu D., Wiebe P.H, Copley N.J, Lawson G.L., Puvanendran V. **(2003)** *Material properties of North Atlantic cod eggs and early-stage larvae and their influence on acoustic scattering.* ICES J. Mar. Sci. **60** (3) *508-515*

Colombo G.A., Mianzan H., Madirolas A. **(2003)** *Acoustic characterization of gelatinous-plankton aggregations: four case studies from the Argentine continental shelf.* ICES J. Mar. Sci. **60** *650-657*

Cook K.B., Hays G.C. **(2001)** *Comparison of the epipelagic zooplankton samples from a U-Tow and the traditional WP2 net.* J. Plankton Res. **23** *953-962*

Coyle K.O. **(1998)** *Neocalanus scattering layers near the western Aleutian Islands.* Journal of Plankton Research **20** (6) *1189-1202*

Costello J.H, Pieper R.E., Holliday D.V. **(1989)** *Comparison of acoustic and pump sampling techniques for the analysis of zooplankton distributions.* J. Plankton Res. **11** *703-709*

Coull K.A., Johnstone R., Rogers S.I. **(1998)** *Fisheries Sensitivity Maps in British Waters.* Pub. UKOOA, Aberdeen, Scotland.

Daly K.L., Samson S., Hopkins T., Remsen A., Sutton T., Langebrake L. **(2001*)*** *Sensor Technology for Zooplankton Assessment.* International Workshop on Autonomous Measurements of Biogeochemical Parameters in the Ocean, Honolulu, 2001

Davenport J. **(1999)** *Acoustic models of fish: the Atlantic Cod (Gadus morhua).* J. Acoust. Soc. Am. **96** *1661-1668*

Davis C.S., Gallager S.M. **(2000)** *Data report for Video Plankton Recorder cruise OSV Peter W. Anderson February 23-28 1999.* Boston: Massachussets Water Resources Authority. Report ENQUAD 00-03 *132pp*

Davis C.S., Gallager S.M., Marra M., Stewart W.K. **(1996)** *Rapid visualisation of plankton abundance and taxonomic composition using the Video Plankton Recorder.* Deep Sea Research II, **43** *1947-1970*

Del Grosso V.A., Mader C.W. **(1972)** *Speed of sound in pure water.* J. Acoust. Soc. Am. **52** *1442-1446*

Demer D.A., Conti S.G. **(2003a)** *Reconciling theoretical versus empirical target strengths of krill; effects of phase variability on the distorted-wave Born-approximation.* ICES Journal of Marine Science **60** *2429–434*

Demer D.A., Conti S.G. **(2003b)** *Validation of the stochastic, distorted-wave Born-approximation model with broadbandwidth, total target-strength measurements of Antarctic krill.* ICES Journal of Marine Science **60** *625–635*.

Demer D.A., Conti S.G. **(2005)** *New target strength model indicates more krill in the Southern Ocean.* ICES J. Mar. Sci. **62** (1) *25-32*

Demer D.A., Hewitt R.P. **(1995)** *Bias in acoustic biomass estimates of Euphausia superba due to diel vertical migration.* Deep Sea Res. I **42** (4) *455-475*

Dessureault J.G. **(1976)** *Batfish: a depth controllable towed body for collecting oceanographic data.* Ocean Engineering **3** *99-111*

Dragesund O., Olsen S. **(1965)** *On the possibility of estimating year class strength by measuring echo abundance of 0-group fish.* FiskDir. Skr. Ser. Havunders **13** *47-75*

Dunn J., Hall C.D., Heath M.R., Mitchell R.B., Ritchie B.J. **(1993)** *ARIES – a system for concurrent physical, biological and chemical sampling at sea.* Deep Sea Research **40** *867-878*

Endo Y. **(1993)** *Orientation of Antarctic krill in an aquarium.* Nippon Suisan Gakkaishi **59** *3465–468*

Envirotech **(2003)** *U-Tow: Undulating Towed Vehicle.* Corporate information leaflet.

Everson I, Bone DG **(1986)** *Detection of krill (Euphausia superba) near the sea surface: preliminary results using a towed upward-looking echo-sounder.* Br. Antarct. Surv. Bull. **72** *61-70.*

Falkowski P.G., Kolber Z **(1995)** *Variations in Chlorophyll Fluorescence Yields in Phytoplankton in the World Oceans.* Australian Journal of Plant Physiology **22** (2) *341 – 355*

Farmer D.M. **(1996)** *Measuring currents with acoustic propagation.* Report of Acoustical Society of America 132nd Meeting, Hawaii, December 1996 **1aAO4**

Fernandes P.G., Brierley A.S., Simmonds E.J., Millard N.W., McPhail S.D., Armstrong F., Stevenson P., Squires M. **(2000)** *Fish do not avoid survey vessels.* Nature **404** *35-36*

Fernandes P.G., Gerlotto F., Holliday D.V., Nakken O., Simmonds E.J. **(2002)** Acoustic applications in fisheries science: the ICES contribution. ICES Mar. Sci. Symp., **215**

Fielding S., Crisp N., Allen J.T., Hartman M.C., Rabe B., Roe H.S.J. **(2001)** *Mesoscale subduction at the Almeria-Oran fron part 2 - biophysical interactions.* Journal of Marine Systems **30** *287-304*

Fielding S., Griffiths G., Roe H.S. **(2004)** *The biological validation of ADCP acoustic backscatter through direct comparison with net samples and model predictions based on acoustic-scattering models.* ICES J. Mar. Sci. **61** 184-200

Fisher F.H., Simmons V.P. **(1977)** *Sound absorption in sea water.* J. Acoust. Soc. Am. **62** *558-564*

Foote K.G. **(1980)** *Importance of the swimbladder in acoustic scattering by fish: a comparison of gadoid and mackerel target strength.* J. Acoust. Soc. Am. **67** *2084-2089*

Foote K.G. **(1983)** Linearity of fisheries acoustics, with additional theorems. J. Acoust. Soc. Am. **73** 1932-1940

Foote K.G., Knudsen H.P., Vestnes G., Maclennan D.N., Simmonds E.J. **(1987)** *Calibration of acoustic instruments for fish density estimation: a practical guide.* ICES Coop. Res. Rep. No. 144 *57pp*

Foote K.G., Stanton T.K. **(2000)** Acoustical methods in ICES Zooplankton Methodology Manual eds. Harris R.P, Wiebe P.H., Lenz J., Skjoldal H.R., Huntley M. Academic Press, London *223-258*

Foster E., Watson J. **(1997*)*** *Holography for underwater inspection and measurement: an overview of current work.* Optics and Laser Technology **29** (1) *17-23*

Francois R.E.. Garrison G.R. **(1984)** *Sound absorption based on oceanic measurements. Part II: Boric acid contribution and equation for total absorption.* J. Acoust. Soc. Am. **72** *1879-1890*

Gehringer J.H. **(1952)** *An all-metal plankton sampler (model Gulf III).* US Fish and Wildlife Service, Spec. Sci. Rep. Fish. **88** *7-12*

Goss C., Middleton D., Rodhouse P. **(2001*)*** *Investigations of squid stocks using acoustic survey methods*. Fisheries Research **54** *111-121*

Greenlaw C.F. **(1977)** *Backscattering spectra of preserved zooplankton.* J.Acoust. Soc. Am. **62** *44-52*

Greenlaw C.F. **(1979)** *Acoustical estimation of zooplankton populations.* Limnol. Oceanogr. **24** (2) *226-242*

Greenlaw C.F. Johnson R.K. **(1983)** *Multiple-frequency acoustical estimation.* Biological Oceanography **2** *227-252*

Harden-Jones F.R. **(1951)** *The swimbladder and vertical movements of teleost fishes. I. Physical factors.* J. Exp. Biol. **28** 553-566

Hardy A.C. **(1926)** *A new method of plankton research.* Nature **118** *630*

Harris M.P., Beare D., Toresen R., Nøttestad L., Kloppmann M., Dörner H., Peach K., Rushton D.R.A., Foster-Smith J., Wanless S **(2007)** *A major increase in snake pipefish (Entelurus aequoreus) in northern European seas since 2003: potential implications for seabird breeding success.* Marine Biology *(in press).*

Haury L.R., McGowan J.A., Wiebe P.H. **(1978)** *Patterns and processes in the time-space scales of plankton distributions.* in Spatial pattern in plankton communities, ed. Steele J.H., Plenum Press, New York *277-327*

Haury L.R., Wiebe P.H. **(1982)** *Fine scale multispecies aggregations of oceanic zooplankton*. Deep Sea Research **29** *915-921*

Heath M.R. **(1988)** *Interpretation of in vivo fluorescence and cell division rates of natural phytoplankton using a cell cycle model.* Journal of Plankton Research **10** (6) *1251 – 1272*

Herman A.W. **(1988)** *Simultaneous measurement of zooplankton and light attenuance with a new optical plankton counter*. Cont. Shelf. Res. 8 *205-221*

Herman A.W., Dauphinee T.M. **(1980)** *Continuous and rapid profiling of zooplankton with an electronic counter mounted on a Batfish vehicle*. Deep Sea Research **27A** *79-96*

Herman A.W., Denman K.L. **(1977)** *Rapid underway profiling of chlorophyll with an in-situ fluorometer mounted on a Batfish vehicle*. Deep Sea Research **24** *385-397*

Herman A.W., Sameoto D.D., Longhurst A.R. **(1981)** *Vertical and horizontal distribution patterns of copepods near the shelf break south of Nova Scotia.* Can. J. Fish. Aquat. Sci. **38** 1065-1076

Higginbottom I.R., Pauly T.J.,Heatley D.C. **(2000)** *Virtual echograms for visualisation and post-processing of multiple-frequency echosounder data*. Proceedings of the Fifth European Conference on Underwater Acoustics, ECUA 2000. Ed. Chevret P. and Zakharia M.E., *Lyon, France.*

Higginbottom I.R. **(2001)** *Virtual echograms for visualisation and post-processing of multiple frequency echosounder data.* Report of the Working Group on Fisheries Acoustics Science and Technology, ICES, *Seattle, USA*.

Hobson P.R., Watson J. **(2002)** *The principles and practice of holographic recording of plankton.* J. Opt. A: Pure Appl. Opt. **4** *S34-S49*

Holliday D.V. **(1977*)*** *Extracting biophysical information from the acoustic signatures of marine organisms.* in Oceanic Sound Scattering Prediction eds. Andersen N.R., Zanuranec B.J. Plenum Press, New York

Holliday D.V., Pieper R.E. **(1995)** *Bioacoustical oceanography at high frequencies.* ICES J. Mar. Sci. **52** *279-296*

Holliday D.V., Pieper R.E., Greenlaw C.F., Dawson J.K. **(1998*)*** *Acoustical sensing of small-scale vertical structures in zooplankton assemblages.* Oceanography **11** (1) *18-23*

Holliday D.V., Pieper R.E., Kleppel G.S. **(1989)** *Determination of zooplankton size and distribution with multifrequency acoustic technology.* J. Cons. int. Explor. Mer. **46** *52-61*

Holliday D.V., Pieper R.E., Kleppel G.S. **(1990*)*** *Advances in acoustic methods for studies in zooplankton ecology.* Oceanis **16** (2) *97-110*

Horne J.K. **(2000)** *Acoustic approaches to remote species identification: a review.* Fisheries Oceanography **9** (4) *356-371*

Horne J.K, Clay C.S. **(1998)** Sonar systems and aquatic organisms: matching equipment and model parameters Can. J. Fish. Aquat Sci. 55 1296-1306

Horne J.K, Jech J.M. **(1999)** Multi-frequency estimates of fish abundance: restraints of rather high frequencies ICES J. Mar. Sci. 56 184-199

ICES **(2002)** *Report of the Working Group on Fisheries Acoustics Science and Technology.* Montpellier, France June 17 2002 **ICES CM 2002/B:05**

ICES **(2004)** *Report of the Planning Group for Herring Surveys.* **ICES CM 2004/G:05** *7-9*

Johnson R.K. **(1977)** *Sound scattering from a fluid sphere revisited.* J. Acoust. Soc. Am. **62** *375-377*

Kang M., Furusawa M., Miyashita K. **(2002)** *Effective and accurate use of difference in mean volume backscattering strength to identify fish and zooplankton.* ICES J. Mar. Sci. **59** (4) *794-804*

Keskinen E., Leu E., Nygard H., Rostad A., Thormar J. **(2004)** *New findings of diel vertical migration in high Arctic ecosystems. University Centre of Svalbard, Norway, Publication Series.* ISSN 1503-4410

Kils U. **(1981)** *The swimming behaviour, swimming performance and energy balance of Antarctic krill Euphausia superba.* BIOMASS Scientific Series **No. 3** *122 pp*

Kimura K. **(1929)** *On the detection of fish groups by an acoustic method.* Journal of the Imperial Fisheries Institute, Tokyo **24** *41-45*

Kiørboe T. **(2001)** *Formation and fate of marine snow: small scale processes with large scale implications.* Scientia Marina **65** (Suppl. 2) *57-71*

Kirby R.R., Johns D.G., Lindley J.A. **(2006)** *Fathers in hot water: rising sea temperatures and a Northeastern Atlantic pipefish baby boom.* Biol. Lett. **doi:10.1098/rsbl.2006.0530** *published online*

Kirsch J., Thomas G.L., Cooney R. T. **(2000)** *Acoustic estimates of zooplankton distributions in Prince William Sound, spring 1996.* Fisheries Research **47** *245-260*

Kloser R.J., Ryan T., Sakov P., Williams A., Koslow J.A. **(2002)** *Species identification in deep water using multiple acoustic frequencies.* Can. J. Fish. Aquat. Sci. **59** *1065-1077*

Kogeler J.W., Falk-Petersen S., Kristensen A., Pettersen F., Dalen J., **(1987)** *Density and sound speed contrasts in Sub-Arctic zooplankton.* Polar Biology **7** *231-235*

Korneliussen R.J., Ona E. **(2002)** *An operational system for processing and visualising multi-frequency acoustic data.* ICES J.Mar. Sci. **59** *293-313*

Kullenberg G.E.B. **(1978)** *Vertical processes and the vertical-horizontal coupling.* in Spatial pattern in zooplankton communities ed. Steele J.H. Plenum Press, New York *43-71*

Kyle H.M. **(1926)** *The Biology Of Fishes.* Sidgwick & Jackson Ltd, London. *396pp*

LeBourges-Dhaussy A., Ballé-Béganton J. **(2004)** *Multifrequency multimodel zooplankton classification.* **ICES CM 2004/R:22**

Lenz J. **(2000)** *Introduction.* in ICES Zooplankton Methodology Manual eds. Harris R.P, Wiebe P.H., Lenz J., Skjoldal H.R., Huntley M. Academic Press, London *p10*

Lenz J., Schnack D., Petersen D., Kreikemeier J., Hermann B., Mees S., Wieland K. **(1995)** *The Ichthyoplankton Recorder: a video recording system for in situ studies of small-scale plankton distribution patterns.* ICES J. Mar. Sci. **52** *409-417*

Lindley J.A., Kirby R.R., Johns D.G., Reid P.C. **(2006)** *Exceptional abundance of the snake pipefish (Entelurus aequoreus) in the northeastern Atlantic Ocean.* **ICES CM 2006/C:06**

Longhurst A.R., Reith A.D., Bower R.E., Seibert D.L.R. **(1966)** *A new system for the collection of multiple serial plankton samples.* Deep Sea Research **13** *213-222*

Mackas D.L., Boyd C.M. **(1979)** *Spectral analysis of zooplankton heterogeneity.* Science **204** *62-64*

MacKenzie K.V. **(1981)** *Nine term equation for sound speed in the oceans.* J. Acoust Soc. Am. **70** *807-812*

MacLennan D.N. **(1990)** *Acoustical measurement of fish abundance.* J. Acoust. Soc. Am. **87** (1) *1-15*

MacLennan D.N., Fernandes P.G. **(2000)** *Acoustical definitions, units and symbols Report of the working group on fisheries acoustics, science and technology.* **ICES CM 2000/B:04 31-33**

MacLennan D.N., Fernandes P.G., Dalen J. **(2002)** *A consistent approach to definitions and symbols in fisheries acoustics.* ICES J. Mar. Sci. **59** *365-369*

MacLennan D.N., Forbes S.T. **(1984)** *Fisheries acoustics: a review of general principles.* Rapp. P.-v Reun. Cons. int. Explor. Mer **184** *7-18*

MacLennan D.N., Holliday D.V. **(1996)** *Fisheries and plankton acoustics: past, present and future.* ICES J. Mar. Sci. **53** *513-516*

MacLennan D.N., Simmonds E.J. **(1992)** *Fisheries Acoustics.* Chapman & Hall, London *325pp*

Madureira L.S.P., Everson I., Murphy E.J. **(1993a)** *Interpretation of acoustic data at two frequencies to discriminate between Antarctic krill (Euphausia superba Dana) and other scatterers.* Journal of Plankton Research **15** (7) *787-802*

Madureira L.S.P., Ward P., Atkinson A. **(1993b)** *Differences in backscattering strength determined at 120 and 38 kHz for three species of Antarctic macroplankton.* Mar. Ecol. Prog. Ser. **93** *17-24*

Martin A.P. **(2003)** *Phytoplankton patchiness: the role of stirring and mixing.* Progress in Oceanography **57** *125-174*

Martin A.P., Srokosz M.A. **(2002)** *Plankton distribution spectra: inter-size class variability and the relative slopes for phytoplankton and zooplankton.* Geophys. Res. Lett. **29** (24) *66.1 – 66.4*

Maxwell K., Johnson G.N. **(2000)** *Chlorophyll fluorescence – a practical guide.* Journal of Experimental Botany **51** (345) *659 – 668*

McCartney B.S. and Stubbs A.R. **(1971)** *Measurement of the acoustic target strength of fish in dorsal aspect, including swimbladder resonance.* Jnl. of Sound Vibration **15** *397–420*

McClatchie S., Thorne R.E., Grimes P., Hanchet S. **(2000*)*** *Ground truth and target identification for fisheries acoustics.* Fisheries Research **47** *173-191*

McGehee D. E., O'Driscoll R.L., Martin Traykovski, L.V. **(1998*)*** *Effects of orientation on acoustic scattering from Antarctic krill at 120 kHz.* Deep-Sea Research II **45**(7) *1273-1294*

McGehee D., Benfield M., Holliday V., Greenlaw C. **(2002)** *Advanced multifrequency inversion methods for classifying acoustic scatterers.* Unpublished material, at http:// zooplankton.lsu.edu/scattering_models/MultifrqInverseMethods.html (February 2006)

McNaught D.C. **(1968)** *Acoustical determination of zooplankton distribution.* in Proc. 11th Conf Great Lakes Res. *76-84*

Morrison C.M. **(1993)** *Histology of the Atlantic Cod, Gadus morhua: an Atlas. Part Four. Eleutheroembryo and Larva* (National Research Council of Canada, Ottawa).

Mukai T., Iida K., Sakaguchi K. Abe, K. **(2000)** *Estimations of squid target strength using a small cage and theoretical scattering models.* The Proceedings of the JSPS-DGHE International Symposium on Fisheries Science in Tropical Area. **10** 135-140

Nakken O., Aung S. **(1980)** *A survey of the fish resources of Burma, September-November 1979.* Reports on Surveys with the R/V "Dr Fridtjof Nansen", Bergen. United Nations Fisheries and Aquaculture Department report.

Nero R.W., Thompson C.H., Jech J.M. **(2004)** *In situ acoustic estimates of the swimbladder volume of Atlantic herring (Clupea harengus).* ICES J. Mar. Sci. **61** *323-337*

Ona E. **(1990)** *Physiological factors causing natural variations in acoustic target strength of fish.* J. Mar. Biol. Ass. UK **70** *107-127*

ONR **(2005)** *Loco for microscopic sea life.* Press Release, ONR Public Affairs Office, Arlington, VA, USA.

Pieper R.E., Holliday D.V. **(1984)** *Acoustic measurements of zooplankton distributions in the sea.* J. Cons. Int. Explor. Mer. **41** 226-238.

Pieper R.E., Holliday D.V., Kleppel G.S. **(1990)** *Quantitative zooplankton distributions from multifrequency acoustics.* Journal of Plankton Research **12** (2) *433-441*

Piontovski S. A., Williams R., Melnick T. A. ***(1995)*** *Spatial heterogeneity and size structure of plankton of the Indian Ocean: some general trends.* Mar. Ecol. Prog. Ser. **117** 229-227

Rayleigh J.W.S. **(1945)** *The Theory Of Sound.* Dover, New York

Renou J., Tchernia P. **(1947)** *Detection des bancs de poissons par ultrasons.* Comite d'Oceanographie des Cotes, Ministiere de la Marine, Paris *21-29*

Rines J., MacFarland M., Donaghay P., Sullivan J., Graff J. **(2006)** *Characterization of the Monterey Bay Phytoplankton Community During the 2005 LOCO (Layered Organization in the Coastal Ocean) Experiment, and the Importance of Species-Specific Characteristics of the Flora to the Dynamics and Properties of Thin Layers.* EOS Trans. AGU **87 (36)** Ocean Sci. Meet. Suppl. **OS33M-05**

Ryer C.H., Orth R.J. **(1987)** *Feeding Ecology of the Northern Pipefish, Syngnathus fuscus, in a Seagrass Community of the Lower Chesapeake Bay Estuaries.* **10** (4) *330-336*

Sameoto D.D., Lewis M.K. **(1990)** *Problems in ground truthing acoustic backscattering layers.* Oceanis **16** (2) *111-116*

Sameoto D.D., Jaroszynski L.O., Fraser W.B. **(1980)** *BIONESS, a new design in multiple net zooplankton samplers.* Can. J. Fish. Aquat. Sci. **37** *722-724*

Sameoto D., Wiebe P., Runge J., Postel L., Dunn J., MIller C., Coombs S. **(2000*)*** *Collecting zooplankton.* in ICES Zooplankton Methodology Manual eds. Harris R.P, Wiebe P.H., Lenz J., Skjoldal H.R., Huntley M. Academic Press, London *pp55-78*

Scott R.L., Biggs D.C., DiMarco S.F. **(2001)** *Spatial and temporal variability of plankton stocks based on acoustic backscatter intensity and direct measurements in the Northeastern Gulf of Mexico.* OCS Study MMS 2001-057 US Department of the Interior, New Orleans, LA. *117pp*

Selivanovsky D.A., Ezersky A.B. **(1996)** *Sound scattering by hydrodynamic wakes of sea animals.* ICES J. Mar. Sci. **53** (2) *377-381*

Selivanovsky D.A., Stunzhas P.A., Didenkulov I.N. **(1996)** *Acoustical investigation of phytoplankton.* ICES J. Mar. Sci. **53** (2) *313-316*

Shulkin M., Marsh H.W. **(1963)** *Absorption of sound in sea water.* J. Brit. Inst. Rad. Eng. **25** *493-499*

Simmonds E.J. **(2003)** *North Sea herring acoustic survey - FRV Scotia 1003s cruise report.* Available from FRS Marine Laboratory library, Aberdeen, Scotland.

Stanton T.K. **(1989)** *Sound scattering by cylinders of finite length III. Deformed cylinders.* J. Acoust. Soc. Am. **86** *691-705*

Stanton T., Chu D. **(2000)** *Review and recommendations for the modelling of acoustic scattering by fluid-like elongated zooplankton: euphausiids and copepods.* ICES J. Mar. Sci. **57** *793-807*

Stanton T., Chu D., Wiebe P.H. **(1996)** *Acoustic scattering characteristics of several zooplankton groups.* ICES J. Mar. Sci. **53** *289-295*

Stanton T.K., Chu D., Wiebe P.H. **(1998)** *Sound scattering by several zooplankton groups. II: Scattering models.* J. Acoust. Soc. Am. **103** (1) *236-253*

Sund O. **(1935)** Echo sounding in fishery research. Nature **135** 953

Swartzman G., Brodeur R., Napp J., Hunt G., Demer D., Hewitt R. **(1999)** *Spatial proximity of age-0 walleye pollock (Theragra chalcogramma) to zooplankton near the Pribilof Islands, Bering Sea, Alaska.* ICES J. Mar. Sci. **56** *545-560*

Szczucka J., Groza K., Porazinski K. **(2002)** *An Autonomous Hydroacoustic System for studying long-term scattering variability.* Oceanologia **44** (1) *111-122*

Tarling G.A., Jarvis T., Emsley S.M., Matthews J.B.L. **(2002)** *Midnight sinking behaviour in Calanus finmarchicus: a response to satiation or krill predation?* Marine Ecology Progress Series **240** *183-194*

Thomas G.L., Kirsch J. **(2000)** *Nekton and plankton acoustics: an overview.* Fisheries Research **47** (2-3) *107-113*

Trevorrow M.V., Mackas D.L., Benfield M.C. **(2005)** *Comparison of multifrequency acoustic and in situ measurements of zooplankton abundances in Knight Inlet, British Columbia.* J. Acoust. Soc. Am. **117** (6) *3574-3578*

Trevorrow M.V., Tanaka Y. **(1997)** *Acoustic and in Situ Measurements of Freshwater Amphipods (Jesogammarus annandalei) in Lake Biwa, Japan.* Limnol. and Oceanog. **42** (1), *121-132*

Urick **(1975)** *Principles of Underwater Sound.* McGraw Hill, New York

Ware D.M., Thomson R.E. **(2005)** *Bottom-up ecosystem trophic dynamics determine fish production in the Northeast Pacific.* Science **308** *1280 – 1284*

Watkins J.L., Brierley A.S. **(1996)** *A post-processing technique to remove background noise from echo integration data.* ICES J. Mar. Sci. **53** *339-344*

Watkins J.L, Brierley A.S. **(2002)** *Verification of the acoustic techniques used to identify Antarctic krill.* ICES J. Mar. Sci. **59** *1326-1336*

Weber L.H., El-Sayed S.Z., Hampton I. **(1986)** *The variance spectra of phytoplankton, krill and water temperature in the Antarctic Ocean South of Africa.* Deep Sea Research Part A – Oceanographic Research Papers **33** (10) *1327-1343*

Wegner G., Ulleweit J. **(2006)** FRV Walther Herwig III, Cruise 283: IBTS 2006 (I) Report. Institute for Sea Fisheries, Hamburg, Germany. *8pp*

Westberry T.K., Siegel D.A. **(2003)** *Phytoplankton natural fluorescence variability in the Sargasso Sea.* Deep Sea Research I **50** (3) *417-434*

Wiebe P.H., Morton A.W., Bradley A.M. **(1985)** *New developments in the MOCNESS, an apparatus for sampling zooplankton and micronekton.* Marine Biology **87** *313-323*

Williamson D.I. **(1962)** *An automatic plankton sampler for use in surveys of plankton distribution.* Rapp. et Proc. Cons. Int. Explor. de la Mer **153** *16-18*

Williamson D.I. **(1963)** *An automatic plankton sampler.* Bull. Mar. Ecol. **6** *1-15*

Wilson W.D. **(1960)** *Equation for the speed of sound in sea water.* J. Ac. Soc. Am. **32** *1357*